10 Uranium-series Chronology and Environmental Applications of Speleothems

David A. Richards

School of Geographical Sciences
University of Bristol
Bristol, BS8 1SS, United Kingdom

Jeffrey A. Dorale

Department of Geological Sciences
University of Missouri - Columbia
Columbia, Missouri, 65211, U.S.A.

1. INTRODUCTION

An increasing number of scientists recognize the value of speleothems[1] as often extremely well-preserved archives of information about past climate, vegetation, hydrology, sea level, nuclide migration, water-rock interaction, landscape evolution, tectonics and human action. Well-constrained data are required to document past changes, reconstruct past patterns and predict future responses of the Earth system at a wide range of spatial and temporal scales. Speleothems are particularly useful in this regard because they can be found in many locations of the globe, sampled at high-resolution and reliably dated using high-precision uranium-series techniques.

Speleothems are bodies of mineral material formed in caves as the result of chemical precipitation from groundwater flowing or dripping in a cave. Most speleothems are composed of calcite formed by slow degassing of CO_2 from supersaturated groundwater, but aragonite and gypsum forms are also common, particularly near cave entrances where evaporative effects are important. A host of different speleothem types decorate the walls, ceilings and floors of caves, and their mineralogy and morphology is a function of fluid flow and chemistry of waters feeding a particular location as well as the ambient conditions (temperature, chemistry, light) in the air or water-filled void. Subaerial forms include the familiar stalagmites, stalactites, draperies, flowstones. Subaqueous forms include rimstone pools, “rafts,” mammillary calcite wall-coatings and “dog-tooth” spar. For an extensive review of the types of speleothem that have been observed, see Hill and Forti (1997).

Speleothems are used in a multitude of ways to explore past environmental conditions, perhaps the most fundamental of which is their very presence or absence. Deposition of speleothems relies on sufficient water supply and soil CO_2 to enable dissolution and transport of reactants in the vadose zone to underlying caves. In arid or glacial times, conditions may not have been favorable for speleothem formation. Thus, speleothem absence/presence or growth frequency can be used as paleoclimatic indicator. The presence of subaerial speleothem forms such as flowstones, stalactites and stalagmites indicates that open passages existed and were not flooded for long intervals during the time of their formation. Age determinations on suitable samples, therefore, provide valuable constraints on the opening of passages and water-table fluctuations, the latter influenced by sea level variation or regional base-level lowering. In addition to

---

[1] In addition to their tremendous value as archives of information about the past state of the Earth’s environment, speleothems have an aesthetic value that satisfies the curiosity of all cave visitors. For this reason, we promote conservation guidelines that have been set in place to preserve the quality of cave environments. In many regions of the world, collection of speleothems is prohibited by legislation. Even if permission is obtained, the utmost effort should be made to minimize the impact of sampling.

1529-6466/00/0052-0010$10.00

presence/absence, a suite of potential indicators are contained within the solid and liquid phase (fluid inclusions) of speleothems, such as trace elements, luminescence, δD, δ^{18}O, δ^{13}C, pollen and internal stratigraphy (growth rate and hiatuses). Also, where speleothems display a clear stratigraphic relationship with sedimentary material that has been deposited, disrupted or altered, valuable age constraints can be obtained for events of interest, such as flooding, seismicity, or human occupation. Attempts have also been made to investigate past records of geomagnetic and/or heliomagnetic intensity by analyzing magnetic minerals and concentrations of cosmogenic nuclides within speleothems.

Essential to all the above applications are constraints on the timing of speleothem growth. Initial attempts to obtain chronological information from speleothems by radiocarbon (e.g., Broecker et al. 1960; Geyh 1970) or uranium-series (e.g., Rosholt and Antal 1962; Cherdyntsev et al. 1965) techniques were poorly constrained, but better understanding of chronological techniques in the late 1960s and 1970s, coupled with the use of stable isotopes of hydrogen, oxygen and carbon to obtain paleoclimatic information (Hendy and Wilson 1968; Duplessy et al. 1972; Schwarcz et al. 1976; Harmon et al. 1978; Gascoyne et al. 1978) indicated that speleothems offered considerable potential. Uranium-series methods now provide by far the most reliable and precise method for dating speleothems <0.5 Ma. Electron spin resonance (Ikeya 1975; Bassiakos 2001) and paleomagnetic (Latham and Ford 1993) techniques can be used to extend the dateable range, but suffer from relatively poor precisions.

A surge in interest in speleothems as archives of geological and archaeological information during the past two decades can be attributed in part to improvements in analytical techniques and also to a better understanding of Earth surface processes at the local to global scale that contribute to variation in proxy evidence contained within speleothems. Improvements in technology are readily illustrated by comparison of paleoclimate information obtained from speleothems 20 years ago with that of most recent studies. Through the mid-1980s, the highest resolution geochemical records (e.g., δ^{18}O and δ^{13}C) were obtained at mm-scale resolution with age control based on sub-samples >10 g with 2σ age uncertainties of the order of 2-10% at 10 ka. In contrast, a recent study of a stalagmite from the west coast of Ireland using an ion microprobe (Baldini et al. 2002) illustrates annual variation in trace elemental (P and Sr) concentration at 10 μm spatial resolution (Fig. 1) for calcite deposited during a period known as the "8.2 ka cold event." Such trace elemental data can be used as proxy evidence for paleo-recharge because they are related to water-soil-rock residence times. A parallel study using laser-ablation gas-chromatography isotope-ratio mass spectrometry to analyze sub-samples of <250 μm diameter from the same stalagmite section (McDermott et al. 2001) highlights a negative δ^{18}O anomaly for the same period (Fig. 1), which is ascribed to a combination of cold temperatures and freshening of ocean surface waters in the North Atlantic, the dominant source region for precipitation in western Ireland, and is linked with anomalies in marine and ice core records of the high latitude North Atlantic and Greenland. The timing of the cold event is constrained by mass-spectrometric uranium-series ages for sub-samples of calcite <1 g with precisions of ± 80 years. This dramatic event was probably caused by a catastrophic draining of the glacial lakes Agassiz and Ojibway into the North Atlantic. This study highlights a vast improvement on sample sizes required for analysis and, hence, temporal resolution, which has enabled construction of records with resolutions approaching those of tree-ring, coral and ice core records. In many ways, the technical developments of the past decade have had particular influence on speleothem studies in comparison to other carbonate deposits because U concentrations and growth rates are typically limiting in speleothems.

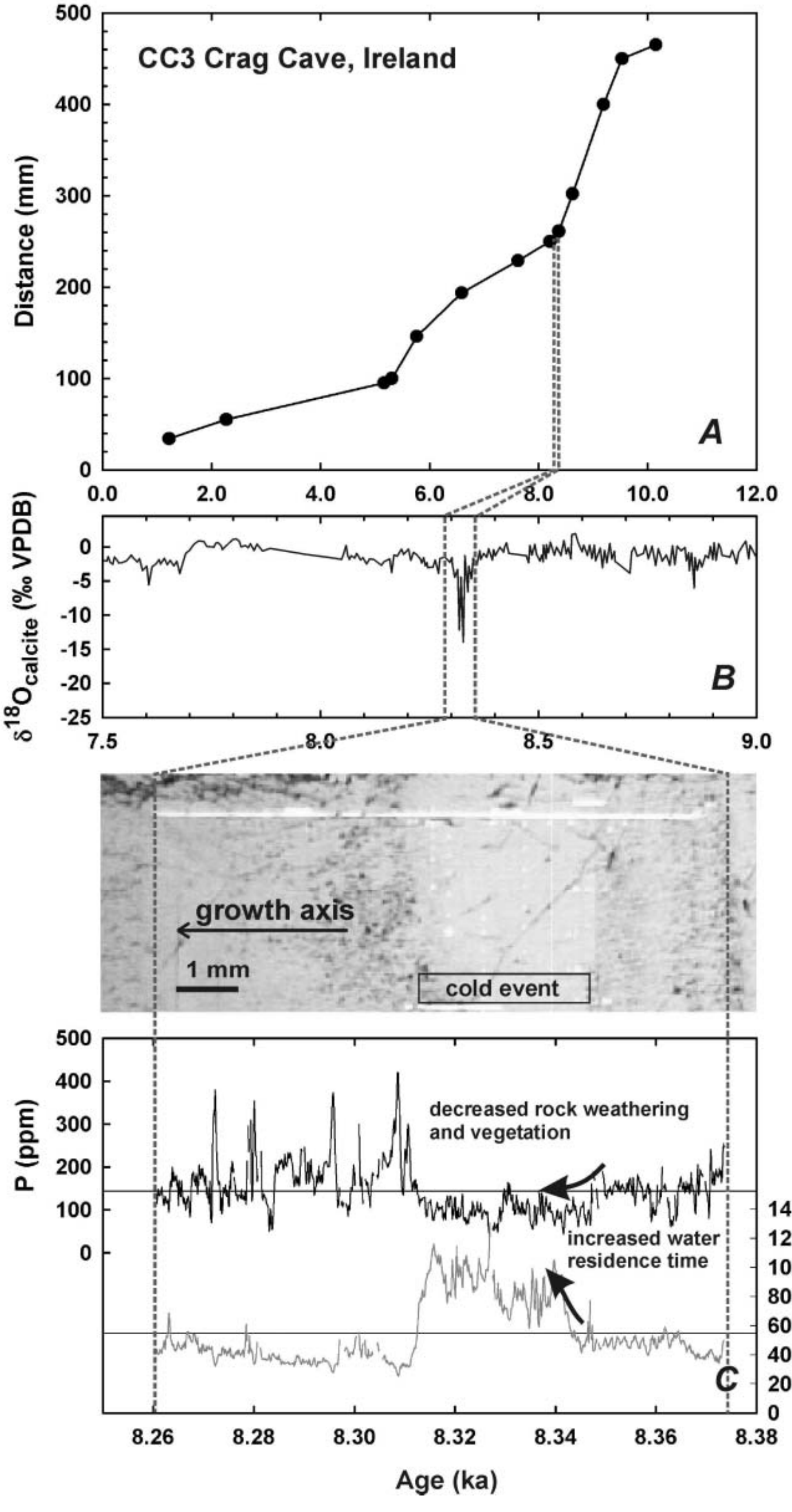

Figure 1. High resolution record of $\delta^{18}O_{calcite}$ and trace elements, Sr and P, for a speleothem from western Ireland (McDermott et al. 2001; Baldini et al. 2002). A) ^{230}Th age vs. distance relationship. Symbols larger than 2σ errors, which range from ± 0.2 to 0.8 ka. B) Negative $\delta^{18}O_{calcite}$ anomaly related to changes in $\delta^{18}O_{water}$ of rainfall during cold event triggered by meltwaters from Laurentide ice sheet. Sample resolution of ~250μm using laser-ablation gas-chromatography isotope-ratio mass spectrometry. C) P and Sr concentrations at ~10 μm resolution for period encompassing cold event. Trace element variation is related to water-rock residence times and vegetation changes in the vadose zone above the sample.

We do not intend to provide an exhaustive review of the development of uranium-series techniques and environmental applications in this chapter because there have been many notable reviews written during the past twenty years (Gascoyne et al. 1978; Gascoyne 1992a; Schwarcz 1986; Latham and Schwarcz 1992; Schwarcz and Blackwell 1992; Atkinson and Rowe 1992; Gascoyne and Harmon 1992; Ford 1997; Ku 2000). Here, we outline considerations that must be made by practicing geochronologists when analyzing speleothems, and illustrate the wide range of recent applications that are informed by ages and geochemistry of these deposits. We focus on the applications of uranium-series dating to speleothems and environmental change of the past million years. There are obvious reasons for this:

(1) Uranium-series dating is by far the most widely-used dating technique applied to speleothems, and is only applicable to material that is currently in a state of disequilibrium. Given the rates of ingrowth of daughter isotopes of ^{231}Pa and ^{230}Th, conditions of uranium-series disequilibrium in systems which have remained isotopically-closed are generally restricted to materials <~500 ka (^{230}Th) and 200 ka (^{231}Pa).

(2) Comparable evidence for environmental change is available from high resolution ocean cores, loess sequences, ice cores and other archives.

We do, however, also include brief discussion of the principles and application of U-Th-Pb dating which can theoretically be applied to material up to the age of the Earth.

2. BASIC GEOCHRONOLICAL PRINCIPLES AND ASSUMPTIONS

2.1. General principles of ^{230}Th-^{234}U-^{238}U and ^{231}Pa-^{235}U dating

A state of secular equilibrium between parent and daughter nuclides in the ^{238}U and ^{235}U radioactive decay-series will have been established in any naturally-occurring material that has remained undisturbed for several million years because the half-life of the parent isotopes is much greater than that of the intermediate daughters in the decay chains. The decay-series in secondary deposits formed from the dissolution and subsequent precipitation of such material, however, will be in a state of disequilibrium at time of formation with either an excess or deficiency of intermediate nuclides because of one or a combination of chemical, physical or nuclear fractionation processes. The extent to which the uranium-series decay chains in the secondary deposit have returned to secular equilibrium in a closed system from an initial state of disequilibrium can be expressed by a straightforward function of time using the decay constants of the radioactive isotopes involved if the following criteria are satisfied: (1) intermediate and daughter decay products at time of formation were absent, or if present, can be corrected for; (2) no gain or loss of the parent nuclide or daughter products occurred since the time of formation.

Uranium-series dating of speleothems is based on the extreme fractionation of the parent U isotopes (^{238}U, ^{235}U and ^{234}U) from their long-lived daughters ^{231}Pa and ^{230}Th in the hydrosphere. The average abundances of U and Th in the Earth's continental crust are 1.7 and 8.5 μg g^{-1} (Wedepohl 1995). Their relative abundances in the hydrosphere, however, are markedly different, principally because of the different solubility of U and Th species in the surface and near-surface environments [see *http://earthref.org/GERM* for database of elemental abundances in major reservoirs of the Earth].

Uranium is readily mobilized in the meteoric environment, principally as the highly soluble uranyl ion (UO_2^{2+}) and its complexes, the most important of which are the stable carbonate complexes that form in typical groundwaters ($pH > 5$, $p\text{CO}_2 = 10^{-2}$ bar) (Gascoyne 1992b; Grenthe et al. 1992; see also Langmuir (1997) for review). Uranium is also known to be strongly associated with organic matter, such as fulvic and humic acids, and inorganic colloids. Uranium concentrations in meteoric waters are highly variable (0.01 to 100 μg L^{-1}; Osmond and Cowart 1982) depending on ionization potential, pH, U concentration and solubility of mineral phase in the source rock, water-rock interaction time, and presence of complexing ligands. Groundwaters with the highest U contents are associated with mineralized areas or organic rich deposits such as black shales. Most analyzes have been conducted on rivers and groundwaters, while relatively few have been conducted on vadose drip waters that feed speleothems.

In contrast to U, the long-lived daughter products Th and Pa typically exist in +4 and +5 oxidation states, respectively, and are readily hydrolyzed and either precipitated or adsorbed on detrital particulates (inorganic or organic), clay minerals and iron (oxy)hydroxides. Thorium and Pa can be readily transported, therefore, in association with calcite colloids, humic acids and goethite, for example, and while turbid waters can be expected to have higher Th concentrations, waters feeding secondary calcite and aragonite deposits will generally have negligible Th concentrations. Protactinium and Th associated with airborne particulates can be incorporated into secondary deposits. Also, intermittent flooding events can transport a supply of detrital material.

U and Th concentrations in secondary deposits precipitated from solution generally reflect relative abundances in the hydrosphere. Uranium is co-precipitated with $CaCO_3$ in subaerial environments on exsolution of CO_2 (or evaporation), while the immediate daughter products are essentially absent. This represents extreme chemical fractionation of parent and daughter isotopes within the hydrosphere.

In a closed system, the extent to which the $(^{230}\text{Th}/^{238}\text{U})_A$ and $(^{231}\text{Pa}/^{235}\text{U})_A$ activity ratios (denoted by subscript A) have returned to unity is a function of time (T) and governed respectively by the following equations, assuming $(^{234}\text{U}/^{238}\text{U})_A = 1$ and an initial state of $^{230}\text{Th} = {}^{231}\text{Pa} = 0$.

$$\left(\frac{^{230}\text{Th}}{^{238}\text{U}}\right)_A = 1 - e^{-\lambda_{230}T} \tag{1}$$

$$\left(\frac{^{231}\text{Pa}}{^{235}\text{U}}\right)_A = 1 - e^{-\lambda_{231}T} \tag{2}$$

While it is expected that the source rocks for the radionuclides of interest in many environments were deposited more than a million years ago and that the isotopes of uranium would be in a state of radioactive equilibrium, physical fractionation of ^{234}U from ^{238}U during water-rock interaction results in disequilibrium conditions in the fluid phase. This is a result of (1) preferential leaching of ^{234}U from damaged sites of the crystal lattice upon alpha decay of ^{238}U, (2) oxidation of insoluble tetravalent ^{234}U to soluble hexavalent ^{234}U during alpha decay, and (3) alpha recoil of ^{234}Th (and its daughter ^{234}U) into the solute phase. If initial $(^{234}\text{U}/^{238}\text{U})_A$ in the waters can be reasonably estimated *a priori*, the following relationship can be used to establish the time T since deposition,

$$\delta^{234}\text{U}(T) = \delta^{234}\text{U}(0)e^{-\lambda_{234}T} \tag{3}$$

where $\delta^{234}\text{U} = 1000*[(^{234}\text{U}/^{238}\text{U})_m/(^{234}\text{U}/^{238}\text{U})_{\text{eq}} - 1]$, $(^{234}\text{U}/^{238}\text{U})_m$ is the measured mass ratio and $(^{234}\text{U}/^{238}\text{U})_{\text{eq}}$ is the mass ratio at secular equilibrium. Reasonable age estimates have been derived for subaqueous speleothem deposits from groundwaters that exhibit minimal long-term variation in δ^{234}U(0) (Winograd et al. 1988; Ludwig et al. 1992). However, secular variation of δ^{234}U(0) within individual samples is commonly observed (see Section 2.4), thus limiting the applicability of this technique.

Nearly all natural waters contain ^{234}U and ^{238}U in a state of disequilibrium (i.e., $(^{234}\mathrm{U}/^{238}\mathrm{U})_A \neq 1$). Generally $(^{234}\mathrm{U}/^{238}\mathrm{U})_A > 1$, and in some cases as high as 30 (Osmond and Cowart 1992), hence, a second term must be added to Equation (1), which gives the standard ^{230}Th/^{238}U age equation (from Kaufman and Broecker 1965):

$$\left(\frac{^{230}\mathrm{Th}}{^{238}\mathrm{U}}\right)_{\mathrm{A}} = 1 - \mathrm{e}^{-\lambda_{230}\mathrm{T}} + \left(\frac{\delta^{234}\mathrm{U(T)}}{1000}\right)\left(\frac{\lambda_{230}}{\lambda_{230} - \lambda_{234}}\right)\left(1 - \mathrm{e}^{(\lambda_{234} - \lambda_{230})\mathrm{T}}\right) \tag{4}$$

Figure 2 shows $(^{230}\mathrm{Th}/^{238}\mathrm{U})_A$ plotted as a function of T for different values of $\delta^{234}\mathrm{U}(0)$. As T becomes large, $(^{230}\mathrm{Th}/^{238}\mathrm{U})_A$ approaches unity and the age limit of the technique is reached. The actual limit depends on the precision of the isotopic determinations and $\delta^{234}\mathrm{U}(0)$. Equations (2) and (4) can be combined to give an expression of ^{231}Pa/^{230}Th

$$\left(\frac{^{231}\mathrm{Pa}}{^{230}\mathrm{Th}}\right)_{\mathrm{A}} = \frac{\left(\frac{^{235}\mathrm{U}}{^{238}\mathrm{U}}\right)_{\mathrm{A}}\left(1 - \mathrm{e}^{-\lambda_{231}\mathrm{T}}\right)}{1 - \mathrm{e}^{-\lambda_{230}\mathrm{T}} + \left(\frac{\delta^{234}\mathrm{U(T)}}{1000}\right)\left(\frac{\lambda_{230}}{\lambda_{230} - \lambda_{234}}\right)\left(1 - \mathrm{e}^{(\lambda_{234} - \lambda_{230})\mathrm{T}}\right)} \tag{5}$$

2.2. Initial conditions

The equations governing the age of secondary carbonate deposits stated above assume that all ^{230}Th or ^{231}Pa present in the mineral is formed *in situ* by radioactive decay of co-precipitated U. Thorium and Pa content at time of formation can often be considered to be negligible in the pure authigenic phase of calcite or aragonite

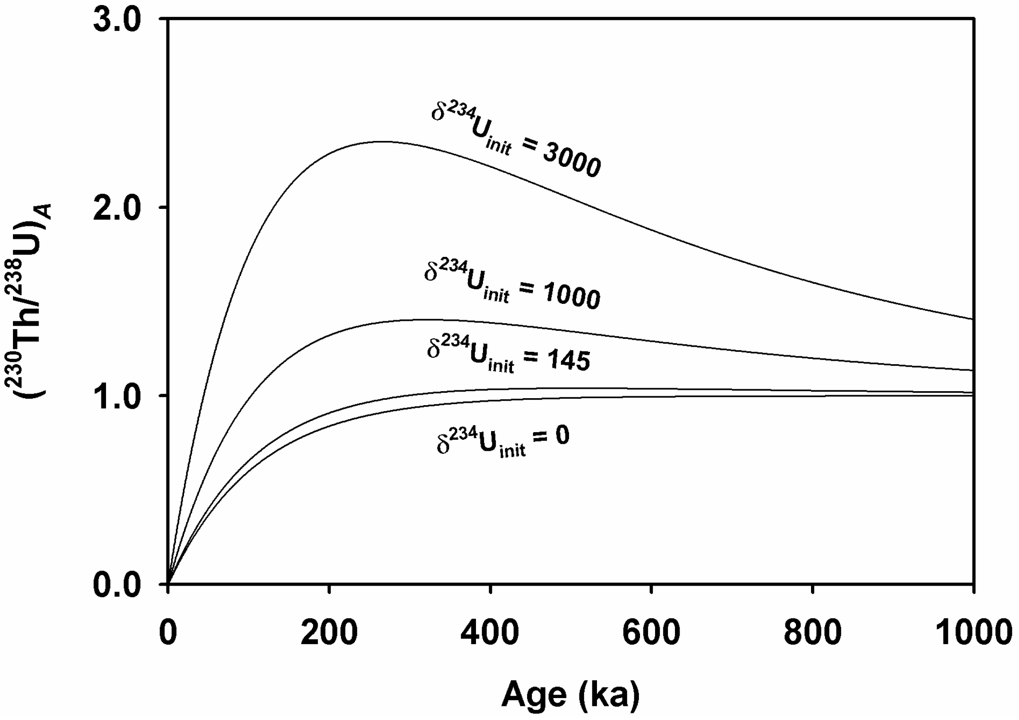

Figure 2. $(^{230}\mathrm{Th}/^{238}\mathrm{U})_A$ versus time for different $\delta^{234}\mathrm{U}(0)$ values assuming closed system and initial $^{230}\mathrm{Th} = 0$ (Eqns. 1 and 2). For those cases where $(^{230}\mathrm{Th}/^{238}\mathrm{U})_A > 1$, a unique combination of $(^{230}\mathrm{Th}/^{238}\mathrm{U})_A$ and $\delta^{234}\mathrm{U}_m$ defines the age T. $\delta^{234}\mathrm{U}(0) > 6000$ have been observed in speleothems (Plagnes et al. 2002) but are generally −100 to 1000.

speleothems, however, this component is often accompanied by allochtonous material with a significant amount of Th and Pa. Various methods are available to account for the presence of inherited daughter isotopes but the uncertainty of the final estimate is greater than would be expected for pure material.

Initial ^{230}Th and ^{231}Pa are generally considered to be associated with a detrital component that becomes cemented, or occluded, within the speleothem. This component may be composed of clays, alumino-silicates or Fe-oxyhydroxides (Fig. 3) with strongly adsorbed Th^{4+} and Pa^{5+}. Th and Pa incorporated in speleothems and similar deposits may also have been transported in colloidal phases (Short et al. 1998; Dearlove et al. 1991), attached to organic molecules (Langmuir and Herman 1980; Gaffney et al. 1992) or as carbonate complexes in solution (Dervin and Faucherre 1973a, b; Joao et al. 1987).

***A priori* estimation of $^{230}Th/^{232}Th_0$ (or R_0).** The extent of initial Th contamination can be monitored by measurement of ^{232}Th, which is the most abundant, extremely long-lived isotope of Th with a half-life of 1.401×10^{10} a. Where ^{232}Th content is high, initial ^{230}Th concentration is also expected to be significant. To a first approximation, correction can be made for the detrital component of ^{230}Th by using the ^{232}Th concentration as an index of contamination and assuming an appropriate value of $^{230}Th/^{232}Th$ for the sedimentary context. By assuming that ^{232}Th was incorporated at the time of formation, and that the excess ^{230}Th associated with this ^{232}Th decayed over time T since then, $(^{230}Th^{*}/^{238}U)_A$ (*in situ* ingrowth within authigenic carbonate phase) can be calculated using the following equation:

$$\left(\frac{^{230}\mathrm{Th}^{*}}{^{238}\mathrm{U}}\right)_{A} = \left(\frac{^{230}\mathrm{Th}}{^{238}\mathrm{U}}\right)_{Am} - \left(\frac{^{232}\mathrm{Th}}{^{238}\mathrm{U}}\right)_{A} R_0 e^{-\lambda_{230}T} \tag{6}$$

where R_0 is the $^{230}Th/^{232}Th$ activity ratio in the detritus at time of formation and is estimated from other sources, subscript m refers to the measured value of the dissolved

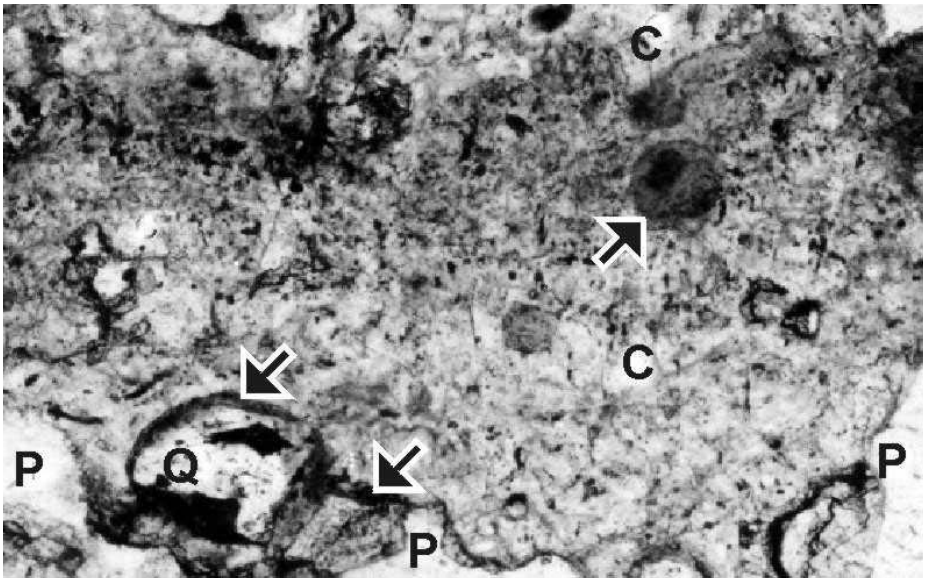

Figure 3. Grain of clay and Fe oxide (upper arrow) and quartz grain (Q) with coating of similar material (lower arrows) amidst calcite (C) in a speleothem from Drotsky's Cave, Botswana. "P" indicates pores. Energy-dispersive X-ray analysis suggests that clay is Mg-bearing smectite and confirms presence of Fe (Railsback et al. 1999). Plane-polarized light; field of view 0.7 mm wide. Stalagmite DS87; thin section BDS1.5-2; sample collected by Drs. G. A. Brook and J. Cooke. [see Atlas of Speleothem Fabrics http://www.gly.uga.edu/railsback/speleoatlas/SAintro1.html]

authigenic and detrital fraction. The concentrations of ^{234}U and ^{238}U in the authigenic carbonate are assumed to equal their concentrations in the leachate that includes the portion of detritus that has entered solution. Kaufman and Broecker (1965) established a mean value for R_0 of 1.7 ± 0.17 (1σ) for Lake Lahontan lacustrine sediments, which was confirmed by subsequent analyzes by Lin et al. (1996). Kaufman (1993) reviews the average values obtained for detritus in carbonate materials (shells, molluscs, tufas) from different locations of the globe and considers the value of 1.7 with a more conservative uncertainty of ± 0.7 (1σ) to be a reasonable *a priori* estimate in the absence of any pertinent data for the region or context of study. Others have generally adopted a value that reflects the Th/U ratio in the terrestrial upper continental crust, which has a range of 3.6 to 3.8 (Taylor and McClennan 1995; Wedepohl 1995). Assuming secular equilibrium between ^{230}Th and ^{238}U, this would give $(^{230}\text{Th}/^{232}\text{Th})_A$ = 0.83-0.87. If the full range of Th/U values for sediments is used (see Rogers and Adams 1969), a conservative mean value would be 0.8 ± 0.8 (2σ). There is a significant difference between the arbitrary values adopted in published studies. It is accepted that where ^{232}Th contamination is minimal, the effect of using the incorrect ^{230}Th/^{232}Th initial ratio will be negligible, however, caution must be adopted because anomalous values of $^{230}\text{Th}/^{232}\text{Th}_0$ may be have been inherited in some environments

Isochron methodology. To thoroughly check for, and accommodate, initial ^{230}Th in bulk carbonate material, we advocate total dissolution and isochron methodologies and application of rigorous statistical treatment (Luo and Ku 1991; Bischoff and Fitzpatrick 1991; Ludwig and Titterington 1994; Ludwig 2003). While various leach-leach, leach-residue methodologies have been promoted to distinguish between the isotopic ratios in the authigenic and detrital phases (Osmond et al. 1970; Ku and Liang 1984; Schwarz and Latham 1989), only total dissolution techniques deal with both lattice-bound and adsorbed Th. Bischoff and Fitzpatrick (1991) demonstrated that these two components could not be adequately separated by selective leaching techniques. Also, ^{230}Th released from the authigenic phase during etching can reabsorb to detrital material present during incomplete dissolution. Henderson et al. (2001) also advocate whole-sample dissolution because of the problems associated with post-depositional mobility of nuclides as a result of α-recoil. For samples with a major component of detrital material, however, there may be insufficient variation in the Th/U ratio of totally dissolved sub-samples of coeval material to arrive at meaningful isochrons, in which case selective dissolution techniques must be employed.

The construction of isochrons is standard methodology in radiometric geochronology where two or more cogenetic mineral phases can be separated from bulk sample and analyzed separately to distinguish between the amount of ingrown radiogenic end-member and its initial abundance (Rb-Sr, U-Pb, Sm-Nd, etc.) Measured U and Th isotopic data for two or more sub-samples of coeval carbonate material with different ^{232}Th/^{238}U should lie on a straight mixing line in ^{230}Th/^{232}Th-^{238}U/^{232}Th and ^{234}U/^{232}Th-^{238}U/^{232}Th space, or ^{230}Th/^{238}U-^{232}Th/^{238}U and ^{234}U/^{238}U-^{232}Th/^{238}U space if the material (1) has behaved as closed system and (2) is a two-component system (i.e., variable quantities of authigenic $CaCO_3$ and homogenous detrital phase). The ^{230}Th/^{238}U and ^{234}U/^{238}U isotopic ratios of the ^{232}Th-free endmember (used to calculate the ^{230}Th-^{234}U-^{238}U age) and $^{230}\text{Th}/^{232}\text{Th}_0$ can calculated from intercept and gradient of the straight line that best estimates the relationship in the data.

Weighted regression of ^{238}U-^{234}U-^{230}Th-^{232}Th isotope data on three or more coeval samples provides robust estimates of the isotopic information required for age calculation. Ludwig (2003) details the use of maximum likelihood estimation of the regression parameters in either coupled *XY-XZ* isochrons or a single three dimensional *XYZ* isochron, where *X*, *Y* and *Z* correspond to either (1) ^{238}U/^{232}Th, ^{230}Th/^{232}Th and

^{234}Th/^{232}Th or (2) ^{232}Th/^{238}Th, ^{230}Th/^{238}U and ^{234}U/^{238}U, respectively.

Stalagmites often have observable differences in the quantity of detrital material along growth layers because of the nature of fluid flow on the surface of the sample. Commonly, the central portion at the locus of drip contact is the cleanest material, presumably because the energy of drip impact is greatest at this point. The extent of homogeneity of initial ^{230}Th/^{232}Th in a single layer from a stalagmite (SVC-98-3.B) from Spring Valley Caverns, Minnesota was analyzed using isochron methodology by Dorale et al. (2003). Variation in detrital Th content was confirmed by ^{238}U/^{232}Th measurements, which vary by two orders of magnitude from the core to the periphery of the growth layer. Isotopic data show a linear relationship in ^{230}Th/^{238}U-^{232}Th/^{238}U and ^{234}U/^{238}U-^{232}Th/^{238}U space, however there is excess scatter with a mean square of weighted deviates value of 7.9 (Fig. 4). The resolved ^{230}Th/^{232}Th is 0.801 ± 0.152, which is very similar to the bulk Earth value.

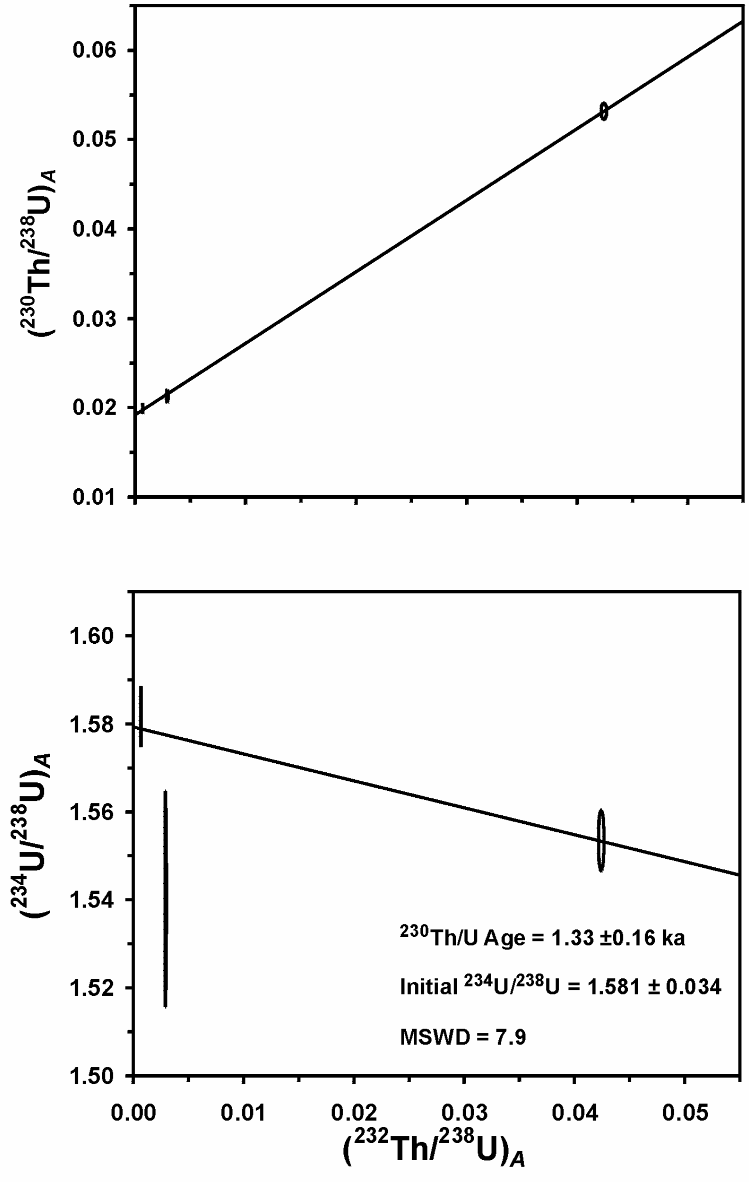

Figure 4. Osmond type II isochron plot for sub-samples from single growth layer in stalagmite SVC-98-3.B from Spring Valley Caverns (Dorale et al. 2003).

The most likely cause of scatter in isochrons is a combination of more than one source of initial Th. Lin et al. (1996) identify three sources of initial ^{230}Th in lacustrine carbonates from Lake Lahontan, USA: (1) detrital Th, (2) hydrogenous Th adsorbed to detritus and (3) hydrogenous Th directly incorporated by carbonates. Detrital Th is assumed to have a Bulk Earth value and be composed of aluminosilicates, however the total initial ^{230}Th/^{232}Th signal is possibly offset to high values by an abundant "hydrogenous" component, which has an additional source of ^{230}Th from *in situ* decay of uranium. Schramm et al. (2000) also identify a hydrogenous component in carbonates deposited in Lake Lisan (last glacial Dead Sea). Here, a sample of modern aragonite material, essentially free of insoluble detritus, had a finite age of 2556 ± 30 years indicating that substantial corrections must be made to ages to account for initial conditions.

A significant hydrogenous component of initial ^{230}Th was also discovered in a speleothem from the Bahamas by Beck et al. (2001). Using a correction for initial ^{230}Th based on measured ^{232}Th concentration and assumed Bulk Earth $(^{230}\mathrm{Th}/^{232}\mathrm{Th})_A$ of 0.8 ± 0.8, they observed that samples with high ^{232}Th concentrations had significantly older ^{230}Th ages than proximal samples with lower ^{232}Th concentrations, indicating that a greater value of $(^{230}\mathrm{Th}/^{232}\mathrm{Th})_0$ was required. In all cases, no insoluble residue or "detrital component" remained after dissolution in dilute acid and, for this reason, they considered the initial component of Th in meteoric waters to be dissolved or scavenged by colloids and co-precipitated with U in the calcite. Variation in ^{238}U/^{232}Th was substantial; two orders of magnitude range and sufficiently different between sub-samples of the same approximate age that ^{230}Th/^{232}Th of the scavenged component could be estimated using isochron techniques. Estimates of the present value of scavenged $(^{230}\mathrm{Th}/^{232}\mathrm{Th})_A$ (or $(^{230}\mathrm{Th}/^{232}\mathrm{Th})_0.e^{\lambda_{230}T}$) were obtained by plotting the isotopic results for sets of 2 or more sub-samples that could be considered as coeval in $(^{238}\mathrm{U}/^{232}\mathrm{Th})$-$(^{230}\mathrm{Th}/^{232}\mathrm{Th})$-$(^{234}\mathrm{U}/^{232}\mathrm{Th})$ space (Fig. 5). A mean value for $(^{230}\mathrm{Th}/^{232}\mathrm{Th})_0.e^{-\lambda_{230}T}$ of 15.8 ± 2.3 ($2\sigma_{\mathrm{mean}}$, $n = 10$) was obtained and used to correct measured ^{230}Th/^{238}U prior to calculation of ages (Fig. 6). This value is at least an order of magnitude higher than commonly used values for initial Th corrections and careful consideration should be given to previously published analyzes where the measured ^{230}Th/^{232}Th activity ratio is $< \sim 200$ and contamination appeared to be insignificant based on lack of insoluble detritus.

One might expect the ^{230}Th/^{232}Th ratio of meteoric waters in the shallow vadose zone of a middle Pleistocene age carbonate platform such as Grand Bahama to be high because the carbonate sediments in the dune ridges that house the cave system are relatively free of silicate material and of sufficient age that ^{230}Th and ^{238}U are expected to be near secular equilibrium. Carbonate material dominates, with a much greater ^{230}Th/^{232}Th than Bulk Earth. Dissolution of this material and subsequent adsorption of hydrogenous Th by Fe-oxyhydroxides and colloids results in transport of Th with elevated ^{230}Th/^{232}Th values to the speleothem. Similar middle Pleistocene oolitic-peloidal deposits from Eleuthera, Bahamas yield ^{230}Th/^{232}Th of 3.43×10^{-4} (Hearty et al. 1999). It should be noted that even though a high initial ^{230}Th/^{232}Th value was derived for the Bahamas speleothem GB-89-24-1 (Beck et al. 2001) and corrections of as much as 3 ka were applied to some sub-samples, many of the sub-samples had such low ^{232}Th concentrations that corrections were negligible. The resulting initial ^{230}Th corrected ages present a remarkably coherent chronology (Fig. 6).

Zero(?) age deposits and waters. Perhaps the most sensitive test of initial conditions for speleothems and analogous carbonate deposits is to undertake U-series measurements of the most recent calcite in actively growing samples such as straw stalactites and the waters that feed them. Surprisingly, few such measurements have been published.

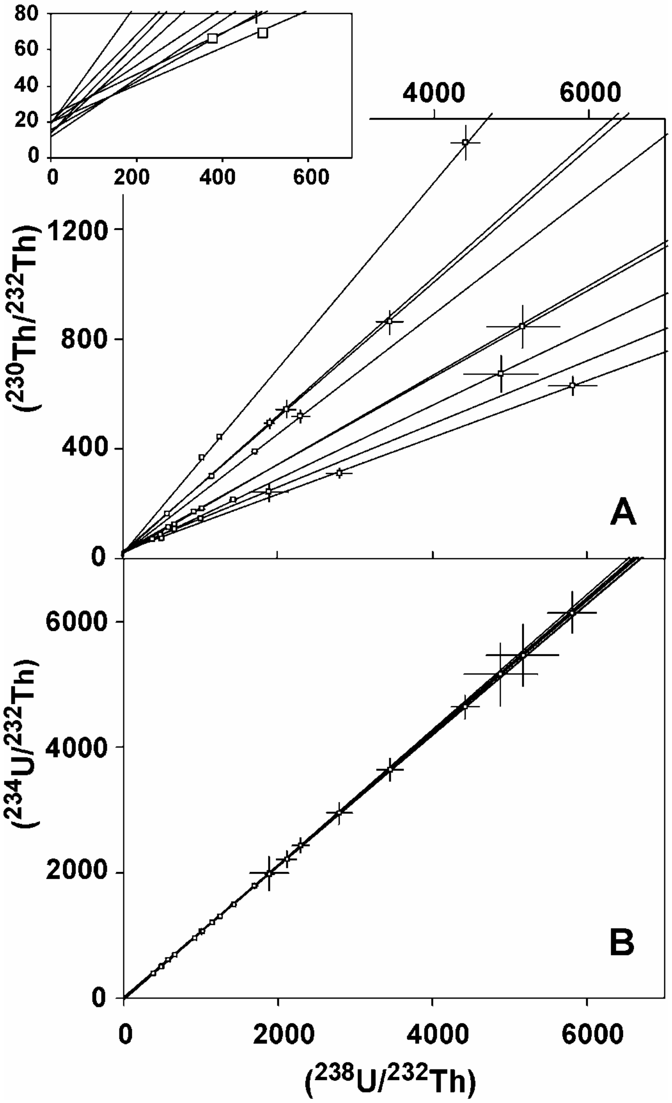

Figure 5. U and Th isotope measurements for 9 coeval sets of sub-samples from GB-89-24-1, Grand Bahama (Beck et al. 2001) are plotted in (A) (^{230}Th/^{232}Th)$_A$-(^{238}U/^{232}Th)$_A$ and (B) (^{234}U/^{232}Th)$_A$-(^{238}U/^{232}Th)$_A$ space (Rosholt Type-II' diagram). Intercepts of isochrons with abscissa in A are equivalent to (^{230}Th/^{232}Th$_{init}$).e$^{-\lambda 230t}$ of the scavenged Th component, while the gradient is equivalent to (^{230}Th*/^{238}U) and can be used to calculate the age T. Ages calculated using isochrons are in correct stratigraphic order. Using T for each isochron, a weighted mean (^{230}Th/^{232}Th)$_0$ activity ratio of 18.67 ± 2.9 ($2\sigma_m$) was obtained, equivalent to an atomic ratio of 1.04×10^{-4} and significantly greater than bulk earth atomic ratio of 4.4×10^{-6}. This value was subsequently used to correct the measured (^{230}Th/^{238}U) in all sub-samples (Fig. 6) The gradient in B is equivalent to the present value of (^{234}U/^{238}U)$_A$. Correction to initial values, using T, yields δ^{234}U(0) = 59 ± 6 ($2\sigma_m$), which is indistinguishable from the mean value of all other sub-samples; 59 ± 3 ($2\sigma_m$, n = 56). No significant relationship between T and δ^{234}U(0) was found.

Whitehead et al. (1999) present finite alpha-spectrometric ^{230}Th-^{238}U and ^{231}Pa-^{235}U ages >2 ka for two straw stalactites considered to be actively forming at the time of sampling and declare that ^{230}Th and ^{231}Pa contamination at zero age is a possible limitation of U-series dating methodology, however, these samples were uncorrected for initial Th, which is known to be relatively high (^{232}Th/^{238}U = 0.0283 and 0.0126), at least two orders of magnitude higher than typical surface corals (^{232}Th/^{238}U < 0.0003), for example.

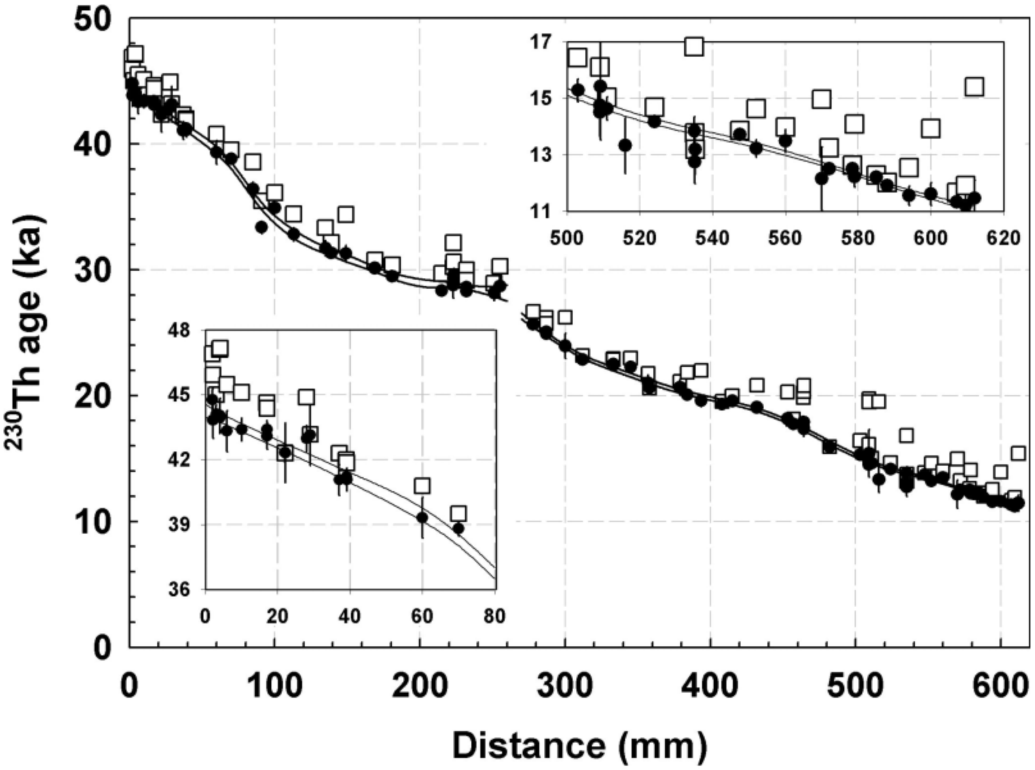

Figure 6. ^{230}Th age vs. distance along the longitudinal growth axis of GB-89-24-1, a submerged speleothem from Grand Bahama (Beck et al. 2001). Estimates of ^{230}Th age are corrected for initial Th using $(^{230}Th/^{232}Th)_0$ activity ratio with Bulk Earth value of 0.8 ± 0.8 ppm (open squares) and significantly higher value of 18.67 ± 2.9 based on isochron results illustrated in Figure 5 (filled squares). The latter correction results in a smooth, monotonic distance-age relationship.

Richards (1995) analyzed U and Th isotopic concentrations in a straw stalactite (TC-92-3) and an unfiltered sample of dripwater from Middle Caicos, British West Indies (Table 1). Further analyzes of waters during the summer of 1999 confirmed the elevated value of $(^{230}Th/^{232}Th)_A$ in drip waters (average = 15.0 ± 7.7, 1σ, n = 19), which is significantly higher than the value of Bulk Earth (~0.8). This value is similar to that predicted using isochrons for a speleothem from Grand Bahama and indicates that $(^{230}Th/^{232}Th)_A$ is high in pure carbonate terrain and initial ^{230}Th must be investigated in detail. In a ^{230}Th/^{232}Th vs. 1/[Th] plot for the Turks and Caicos dripwaters (Fig. 7) it can be seen that the points sit on or above a mixing plane between two or more components, Bulk Earth and various radiogenic “hydrogenous” phases.

In a detailed study of numerous suites of co-eval sub-samples from speleothems from Soreq Cave, Israel, Kaufman et al. (1998) demonstrate that Th is positively correlated with Si, Fe and Al, which suggest that ^{232}Th is associated primarily with

Table 1. U, Th data for active straw stalactite and drip water from Conch Bar Cave, Middle Caicos

Sample	^{238}U $(ng\ g^{-1})$	^{232}Th $(ng\ g^{-1})$	$(^{230}Th/^{232}Th)_A$	*Th/U*	$\delta^{234}U(0)$ (‰)	$(^{230}Th/^{238}U)_A$	*Uncorrected Age* (*ka*)
TC-92-3B	724.3	0.10	18.3±2.2	.000138	24.3±1.5	$80(\pm 1)\times10^{-4}$	0.09±0.01
TC-92-H20	0.3884	2.7×10^{-4}	5.18±0.85	.000695	97.4± 2.0	$120(\pm2)\times10^{-4}$	0.12±0.02

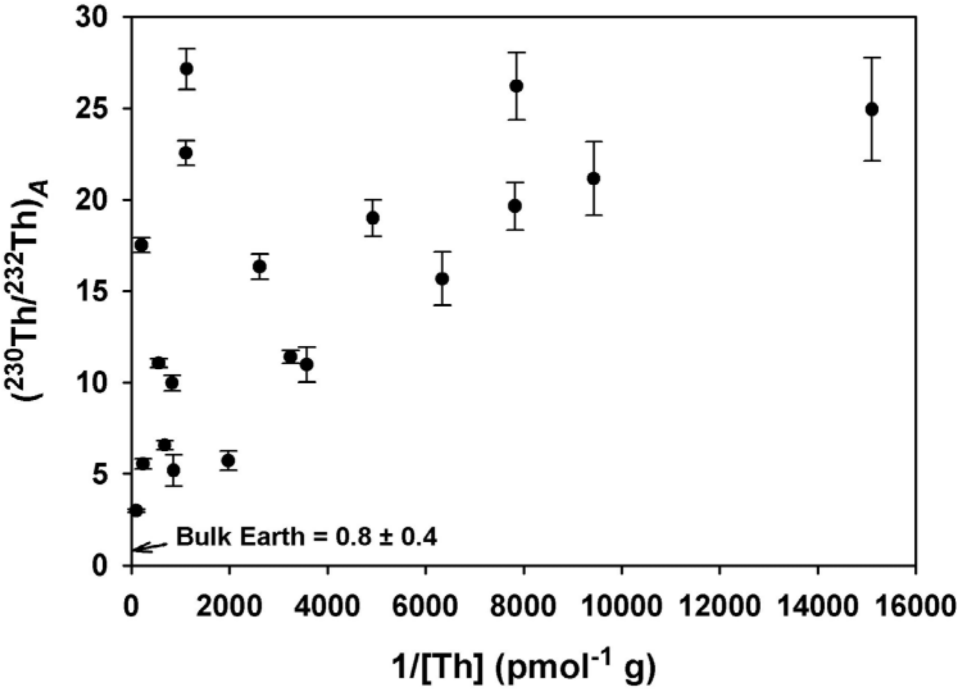

Figure 7. $(^{230}Th/^{232}Th)_A$ vs. 1/[Th] of dripwaters from Conch Bar Caves, Middle Caicos, British West Indies. In all cases dripwaters have $(^{230}Th/^{232}Th)_A > 0.8$ (bulk Earth value).

detrital silicates and ferric-oxyhydroxides. Isochron analyzes reveals a R_0 value of 1.3 to 2.9. Assuming secular equilibrium, this suggests a $^{232}Th/^{238}U$ atomic ratio of 1.08 to 2.4, which is below that of the average crustal value. Analysis of filtered and unfiltered cave drip waters from the same location indicate that ^{232}Th in this environment is associated with detrital particulates, but they also discovered that such material has adsorbed large quantities of U, as has been found for colloids and ferric-oxyhydroxides in rivers and estuaries (Porcelli and Swarzenski 2003; Swarzenski et al. 2003).

2.3. Closed system decay

One of the major assumptions of the ^{230}Th and ^{231}Pa dating schemes presented above is that the U-series radionuclide system should be closed to post-depositional migration or addition constituent nuclides. Authigenic material that shows evidence of weathering should be avoided. Also, any sign of recrystallization, such as conversion from aragonite to calcite, is indicative of potential nuclide migration, as is alteration from "length-fast" palisade low magnesium calcite to blocky, equant low magnesium calcite (Bar Matthews et al. 1997). Dense, macrocrystalline calcite provides the most reliable material.

After material has been analyzed, an extra degree of confidence can be ascribed to the ages if a combination of the following criteria are met:

(1) Age determinations are consistent with their stratigraphic position, either within the sample itself or in the context of the surrounding deposits and sample location.

(2) Combined ^{230}Th-^{238}U and ^{231}Pa-^{235}U dating techniques yield concordant results.

(3) Agreement is found for ages determined on the same material by independent dating methods

In addition to the above, one should also look for internal consistency of the derived values of initial $^{234}U/^{238}U$ and also demonstrate that secular equilibrium conditions have been established and maintained in material >1 Ma, if available, from the same location.

Stratigraphic consistency. The advent of high-resolution U-series techniques has brought about the standard practice of measuring multiple sub-samples along the growth axis of speleothems to provide detailed chronologies and growth rate information. Such data provide an opportunity to look for internal consistency in the derived ages. Beck et al (2001) made 81 U and Th measurements on sub-samples from the growth axis of a speleothem from the Bahamas, which is composed of clear dense calcite with no evidence of post-depositional alteration. After correction of the U and Th isotopic results for the presence of initial ^{230}Th contamination (see above), a smooth relationship is observed between longitudinal position and age, with no statistically significant age reversals (Fig. 6).

The most susceptible material for post-depositional loss or addition of radionuclides is the outer layer of samples that have been exposed to moisture for a long duration. Stratigraphic consistency between ages of the outermost material and that deposited prior to this provides valuable constraints on the technique. Four ages were derived for a band of clear, white calcite deposited on a stalactite from 53.6 m below sea level in a blue hole of Andros, Bahamas (Richards et al. 1994). Isotopic data for the outermost surface, which had been exposed to sea water for at least 8 ka was indistinguishable from the internal material (Fig. 8).

Combined ^{231}Pa-^{235}U and ^{230}Th-^{234}U-^{238}U dating. For secondary carbonate deposits less than about 200 ka, finite ^{230}Th and ^{231}Pa ages can be derived using the Equations (4) and (2), respectively. A combined $^{230}Th/^{231}Pa$ age can also be derived (Eqn. 5). Based on the assumptions that negligible Pa and Th was incorporated in the secondary deposit at

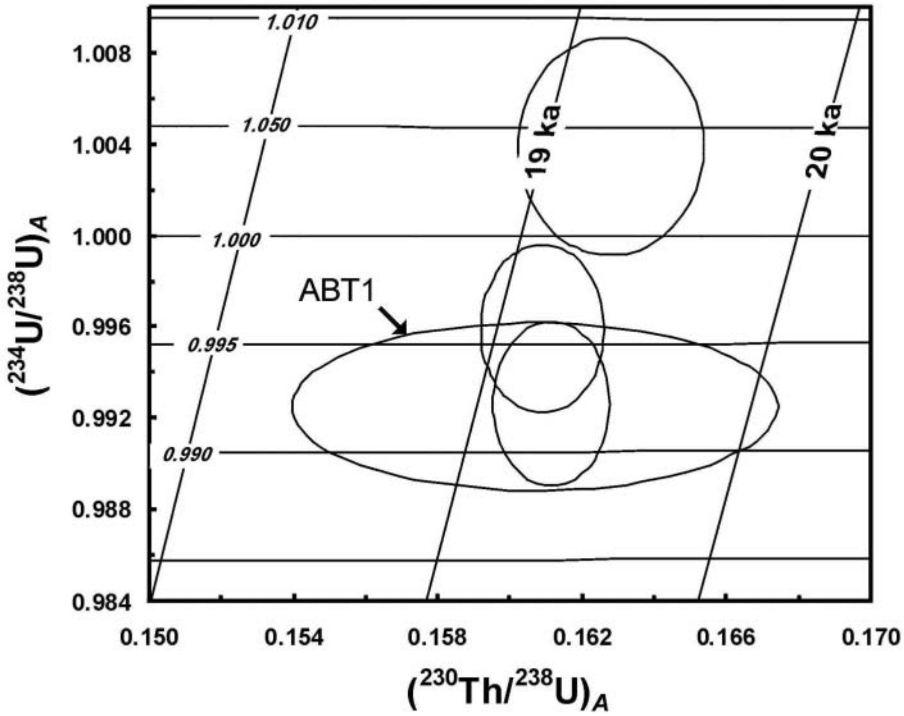

Figure 8. TIMS ^{230}Th ages of latest phase of growth of GB-89-23-2 (Richards et al. 1994). Outermost sample (ABT1; n = 4) indistinguishable from ages of older material up to 10 mm inside outer surface of this stalactite. GB-89-23-2 was collected from a depth of 53.6 m below present sea level in Stargate, Andros, Bahamas, and was submerged since inundation by rising sea levels during the last deglaciation.

the time of formation and decay has proceeded as a closed system, one should expect the ages to agree within analytical precision. If there has been significant episodic or continuous loss or gain of U, Th and Pa since deposition, discordant ages will result. Isotopic data for material with initial $^{230}Th/^{238}U$ and $^{231}Pa/^{235}U = 0$ and closed system decay will plot on an evolution curve, which has a form dictated by initial $^{234}U/^{238}U$. Combined measurements of U, Th and Pa measurements can be used to investigate open system behaviour and diagenesis in much the same way as has been used in U-Th-Pb system (Allègre 1964; Ku et al. 1974; Szabo 1979; Kaufman et al. 1995). Prior to the development of high-precision mass-spectrometric techniques, however, the precision of alpha-spectrometric techniques was insufficient to investigate many dating problems using Pa.

Early attempts to demonstrate concordance between speleothem ages derived from each of the ^{238}U and ^{235}U decay chains were presented by Thompson et al. (1976) and Gascoyne (1985), who used ^{227}Th to deduce the activity of ^{231}Pa. This is possible because the half-life of the intermediate daughter, ^{227}Ac, is only 22 yr and material older than a few hundred years has ^{227}Th activity in equilibrium with that of ^{231}Pa. They demonstrated reasonable concordance in some samples, but overall results were equivocal, possibly as a result of coprecipitation of ^{231}Pa during formation, and thus excess ^{227}Th, in some samples (see also discussion in Whitehead et al. 1999). Shen (1996) was more successful in applying the technique to speleothem samples from caves of China and demonstrates reasonable concordance for a suite of sub-samples with ages up to and beyond 200 ka. The analytical uncertainties, however, are generally greater than 10%.

Now that ^{231}Pa measurements can be obtained with precisions approaching that of ^{230}Th measurements on material deposited during the past 50 ka, researchers are in a much better position to verify their U-Th chronologies by testing for age concordancy and diagenetic processes. Using a modified technique of that developed by Pickett et al. (1994), Edwards et al. (1997) tested the accuracy of ages that had been obtained using the ^{230}Th chronometer. They obtained U, Th and Pa isotopic data for numerous corals to demonstrate closed system uranium-series decay from an initial state of $^{231}Pa = ^{230}Th = 0$ and $\delta^{234}U_{init} = 140‰$. Also, two sub-samples from Devils Hole calcite vein, which had a ^{230}Th chronology suggesting an earlier timing for the penultimate deglaciation of (Ludwig et al. 1993) than that suggested by orbitally-tuned marine cores, provided concordant ages and similar $\delta^{234}U_0$ of 1800‰.

Edwards et al. (1997) demonstrate that for samples with similar $\delta^{234}U(0)$, such as corals that grew in open marine water, and remained closed system since time of formation, isotopic data plot on or close to an ideal concordia in ^{231}Pa-^{235}U vs. $^{230}Th/^{234}U$ space. Concordia represent the loci of points for which ^{231}Pa and ^{230}Th ages are identical for a given $\delta^{234}U(0)$, and are more useful for systems with constant $\delta^{234}U(0)$ than deposits formed from meteoric water where it is well known that secular variation of $\delta^{234}U(0)$ is exhibited because of the changing nature of water-rock interaction and chemistry of percolating waters. Where $\delta^{234}U(0)$ varies significantly in individual samples or between samples, concordance is better demonstrated on a ^{231}Pa versus ^{230}Th age plot. The suitability of speleothem calcite for uranium-series dating is well-demonstrated by Figure 9, where isotopic data and ages for material analyzed in the past few years at the University of Minnesota (Beck et al. 2001, Musgrove et al. 2001, Dorale et al. 2003) plot on the $^{230}Th = ^{231}Pa$ line (Fig 9B). The same data are plotted in ^{231}Pa-^{235}U vs. $^{230}Th/^{234}U$ space in Fig 9A. Generally, data for individual samples plot on or near concordia indicating limited secular variation of $\delta^{234}U(0)$, however, two sub-samples from a speleothem from Crevice Cave, Missouri have different $\delta^{234}U(0)$ of 3007 at 89.7 ka and 2589 at 78.9 ka.

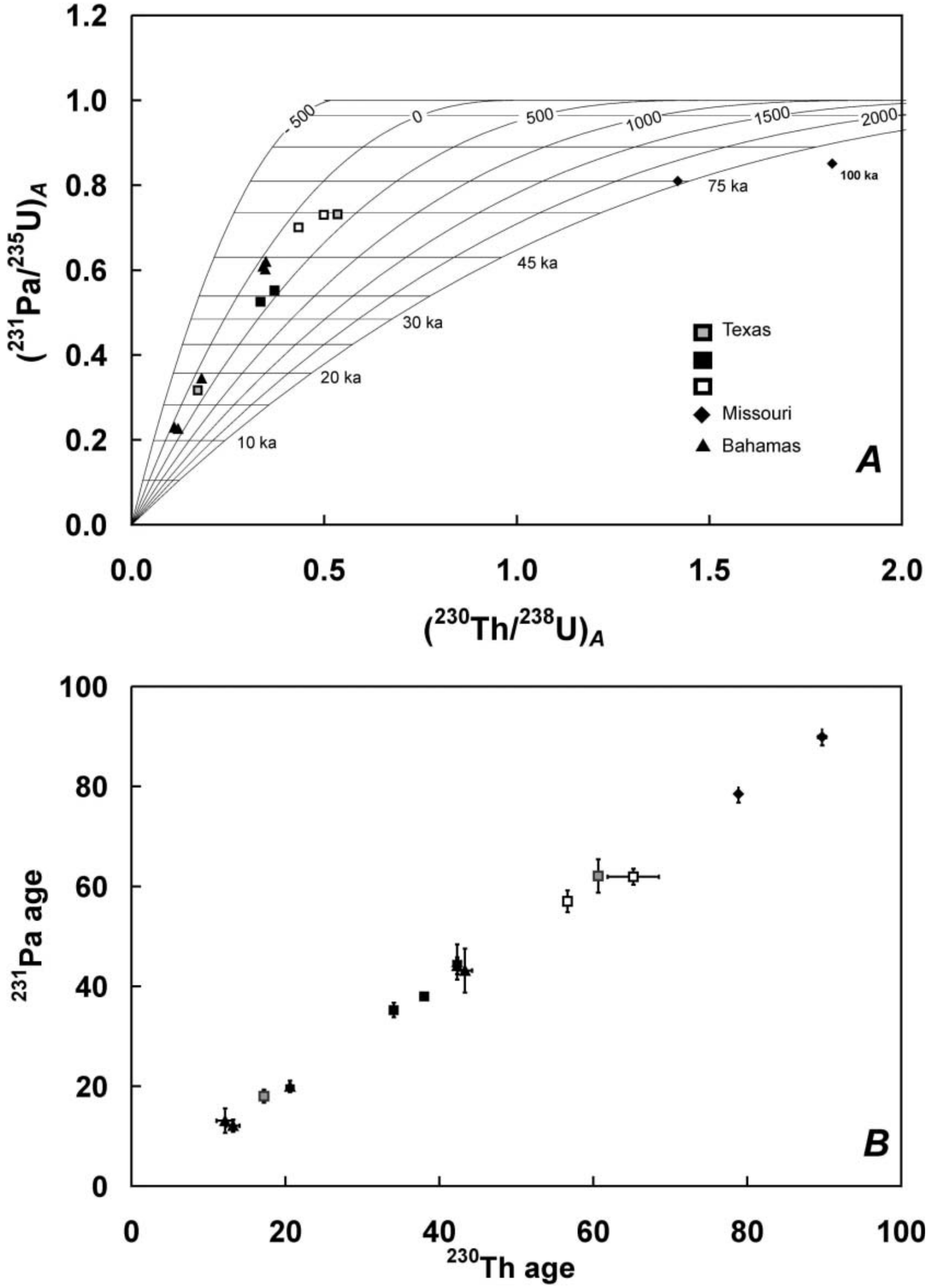

Figure 9. U, Th and Pa isotopic data and ages for speleothems (Beck et al. 2001; Musgrove et al. 2001, Dorale et al. 2003). A.) $(^{230}Th/^{238}U)_A$ vs. $(^{231}Pa/^{235}U)_A$ concordia plot. Evolution curves for different $\delta^{234}U(0)$ are shown. Horizontal lines represent isochrons. B.) ^{230}Th vs. ^{231}Pa ages for the same samples. All data plot within error of the 1:1 line, illustrating age concordance.

A unique strength of concordia diagrams is their ability to reveal modes of diagenetic disturbance. If U-Th-Pa isotopic data for numerous co-eval sub-samples that have experienced different degrees of the same diagenetic process are plotted in $^{231}Pa/^{235}U$ or $^{230}Th/^{238}U$ vs. $^{234}U/^{238}U$ space, they should fall on a curve or straight line that can be used to estimate the true crystallization age and the mode of disturbance. This is similar to methods used in U-Pb geochemistry and is described in detail by Cheng et al. (2000), who illustrate the use of combined U-Th-Pa data to investigate open-system behavior in corals from a last interglacial terrace on Barbados. To the best of our knowledge similar methods have yet to be applied to speleothems.

Comparison with independent "dating" methods. Advances in technology during the past have made uranium-series dating potentially the most precise and/or highest resolution method for dating carbonate material. Alternative radiometric methods are often fraught with additional complications. Only AMS ^{14}C dating can achieve comparable precisions, but as we discuss in Section 4.2, *a priori* assumptions of initial ^{14}C concentrations in speleothem are poorly constrained and accuracy is less reliable. However, confidence can be ascribed to a uranium-series age determination if consistent timing is observed between regional or global events recorded by trace elements or stable isotopes in a speleothem and that observed in other archives, such as ocean cores or ice cores. For example, McDermott et al. (2001) and Baldini et al. (2002) observe a $\delta^{18}O$ and trace element anomaly (~8.3 ka) in a speleothem from western Ireland (Fig. 1) that is synchronous, within 2σ dating uncertainties, with an abrupt and short duration shift to cold climate in the high latitude Northern Hemisphere as recorded in Greenland ice cores (Grootes et al. 1993, Alley et al. 1997).

Dramatic shifts in ocean or atmospheric circulation can result in shifts in $\delta^{18}O$ of precipitation falling above the cave location. Speleothems, therefore, can be used to infer timing of regional or global scale changes in past climate. A high degree of synchroneity between the timing of abrupt shifts of $\delta^{18}O$ records in speleothem calcite and marine and ice cores for the last interglacial-glacial period, therefore, has been also used to indicate the reliability of uranium-series ages speleothems (Dorale et al. 1998, Bar-Matthews et al. 1998; McDermott et al. 2001, Burns et al. 2001 Spötl and Mangini 2002; Wang et al. 2002 *inter alia*; see Section 4.2). We should stress, however, that observation of apparent synchroneity between events in speleothems and other records does not provide unequivocal constraints on the age determination because there exists the possibility of diachronous response to the same forcing events. Researchers should also be aware that in many cases the marine cores and ice cores records are themselves reliant on dating methods that are subject to debate, such as ice flow models, radiocarbon and orbital tuning.

2.4. $^{234}U/^{238}U$ dating methodology

^{230}Th-^{234}U-^{238}U and ^{231}Pa-^{235}U techniques are only applicable to deposits typically less than ~500 ka and ~200 ka respectively. The half-life of ^{234}U is such that the dateable age range can be extended to at least 1 Ma (using Eqn. 3) if robust estimates of $\delta^{234}U(0)$ can be made for a particular cave system. However, speleothems exhibit significant secular and intra-regional variation of $\delta^{234}U(0)$ in most settings because of changes in water-rock interaction times, soil $p\mathrm{CO}_2$, pH and other climate- and hydrology-related factors, thus precluding the use of this technique for dating purposes in most cases (Harmon et al. 1975). Some have advocated the use of a regional best estimate to obtain low precision ages where numerous modern drip waters and material with resolvable U/Th ages from the same cave or region show little variation in $\delta^{234}U(0)$. For example, Gascoyne et al. (1983) showed that the standard deviation of $\delta^{234}U(0)$ for numerous dated speleothems from Victoria Cave, northwest England was sufficiently low that reasonable age estimates could be obtained for material up to 1.5 Ma. Successful attempts have been made to use this technique under marine (Bender et al. 1979; Ludwig et al. 1991), groundwater (Winograd et al. 1988; Ludwig et al. 1992), lacustrine (Kaufman 1971) and soil (Ludwig and Paces 2002) settings where δ^{234}U(0) is more likely to remain reasonably stable for long periods of time. Ludwig et al. (1992) adopted a mean δ^{234}U(0) value of 1750 ± 100 to calculate ages >360 ka for sub-samples from a calcite vein from Devils Hole, Nevada. The uncertainty propagated through the age equation encompasses the full range of variation of δ^{234}U(0) for ages younger <360 ka.

2.5. U-Th-Pb dating of secondary carbonates of Quaternary age

Standard ^{230}Th-^{234}U-^{238}U dating techniques can only be applied usefully to material that satisfy the above criteria and have activity ratios that are distinguishable from unity. For speleothems, this means that the upper age limit is <~500 ka, unless the calcite precipitated from waters with extremely high initial values of ^{234}U/^{238}U (see Fig. 2). Speleothems and other secondary carbonate deposits such as tufa, travertines, lake carbonates and vein calcites have the potential to provide valuable information about past climate, hydrogeochemistry, landscape development and hominid evolution during the early Quaternary and Tertiary periods. Electron-spin resonance (Grün 1989, Rink 1997) and ^{234}U-^{238}U disequilibrium methods (Ludwig et al. 1992) have proved to be useful in extending the dateable range beyond 0.5 Ma but suffer from lack of precision or poorly constrained initial conditions. An alternative geochronological technique is U-Th-Pb dating, which uses the ingrowth of the stable Pb isotopes ^{206}Pb and ^{207}Pb from the decay of their respective long-lived parent isotopes, ^{238}U and ^{235}U. U-Th-Pb dating techniques are more commonly used for much older deposits, indeed up to the age of the Earth. Since the work of Moorbath et al. (1987), U-Pb and Pb-Pb methods have been applied to various ancient carbonates (Paleozoic and Mesozoic), such as limestones (Smith and Farquhar 1989), metamorphosed marbles (Jahn and Cuvellier 1994), calcite concretions (Israelson et al. 1996), paleosol calcite (Rasbury et al. 1997) and scalenohedral calcite (Lundberg et al. 2000). For deposits less than a few million years, the amount of radiogenic Pb present is very small because of the extremely long half-lives of the parent isotopes and, until recently, it has been considered impractical to obtain ages with reasonable precision. Getty and DePaolo (1995) presented a novel method for dating Quaternary volcanic rocks using U-Th-Pb techniques and Richards et al. (1998) demonstrated the feasibility of using U-Th-Pb isochron methodology to date young carbonate materials with high U concentrations, very low Pb concentrations, and sufficient range in U/Pb ratios. More recently, preliminary U-Th-Pb ages have been obtained for Quaternary sedimentary carbonates from Olduvai Gorge that are associated with hominid remains (Cole et al. 2001), speleothems with extremely high U concentrations (> 300 ppm) from Spannagel Cave, Austria (Cliff and Spötl 2001) and corals of middle Pleistocene age from Costa Rica (Getty et al. 2001). The most extensive U-Th-Pb dating study on deposits of Quaternary age is that conducted by Neymark et al. (2000) on sub-millimeter-thick opal (30 to 313 ppm U) that coats fractures and cavities in Tertiary Tuffs at Yucca Mountain Nevada.

Criteria for successful U-Th-Pb dating are similar to those of standard U-series techniques, but in addition (1) sufficient amounts of ^{206}Pb and ^{207}Pb must have accumulated by radiogenic ingrowth to be distinguished from the initial Pb that is always present at the time of formation and (2) the decay scheme must be closed for all intermediate daughters from ^{230}Th and ^{231}Pa to stable ^{206}Pb and ^{207}Pb, respectively.

Isochrons can be used for coeval samples with a range of U-Pb ratios to determine the age and initial Pb ratio in a similar manner to that used in standard U-Th techniques where initial Th is significant. Ideally, sub-samples of pristine calcite from the same growth layer and exhibiting a considerable range of U/Pb ratios can be used to define isochrons in either ^{206}Pb/^{204}Pb-^{238}U/^{204}Pb or ^{207}Pb/^{204}Pb-^{235}U/^{204}Pb space. The gradient of the isochrons will define ^{206}Pb*/^{238}U and ^{207}Pb*/^{235}U, where ^{206}Pb* and ^{207}Pb* are the radiogenic Pb components. Alternatively, three-dimensional isotope plots, which contain complete information about concordance between the two decay schemes and common Pb (Wendt 1984) can be used. We suggest the use of the variant developed by Wendt and Carl (1985) from Tera and Wasserburg (1972), as implemented in ISOPLOT 2.92 (Ludwig 1994, 1999).

For most geochronological applications of U-Pb methodology, departures from initial secular equilibrium of the U-series decay chain at time of precipitation are generally considered to be insignificant relative to subsequent radiogenic ingrowth. For young samples, however, this becomes a significant consideration (Ludwig 1977; Wendt and Carl 1985) (Figs. 10, 11). It should be noted that with increasing precision of U and Pb measurements even mineral ages as great as 380 Ma can be significantly affected by initial ^{230}Th excess (Amelin and Zaitsev 2002). While this can present a problem to the geochronologist, Oberli et al. (1996) recognize that initial disequilibria can be used to provide detailed information about the nature of chemical fractionation processes involved at the time of formation and perhaps the subsequent metamorphic history.

We have considered initial uranium-series conditions in Section 2.2 above in relation to standard U-Th-Pa techniques. Intermediate daughters such as ^{230}Th, ^{231}Pa are insoluble and strongly adsorbed on suspended sediments such that their incorporation in calcite is generally negligible ($^{230}\mathrm{Th}_0 = {}^{231}\mathrm{Pa}_0 = {}^{227}\mathrm{Ac}_0 = 0$). In nearly all cases, ^{234}U is precipitated in excess of that expected for secular equilibrium with ^{238}U. This must be taken into account by using an independent estimate of δ^{234}U(0). The effects of ^{234}U/^{238}U disequilibrium on calculated age can be seen in Figures 10 and 11, which illustrates the situation for a range of δ^{234}U(0) typical of calcite deposited from freshwater. For a given ^{238}U/^{206}Pb and ^{207}Pb/^{206}Pb the corresponding concordant age can vary significantly depending on initial conditions. It is likely that there will be some ^{226}Ra initially coprecipitated with U because excesses of ^{226}Ra over its parent ^{230}Th have been reported for soils (Dickson and Wheller 1992; Olley et al. 1997), however, the effect of any initial abundance is minor because of the short half-life of 1600 years and is likely to be irrelevant for the applicable age range of this technique.

In addition to the assumptions of initial conditions, the validity of U-Pb methodology relies on closed system behavior of U, Pb and intermediate nuclides in the decay chain. Concordance between the two U-series decay chains is most likely to be compromised by Rn loss because Rn is the only gas in the decay chains and has a high diffusivity. Radon-222 in the ^{238}U decay chain has a half life of 3.8 days. This is much longer than the half-life of ^{219}Rn (3.96 s) in the ^{235}U decay chain. Therefore, partial loss of Rn will give rise to an apparent ^{206}Pb*/^{238}U age younger than the true age, whereas the ^{207}Pb*/^{235}U will remain unaffected. There is evidence that Rn loss is negligible from speleothems composed of dense calcite with columnar crystal fabric (Lyons et al. 1989). Richards et al. (1998) investigated the possibility of Rn loss in a stalactite from the Peak District by measuring the activity of ^{230}Th and ^{210}Po, which are either side of ^{222}Rn in the ^{238}U decay chain and expected to be in secular equilibrium for material much greater than 20 ka. The measured (^{210}Po/^{230}Th) activity ratio was 0.942 ± 0.064, which is within error of unity. They obtained a ^{206}Pb*/^{238}U age indistinguishable from a ^{230}Th/^{238}U age for this stalactite using three-dimensional isochron methodology (Ludwig 2003), indicating that U-Th-Pb dating of Quaternary age samples is possible (Figs. 12, 13). Not all calcite is suitable for U-Th-Pb dating, however, because in many cases too much initial Pb is coprecipitated. Ideal material has very high U and low Pb, so that radiogenic Pb can be distinguished from initial Pb. A survey of selected pristine calcite from various locations of the globe

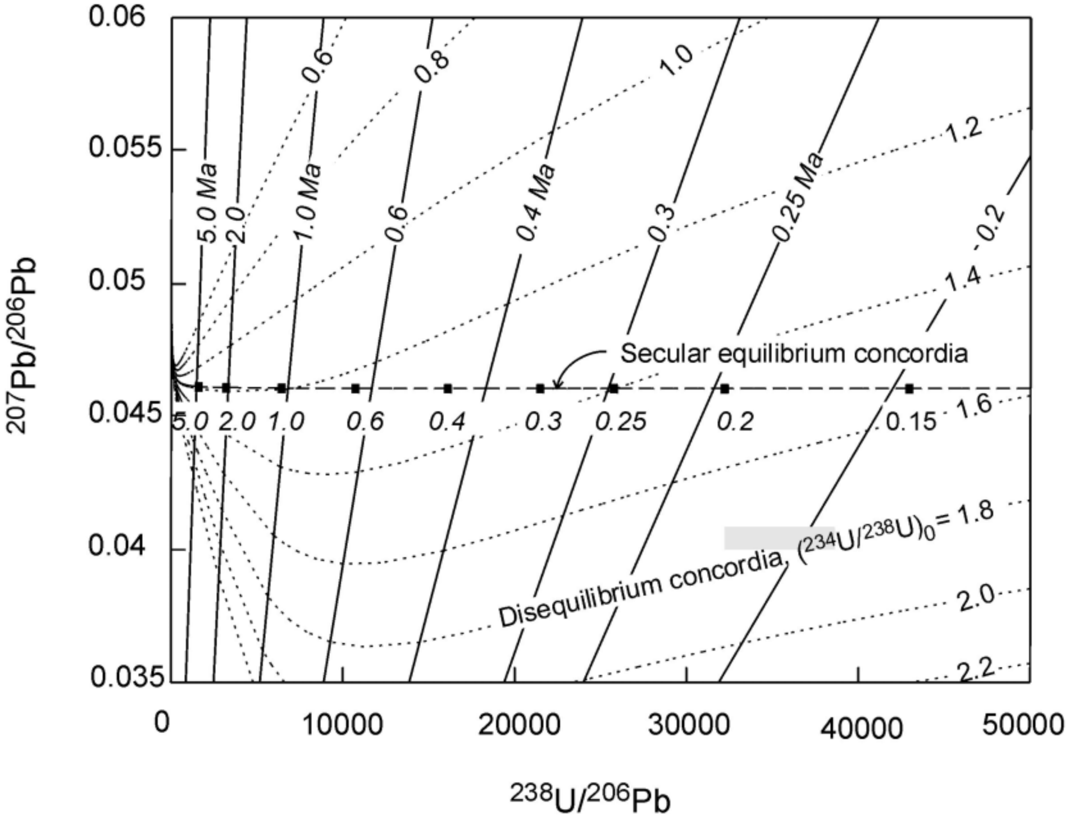

Figure 10. Modified Tera-Wasserburg (^{207}Pb/^{206}Pb-^{238}U/^{206}Pb) plot with disequilibrium concordia (after Wendt and Carl 1985). The curvilinear trajectories (dotted lines), or concordia, show the change in ^{238}U/^{206}Pb and ^{207}Pb/^{206}Pb as age increases for different values of δ^{234}U(0) and ^{231}Pa$_0$ = ^{230}Th$_0$ = ^{226}Ra$_0$ = 0. The near vertical lines (solid) are isochrons. Ages reported in Ma. The secular equilibrium case, where the activity ratios of all parent-daughter pairs in the U-series decay chains are unity is shown by a dashed line. Ages (in Ma) are represented by squares.

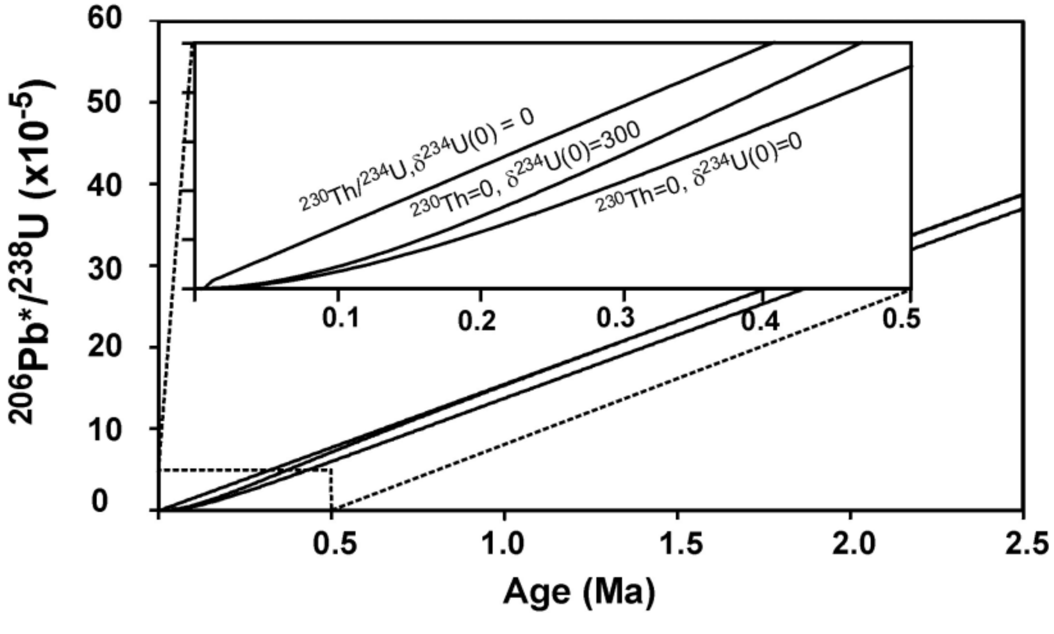

Figure 11. Evolution curves of age vs. ^{206}Pb*/^{238}U for material in secular equilibrium or disequilibrium.

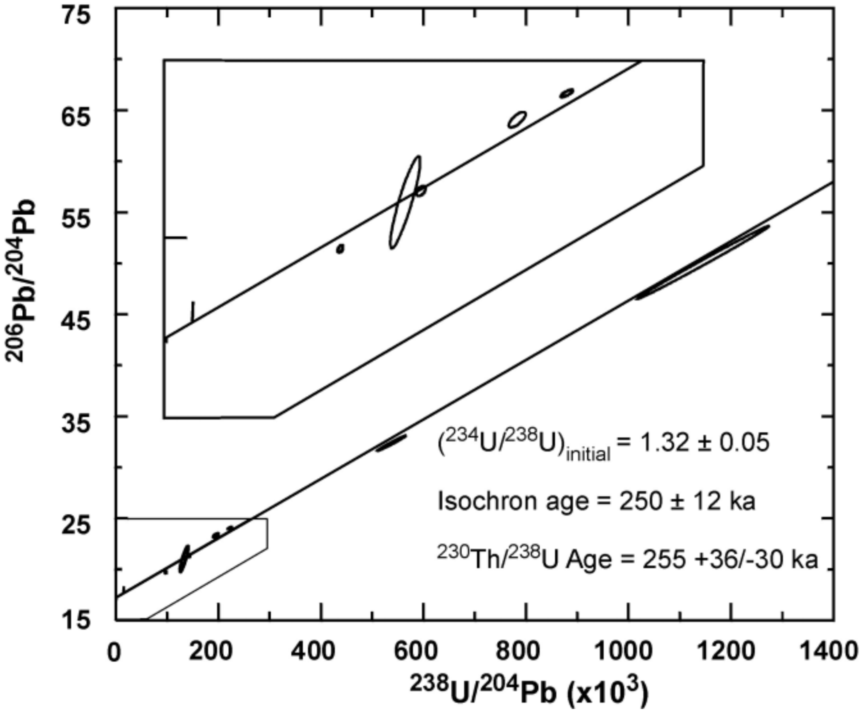

Figure 12. Uranium-lead ($^{238}U/^{204}Pb$-$^{206}Pb/^{204}Pb$) isochron plot for the WHC1 stalactite from Peak District, England (Richards et al. 1998).

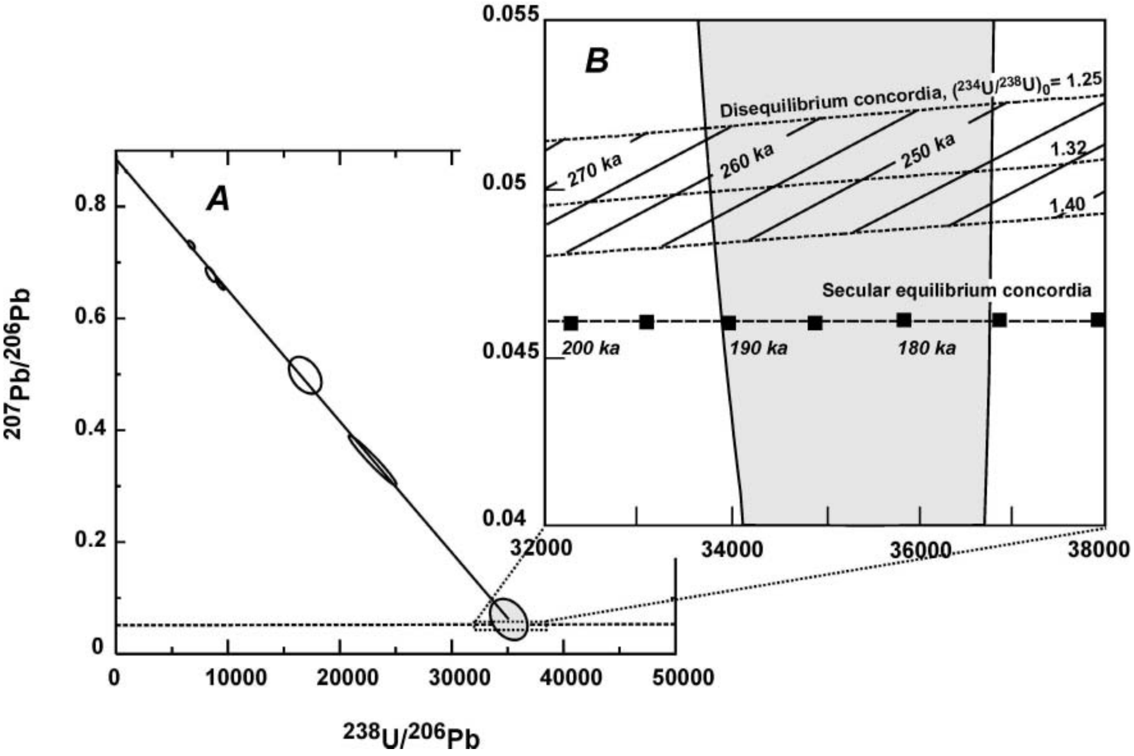

Figure 13. Tera-Wasserburg style three-dimensional concordia plot for the WHC1 stalactite (Richards et al. 1988). Shown is the projection onto the $^{238}U/^{206}Pb$- $^{207}Pb/^{206}Pb$ plane (see Fig. 10 caption). The intercept of the three-dimensional fit with this plane is shown by the shaded error ellipse. A) Three-dimensional regression, disequilibrium concordia ($\delta^{234}U(0)$ = 320; dashed line], and plane intercept. B) Detail of intercept with $^{238}U/^{206}Pb$-$^{207}Pb/^{206}Pb$ plane, disequilibrium concordia (2σ error), regression line, and the secular equilibrium concordia.

using standard ICPMS coupled with data from the literature reveals an extremely large range in U/Pb ratios of eight orders of magnitude (Fig. 14). Clearly, pre-screening for elemental abundance is recommended prior to isotopic analysis.

3. SPELEOTHEM GEOCHRONOLOGY IN PRACTICE

The morphology, crystallography, mineralogy, purity and growth rates of speleothems vary tremendously in relation to their location and the chemistry of waters feeding them. The potential suitability of speleothems is dependent on the intended application. Paleoclimate records, for example, are best derived from samples from the deep-interior of caves that exhibit continuous growth of dense calcite with a simple internal morphology (flowstones and stalagmites), whereas speleothem intercalated with hominid remains are likely to be found near cave entrances and rock shelters. A review of potential applications can be found below in Section 4. Here, we present field sampling strategies, sub-sampling methodology, and post-analytical treatment of ages. Analytical procedures for chemical separation of uranium-series nuclides and instrumental procedures for obtaining high-precision estimates of isotopic abundance are discussed by Goldstein and Stirling (2003). Statistical treatment of isotopic data is also dealt with in Ludwig (2003).

3.1. Speleothem sampling strategy

At the outset here, we reiterate that collection of material from caves is a highly sensitive issue and at all times researchers must be aware of conservation issues regarding cave deposits. To quote from the National Speleological Society (USA) Code of Conduct, scientific collection should be "professional, selective, and minimal."

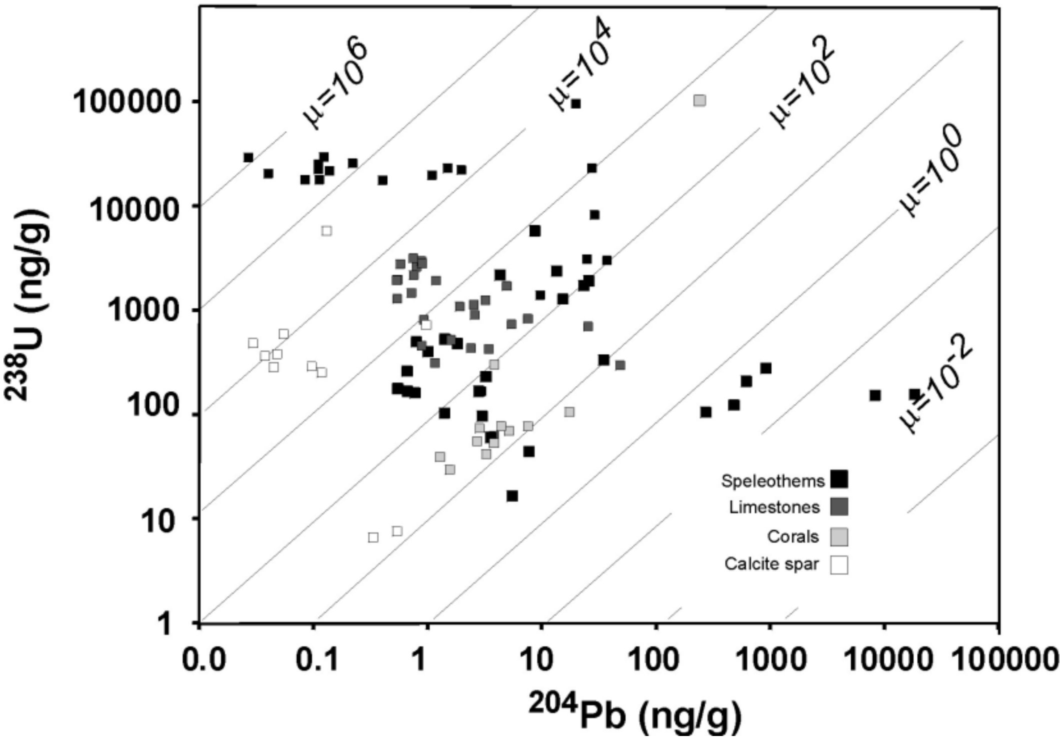

Figure 14. Comparison of U, Pb concentrations in speleothems from the Bristol archive with published data of limestones, corals and calcite spar (Smith et al. 1991; Jones et al. 1995). Eight orders of magnitude variation in ^{238}U/^{204}Pb ratio is observed.

***A priori* considerations.** An extensive review of the form and mineralogy of the secondary cave deposits is provided by Hill and Forti (1997), but also see Ford and Williams (1989). By far the most useful speleothems for geological purposes are the most common forms; stalactites, stalagmites and flowstones composed of calcite, and occasionally aragonite. Other deposits that have been used to derive useful information include travertines, gypsum crusts, calcite veins and scalenohedral calcite (dog-tooth spar).

In a discussion of the suitability of speleothems for dating purposes, Gascoyne and Schwarcz (1982) describe the various types of speleothem that form in the different "zones" of a cave from the entrance to the deep interior. The entrance (or "twilight") zone contains sporadic, fast-growing speleothems that are the often the result of evaporative processes. Alteration by microbial action in biofilms (Jones 1995) is often displayed within this zone, and samples have high, detrital and organic content. Here, speleothems often display a degree of porosity and are contaminated with detritus. Samples from the deep-interior, where humidity levels are at their highest and air circulation is non-existent, are the slowest growing, and are generally composed of the dense calcite and free from detritus, unless the site is subject to periodic flooding. To these subaerial zones could be added the subaqueous zones where phreatic calcite is formed under low temperature conditions or associated with hydrothermal fluids (e.g., Devils Hole vein calcite).

The suitability of speleothems for analysis is determined by their mineralogy and fabric. Material displaying unaltered or primary fabric are required if chronological or paleoenvironmental information is sought. Such mineral fabrics include coarse columnar (or palisade) calcite, equant calcite, microcrystalline calcite, botryoidal clusters of elongate (acicular or fibrous) aragonite crystals. Kendall and Broughton (1978) present an overview of the common calcite fabrics (see also González et al. 1992; Frisia et al. 2000). We suggest routine observation of thin sections because they can reveal the extent of porosity, primary fabric, contaminants, and diagenetic history (Railsback 2000).

Sub-sampling of calcite for dating purposes. Sub-sampling for chronological purposes is not a trivial matter. The primary consideration is quality of material, but also important is the requisite mass and dimensions of sub-samples, which is based on a priori consideration of desired precision. Ideally, the spatial resolution of sampling is based on a compromise between the growth period represented by the sub-sample and the achievable precision. For U-Th ages this is a function of U concentration, δ234U(0), sample age, chemical yield and the ionization/transmission efficiency of the adopted instrumental procedure. The most efficient strategy here is to measure the U concentration of selected sub-samples prior to isotopic analysis. While U concentration can vary dramatically between samples (Fig. 14), there is much less variation along the growth axis of individual samples. It is only after subsequent dating that growth rate can be determined, at which point adjustment of the growth distance represented for further sub-samples can be made. Improvements in ionization and transmission efficiency afforded by plasma source technology (Goldstein and Stirling 2003) have served to further reduce sample sizes, enabling dating of thin cement overgrowths and slow-growing speleothems. Also, Stirling et al. (2000) have demonstrated the feasibility of analyzing speleothems with greater than 100 ppm U by direct *in situ* laser ablation with a spatial resolution of 10-50 μm.

Sub-samples of calcite of between 0.01 and 1 g are usually adequate for most dating applications using mass-spectrometry. Powders can be obtained using micro-drills or wafers can be cut from a slab using a diamond wire saw (0.17-0.3 mm kerf). Milling is generally less destructive to the formation and specific growth layers can be precisely traced. The advantage of sawing is that there is less chance for contamination, and sub-samples can be ultrasonicated to remove cutting debris and detrital material. Growth layers can be followed by adjusting the cutting axis using a micrometer or goniometer stage.

Many samples exhibit growth layers. These may be a result of linear arrays of fluid inclusions, changes in crystal fabric, entrapment of surface contamination such as clays, or changing organic/mineral content of solutions feeding the sample. In many cases, these can provide a useful guide to sub-sampling because they define the past record of growth morphology. We note here that growth layers have been observed at annual intervals or less for some samples using visual (Railsbeck et al. 1994), elemental (e.g., Roberts et al. 1998, 1999; Huang et al. 2000; Baldini et al. 2002) or fluorescence (e.g., Baker et al. 1993, Shopov et al. 1994, Polyak and Asmerom 2001). This could prove to be extremely valuable in terms of correlation with coral, tree-ring and ice core records; however, Betancourt et al. (2002) cautions that the manifestation of a consistent long-term annual signal is likely to be rare because of variability in groundwater residence times and seasonal pattern of soil moisture conditions.

The number of sub-samples that must be obtained for individual speleothems depends on the specific application. When ages are to be used to constrain the periods of continuous growth or hiatuses, sub-samples from the base and outer surface may suffice. For applications based on high-resolution records of environmental change, a suite of ages must be obtained to estimate the distance-age relationship along the axis of growth.

3.2. Treatment of U-series ages

Speleothems offer considerable potential for obtaining high-resolution records of paleoenvironmental change; in fact sub-annual resolution can now be achieved for various proxy indicators. It is therefore important that robust chronologies are also obtained. In many cases speleothem chronologies rely on interpolated estimates of ages for calcite deposited between sub-sample locations. The strategy adopted to obtain a high-resolution chronology for continuous growth periods is often an iterative procedure that considers the variability in growth rate, achievable precision, amount of material sampled and the age derived. Where sample growth is extremely slow, such as opals, models need to be constructed based on integral equations of continuous deposition because standard ages often over-estimate the true age (Neymark and Paces 2000).

A survey of the most recent studies that use multiple uranium-series ages for individual speleothems reveals a range of practices in dealing with interpolation and extrapolation of derived ages. Linear regression, stepwise linear fits, polynomial fits and non-parametric smoothing splines are used to define the most likely age vs. distance relationship for continuous phases of growth. There are advantages with each of these approaches but weighted non-parametric smoothing splines are, perhaps, the most “natural” and “automatic” of curve fitting routines. Non-parametric smoothing methodology consists of techniques that make few assumptions about the form of an underlying function that needs to be estimated. Essentially, these techniques allow the dataset to "speak for itself" in determining the final estimate which is constructed by weighted local averaging, the extent of which is controlled by a smoothing parameter. Unfortunately, interpolation is not trivial because of the non-parametric nature of the function, and we recognize that low-order polynomial fits produce simple-to-use, or readily transferable, formulae for interpolating between dated sub-sample locations. Also, non-parametric smoothing techniques are computationally intensive, but standard statistics software such as S-PLUS® (Venables and Ripley 1999) can be easily used to derive of the age-distance relationship.

Demand for high-resolution records of environmental change from speleothems has led to a dramatic increase in the number of sub-samples required from individual samples to define the distance-age relationships along the axis of growth. Twenty years ago, the age determination of top and bottom sub-samples was generally considered adequate to constrain the growth period. In more recent times, however, many more sub-samples are utilized: Dorale et al. (1998) reported 38 ages (74.0 to 21.4 ka) for sub-samples from 4 stalagmites from Crevice Cave, Missouri, one of which is supplemented by an additional 13 ages in Dorale et al. (2003); Wang et al. (2001) determined ages for 59 sub-samples from 5 samples from Hulu Cave, China (74.9 to 10.9 ka); Zhao et al. (2001) determined 17 sub-sample ages along the axis of a speleothem from Newdegate Cave, Tasmania (154.5 to 100.3 ka); Musgrove et al. (2001) produced ages for a total of 45 sub-samples from 4 samples from central Texas (7.6 to 71 ka); Beck et al. (2001) reported 81 ages (44 to 11 ka) from the growth axis of a single submerged speleothem sample from Grand Bahama. In most of the above examples, the age-distance relationship is represented by a piecewise linear fit. While this is convenient for interpolation purposes, growth rates cannot be adequately represented because of the stepwise nature of the resultant function. For this reason, we advocate the use of curvilinear fits, in particular smoothing splines. Researchers should be aware of the implicit assumptions that are adopted in the various approaches used for interpolation, or more strictly approximation, and extrapolation. Particular caution must be adopted if interpolated results are to be examined in the frequency domain, as is often the case in palaeoclimate research.

4. SPELEOTHEM CHRONOLOGY AND ENVIRONMENTAL CHANGE

There is a critical need to assess natural environmental change at increasingly higher temporal and spatial resolution to elucidate the pattern of response to internal and external forcings and feedbacks in the Earth's system. Speleothems and other secondary carbonate deposits are one of a host of different archives that can be used to provide such information for the past 0.5 Ma, a time period of dramatic and often abrupt change. Speleothem applications can be broadly classified into those based on (1) presence/absence or rate of speleothem growth, or (2) proxy information for environmental change derived from the isotope and chemical composition of the mineral deposits themselves. Essential to both of these classes is the determination of accurate chronologies using the methods described above. By obtaining reliable and high-precision chronologies of environmental and geophysical change for many sites across the globe using speleothems, comparison can be made with independent records from the terrestrial environment, oceans and cryosphere, so that the amplitude and spatial patterning of response to different forcing can be investigated. Below, we illustrate the wide range of possible applications focussing on the most recent literature. We deliberately avoid reviewing the fundamental controls on proxy evidence in each of the categories and concentrate on chronological aspects. For further information on the controls of paleoclimate evidence, we suggest that readers look at the upcoming review by Lauritzen (in press) (see also Gascoyne 1992).

4.1. Applications based on the presence/absence or growth rate of speleothems

Speleothem growth is obviously dependent on the continued supply of seepage water supersaturated with respect to calcite to a point location in a cave. Initiation and cessation of growth can be caused by a range of different factors such as changes in vadose water chemistry, aridity, flooding events, permafrost conditions and random shifts in flow routing. Reliable ages of the period of growth, therefore, can provide valuable spatial and temporal constraints on environmental factors. The spatial extent of the principal factor controlling presence or absence may be global (e.g., eustatic sea level change), regional (influence of advancing ice sheet during glacial periods) or local (e.g., back flooding of cave passage after sediment blockage downstream).

Palaeo-sea (and -water-table) fluctuations. Edwards et al. (2003) describe methods used to obtain valuable information about past sea level elevations and tectonics using U-series ages of well-preserved shallow marine carbonates from uplifted coral reef terraces (e.g., Barbados, Papua New Guinea and Vanuatu) and submerged coral sequences (e.g., Barbados and Tahiti). Most of the information derived from corals is related to either periods of sea level stasis or rise. Well-preserved speleothems found below present sea level can be used as complimentary evidence about the timing and elevation of *low* sea levels in the past because they could only have formed when cave passages were air-filled.

Alpha-spectrometric U-series ages determined for submerged speleothems from the stable platforms of Bermuda (Harmon et al. 1978, 1981, 1983) and Bahamas (Spalding and Mathews 1972; Gascoyne et al. 1979, Gascoyne 1984) provided valuable constraints for the timing of sea level fluctuations above –20 m during glacial and interglacial periods of the past 200 ka. Age uncertainties, however, were typically >5 %. The advent of mass-spectrometric techniques enabled much higher precision chronologies using slower growing samples, such as flowstones. Li et al. (1989) and Lundberg and Ford (1994), for example, presented high-precision ages for a flowstone sequence from −15 m in a cave on Grand Bahama that exhibited interruptions in deposition from 235-230 ka, 220-212 ka, 133-110 ka, 100-97 ka and <30 ka. These hiatuses in growth were caused by submergence during interglacial high sea stands during oxygen isotope stages 7, 5 and 1. Richards et al. (1994) and Smart et al. (1998) present results from a comprehensive suite of samples to depths of −60 m in numerous "blue holes" of the Bahamas that constrain the maximum elevation of sea-level fluctuations during the last and penultimate glacial periods. Continuous growth is observed from 70 to 16 ka at an elevation of −20 m, indicating that maximum sea level during all of isotope stage 3 parts of stages 2 and 4 were no higher than −20 m. Periods of submergence are represented by breaks in deposition and crystal terminations, followed by re-nucleation of calcite growth after sea level regression leaves cave passages air filled. In most cases, material is extremely well-preserved, showing no evidence of dissolution despite submergence for up to 50 ka (Fig. 15A,B). In some cases, however, outer surface may be truncated by dissolution in the aggressive waters of the mixing zone (Fig. 15C,D). Here, top ages for phases of growth may be represent maximum age constraints. Researchers must also be aware that initiation of growth after a hiatus may not be immediate because of paleoclimate control (e.g., regional aridity) or random shifts in flow routes.

Generally, submerged speleothems from inland caves provide the most suitable material for dating purposes because they are less susceptible to mechanical and chemical bioerosion by epilithic and endolithic organisms. Gascoyne et al. (1979) successfully obtained ages of poorly preserved samples by separating primary and altered components of carbonate. Borings and encrustation by marine organisms can, however, provide unambiguous evidence for submergence by rising sea levels. Antonioli and Oliverio (1996) obtained AMS ^{14}C ages for well-preserved fossil shells of the boring mussel *Lithophaga lithophaga* from within a submerged stalagmite from −48 m in a cave off the west coast of Italy. The oldest age obtained for one of the marine colonists was 9.6 ^{14}C kyr BP (or 10.3 ka) and is used to constrain the rate of sea level rise during the last deglaciation by comparison with the sea level curve derived from submerged corals in Barbados (Fairbanks 1989; Bard et al. 1990). Earliest colonization by serpulid worm communities on submerged speleothems from the Tyrrhenian coast of Italy has also been dated by radiocarbon techniques to constrain a regional sea level curve for the Mediterranean region (Antonioli et al. 2001). Recently, Bard et al. (2002a) reported high-precision TIMS ^{230}Th ages for calcite from the core of an encrusted stalagmite from the same coastline. Two continuous growth phases of dense calcite are exhibited with biogenic crust overgrowths formed during high sea-stands. This submerged sample from −18.5 m constrains the timing of the high sea-stand associated with marine isotope stage (MIS) 7.1 (Martinson et al. 1987) to between 201.6 ± 1.8 and 189.7 ± 1.5 ka, which

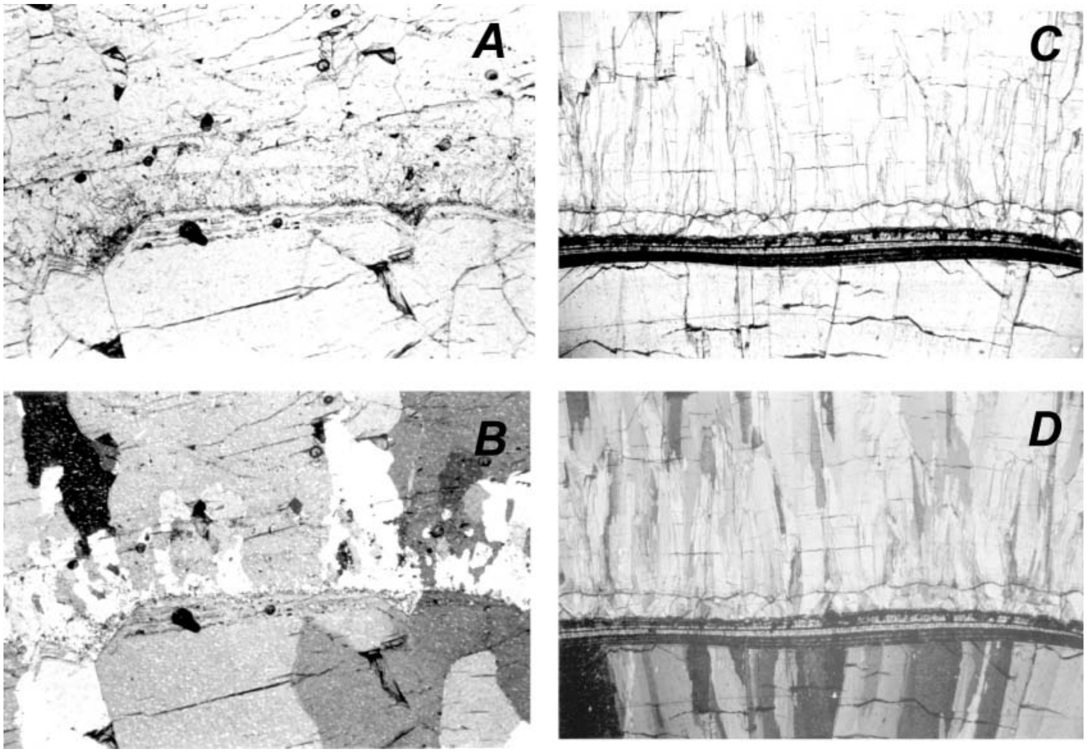

Figure 15. Thin section photomicrographs of hiatuses in Bahamas flowstone and stalagmite sequence from Sagittarius blue hole, Grand Bahama. A,B) GB-89-25-5A (plane and cross-polarized light, respectively; field of view = 2.6 mm). Hiatus represents stage 5 high sea level during which sample was submerged for at least 50 ka. Note well-preserved steep-sided crystal terminations. C,D) GB-89-27-1 (plane and cross-polarized light respectively; field of view = 2.6 mm). Hiatus in growth represents stage 9 high sea levels. Iron-rich red/orange flocculate is observed at hiatus (lepidocrosite and hematite) and crystal termination of lower phase of calcite growth is truncated.

agrees with an estimate of 190 ± 5 ka for sea level fall after stage 7 derived from a flowstone sequence from the Bahamas (Richards et al. 1992) and the youngest ages (200.1 ± 1.2 ka; 200.8 ± 1.0 ka) for the penultimate interglacial (MIS 7) coral reef terrace in Barbados (Gallup et al. 1994). Robinson et al. (2002) report ages as young as 178.4 ka for well-preserved aragonitic material from Bahamas slope sediments considered to be of MIS stage 7 age based on δ^{18}O data and cite confirmatory evidence of speleothem ages from Oman for an interglacial period from 210 to 180 ka (Burns et al. 2001).

Clearly, U-series ages of speleothems can provide valuable constraints for the timing of past sea levels and can be used in conjunction with marine evidence to test the hypothesis that glacial-interglacial fluctuations are related to solar forcing, but there remain some discrepancies and much attention is currently focused on the timing of the penultimate deglaciation, or Termination II. It was the long-held belief that increases in summer insolation in the high latitude regions of the Northern hemisphere were the major cause of the onset of deglaciation and oxygen-isotope records were tuned to changes in northern hemisphere insolation in the frequency domain. The predicted age of the mid-point of penultimate deglaciation (~128 ka) on the basis of such theory is significantly younger than suggested by uranium-series ages on speleothems and marine aragonite deposits. Bard et al. (2002a) report latest growth in a continuous phase of speleothem growth from the submerged Argentarola Cave prior to the penultimate deglaciation of 145.2 ± 1.1 ka, which constrains the maximum age of Termination II, while compilation of minimum ages for latest speleothem growth during the penultimate glaciation in the

Bahamas suggest a younger maximum constraint of >130 ka (Gascoyne et al. 1979; Richards et al. 1994; Lundberg and Ford 1994; Lundberg 1997). Ages for Termination II as recorded in the δ^{18}O record of Devils Hole calcite vein from continental USA predated estimates from Milankovitch theory by some 6 ka at 140 ± 3 ka (Winograd et al. 1992; Ludwig et al. 1992). An earlier termination has also been indicated by marine evidence: Henderson et al. (2000) dated aragonite deposits from the slopes of the Bahama Banks and obtained a well-constrained ^{230}Th age of 135 ± 2.5 ka for Termination II; Gallup et al. (2002) reported ^{230}Th and ^{231}Pa ages of 135.8 ± 0.8 ka for coral samples that were 18 ± 3 m below sea level at time of formation; Esat et al. (1999) obtained ages of corals the Huon Peninsula that suggest sea levels was at least as high as 14 m below present at 135 ka.

Most studies using speleothems to constrain past sea-levels rely on U-series ages of calcite that was deposited at times of low sea level. Vesica et al. (2000) and Fornós et al. (2002), however, present mass-spectrometric ^{230}Th ages for phreatic calcite overgrowths that form on previously vadose speleothems in Mallorca that were submerged by brackish water during high sea stands. Phreatic overgrowths have been documented for each of the high stands associated with MIS 9 or older, 7, 5e, 5c and 5a and conform broadly to the expected time ranges suggested by the Milankovitch theory. With increased precision afforded by the latest techniques, it is envisaged that such material will be re-analyzed to improve upon precisions and investigate phase relationships between Milankovtch forcing and sea level at these much earlier times. One of the key issues is whether or not phase relationships between insolation and sea level and duration of high sea stands are consistent throughout the Quaternary period (Winograd et al. 1997)

Not only does flooding by rising sea levels cause cessation of calcite growth, but also flooding by regional water table fluctuations in areas distant from the sea. Auler and Smart (2001) obtained ^{230}Th ages for water table and subaqueous speleothems formed during last glacial maximum and MIS 6 in Toca de Boa Vista, northeastern Brazil, 13 m above the present water table, indicating that climate was wetter than present during these glacial periods, in marked contrast to other records from lowland Brazil sites and general circulation model results. Regional fluctuations in paleoclimate are also inferred from water table fluctuations documented in Browns Room, an air-filled chamber that is part of the Devils Hole fissure system, Nevada (Szabo et al. 1994). Uranium-series ages of calcite with morphological and petrographical features that can be related to former water levels provide reliable evidence for the timing of former high water tables 5 m above present from 116 to 53 ka, and fluctuations between 5 and 9 m between 44 and 20 ka. This data is in broad agreement with effective moisture records from lacustrine, soil and travertine deposits of the Great Basin, USA.

Paleoclimate. One of the disadvantages of speleothems as paleosea-level indicators is the fact that growth may cease for reasons other than submergence by rising sea levels. For example, Richards et al. (1994) suggest that regional aridity in the Bahamas may have been associated with the onset of deglaciation and in North America, thus halting supply of dripwater to the caves up to 5 ka prior to submergence in some cases. In many studies, however, the recognition that changing environmental conditions control speleothem growth frequency, periods and rates has provided valuable regional paleoclimate information that can be compared with independent evidence such as lake level, paleovegetation, marine and ice core evidence.

Growth frequency. In high latitude regions of the globe, periodic advance of glaciers dramatically affected karst regions; dripwater flow routes to the cave became permanently frozen, rate of production of soil CO_2 was reduced and, in some cases, soil would have been stripped from the surface by ice masses. Harmon et al. (1977) recognized four distinct periods of deposition in the Rocky Mountains of North America based on alpha-spectrometric ages of many U-series ages of speleothems that could be related to periods of low continental ice volume. Since this early work, many regional compilations of alpha-spectrometric ^{230}Th ages have been produced with a view to discerning changing environmental conditions, among them, Gascoyne et al. (1983)—northern England; Hennig et al. (1983)—Europe; Lively (1983)—Minnesota, USA; Gordon et al. (1989)—United Kingdom; Baker et al. (1993)—northwest Europe; Lauritzen (1991, 1993)—Norway; Onac and Lauritzen (1996)—Romania; Hercman (2000)—central Europe; Lauritzen and Mylroie (2000)—New York, USA; Ayliffe and Veeh (1988), Ayliffe et al. (1997)—Naracoote, Australia. The most suitable method for graphical representation of speleothem growth frequency is by probability density functions of age frequency, where each age determination represented by a normal distribution and normalized to equal area (Gordon and Smart 1984) (see Fig. 16). Smooth density functions constructed for compilations of alpha-spectrometric ^{230}Th ages can be compared with other proxy records of climate change. Kashiwaya et al. (1991) analyzed the speleothem frequency curve of Gordon et al. (1989), which is based on several hundred British speleothems, to demonstrate that temporal change in frequency was related to Milankovitch parameters. While speleothem growth generally ceased in high latitudes during glacial conditions, growth in temperate mid-latitude regions continued but at a reduced frequency under conditions of changing vegetation, soil CO_2 levels and soil moisture availability and temperature.

Speleothem frequency distributions have provided a useful tool for broad comparisons, but they suffer from the problem of biased sampling strategies and low resolution at times of known abrupt change. The increased precision afforded by mass-spectrometric techniques will result in fewer studies using this approach to assess of growth frequency and, more often, records of continuous deposition and growth rate studies will be graphically illustrated.

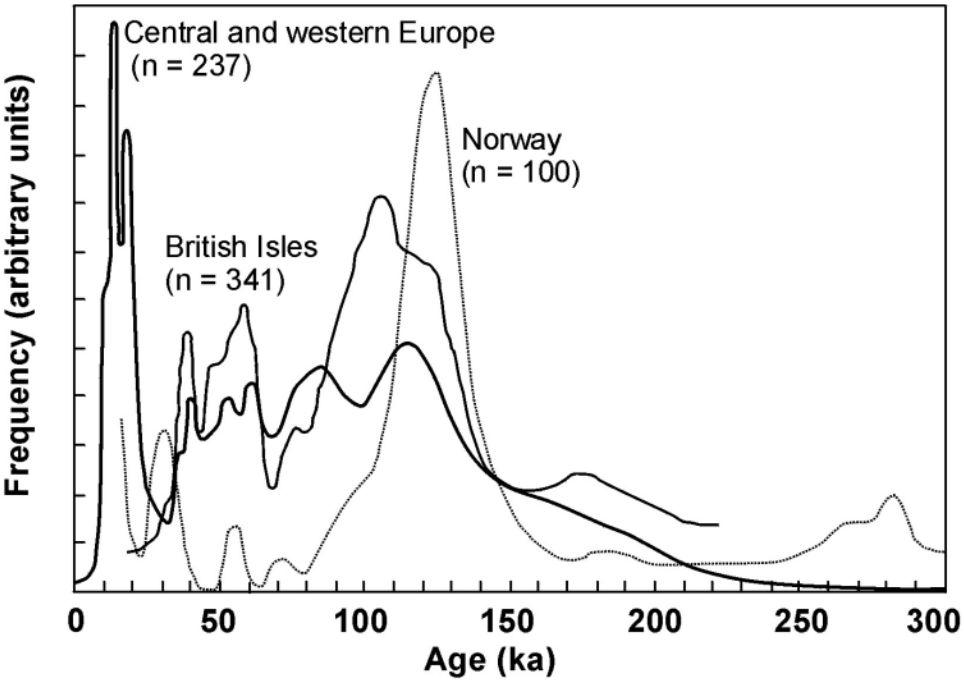

Figure 16. Probability density function of compilations of alpha-spectrometric U-series ages for central and western Europe (Hercmann 2000), British Isles (Gordon et al. 1989) and Norway (Lauritzen 1991, 1993) (redrawn from Hercmann 2000).

Growth periods. Growth phases in individual speleothems, or more ideally suites of speleothems from individual caves, can be used to constrain periods of time when regional environmental conditions were conducive for calcite growth. Mass-spectrometric ages of sub-sample wafers or powders representing < 1 mm growth from close to the base and outer surface of continuous phases of growth in stalagmites, flowstones and stalactites precisely define the growth periods.

Baker et al. (1996) compare the pattern of growth in two flowstone sequences from Yorkshire, England. Six growth periods of both short duration (1 to 3 ka) and fast growth rate are separated by non-depositional hiatuses in a sequence from Lancaster Hole. The ages of these phases were determined to be 128.8 ± 2.7, 103.1 ± 1.8, 84.7 ± 1.2, 57.9 ± 1.5, 49.6 ± 1.3, and 36.9 ± 0.8 ka by mass-spectrometric techniques. There is a remarkably good correlation between the periods of active speleothem growth and the timing of Northern hemisphere solar insolation maxima, which they consider to be related to recharge rates or volume. This sample, they suggest, only grew at times when precipitation was sufficiently high to overcome a threshold and supply dripwater to this location. A flowstone sequence from a nearby cave, Stump Cross Caverns, also exhibits numerous phases of growth. In common with the Lancaster Hole sequence, no growth was found at times of glaciation but there appear to be an additional control on calcite growth because no growth is exhibited during MIS 5. The authors suggest that although conditions were warm and moist enough for flowstone growth as evidenced by hippopotamus faunal remains in hiatus material (Gascoyne et al. 1981) and calcite deposition elsewhere in the cave (Sutcliffe et al. 1985), the location of this flowstone sequence must have been flooded for a long duration. Clearly, this is a site-specific effect and researchers must be careful not to infer regional paleoclimate information on the basis of individual samples.

High-precision TIMS ^{230}Th ages of a flowstone samples from Spannagel Cave, Zillertal Alps (Austria) at 2500 m above sea level demonstrates that this site is highly sensitive to climate changes because growth is restricted to interglacial periods between 207 to 180 ka and 135 to 116 ka (Spötl et al. 2002). The estimated age of initiation of calcite growth after the termination of the penultimate glacial is 135 ± 1.8 ka, which is in remarkable agreement with estimates from the marine realm (Esat et al. 1999; Henderson and Slowey 2000; Gallup et al. 2002) discussed above in Section 4.1.

In contrast to regions in high latitudes, carbonate cave deposits in desert locations might be expected to exhibit growth during the cooler periods of the late Pleistocene. Vaks et al. (2001), for example, determined 41 ^{230}Th ages for material from 13 samples from a cave located at the current desert boundary in Israel. Hiatuses in growth between 160 and 80 ka and the Holocene are ascribed to increased evaporation/precipitation ratio from either higher temperatures or reduced rainfall during interglacial periods. Abundant samples are also observed in tropical regions at times of intensified monsoon activity. Burns et al. (1988, 2001) report fifty-one ^{230}Th ages of speleothems from Hoti Cave, Oman, that are restricted to the intervals 325-300 ka, 210-180 ka, 130-117 ka and 82-78 ka (one sample records three short separate growth periods during MIS 9, 7a and 5e, separated by long intervening periods of non-deposition marked by detrital material). Each growth period corresponds to a continental pluvial period coincident with peak interglacial conditions.

Growth rates. Where many age determinations have been made along the growth axis of individual samples, accumulation rates of calcite can be calculated and related to changing conditions in the vadose zone above the location of drip source. Theoretical models of speleothem growth have been developed based on chemical kinetics of calcite precipitation (Dreybrodt 1980; Buhmann and Dreybrodt 1985a 1985b, Dreybrodt 1997), but the inter-relationships between the various factors are complex. Calcite precipitation rates are dependent on calcium concentration, temperature and drip rates, all of which are likely to change with climate and vegetation changes. Calcium concentration is related to porosity and permeability of limestone, soil $p\mathrm{CO}_2$ levels, moisture and temperature, while drip rates are related excess soil moisture and routing of water in the hydrological system. The nature of flow at the solid-solution interface is also important, with turbulent flow conditions giving rise to greater precipitation rates than stagnant or laminar flow conditions (Dreybrodt 1997). Relatively few studies have compared empirical observations of growth rates within stalagmites collected in artificial and natural "cave" settings with theoretical estimates: Baker and Smart (1995) used flowstone samples that had grown in excavated caves or mines, where it was possible to estimate the maximum time since opening of the void; A. Baker et al. (1998) used recent samples from natural and artificial settings that exhibit annual laminae. In both cases, reasonable agreement was found between empirical and theoretical estimates of mass accumulation, but complicating factors such as seasonality of water supply and variations in calcite porosity were implicated (A. Baker et al. 1998). Positive correlations have also been observed in comparisons between thickness of annual laminae and historical records of effective precipitation (Railsback et al. 1994; Genty and Quinif 1996; Brook et al. 1999) and environmental change based on archaeological records (Polyak and Asmerom 2001). However, it is recognized that the factors involved are complex and not fully determined for sites that are well-monitored and have detailed historical records of climate and vegetation change and only broad conclusions can be deduced from observed variations in growth rate using U-series ages where sub-samples are typically analyzed at intervals of 10^2 to 10^4 years.

Musgrove et al. (2001) reported calcite growth rates that varied by three orders of magnitude during the period 70 to 7 ka based on ^{230}Th ages for 4 speleothems from caves up to 130 km apart in central Texas. The correspondence of fast and slow growth rates in the four samples suggest that a common controlling mechanism is involved at the regional scale. Fastest growth rates are observed at times of rapid Laurentide ice sheet growth in North America (MIS 2 and 4).

In a detailed study of a single stalagmite from Tasmania, Australia, that grew from 155 to 100 ka, Zhao et al. (2001) show that the fastest growth rates (~61.5 mm ka^{-1}) occurred between 129.2 ± 1.6 and 122.1 ± 2.0 ka. They suggest that highest rates of growth are associated with greater moisture supply during the height of the last interglacial because of latitudinal shifts in the band of subtropical highs. In contrast to this pattern, further to the north, in the Naracoorte region of South Australia, speleothems exhibit enhanced growth during stadials rather than interglacials (Ayliffe et al. 1998). Here, effective moisture in the past must have been related to evaporation rates or air temperature.

Landscape evolution. Atkinson and Rowe (1992) review the application of uranium-series dating to investigations of regional uplift, denudation and valley downcutting. The datable range of U-Th techniques is such that rates of change can be established for the past 500,000 years and extrapolated with reasonable confidence for the past few million years. While it is envisaged that future applications of U-Th-Pb dating techniques will extend the range of possibilities (Richards et al. 1998), most studies have relied on alternative dating strategies such as palaeomagnetism, ESR and ^{40}Ar/^{39}Ar to extend the time frame of study.

Speleothems have been most usefully applied to investigations of the rate of valley downcutting, where base level changes are associated with paleo-watertable lowering and draining of cavernous voids. Uranium-series ages of the oldest material found at a particular elevation in a cave system defines the minimum age of change from phreatic to vadose conditions. By plotting the age vs. elevation of numerous speleothems samples, estimates of maximum valley incision rates can be derived. This approach has been used to deduce valley downcutting rates in Yorkshire, England (Atkinson 1978, Gascoyne et al. 1983) of 0.12 m ka^{-1}. Rowe et al. (1988) used a combination of paleomagnetic data and U-series ages of speleothem from the Peak District, England to demonstrate that mean downcutting rates were 0.055 m ka^{-1}. Farrant et al. (1995) deduce a long-term (~2 Ma.) base-level lowering rate of 0.19 ± 0.04 m ka^{-1} based on uranium series, electron spin resonance, and paleomagnetic dating of an extensive sequence of speleothems and limestone caves in Sarawak, Malaysia. Polyak et al. (1998) extend the timeframe for analysis of water table lowering in the Guadalupe Mountains of Mexico, which was originally based on U-series ages (Ford and Hill 1989), by ^{40}Ar/^{39}Ar dating fine-grained alunite that forms during cave genesis by sulfuric acid dissolution. Alunite found up to 1100 m above the present valley floor had ^{40}Ar/^{39}Ar ages of 12 Ma, implying a downcutting rate of ~0.092 m ka^{-1}.

Palaeoseismicity. Uranium-series ages constraining deformation, breakage and differential growth of stalagmites and stalactites in caves can used to provide data on the occurrence of historic and prehistoric earthquakes, and hence return periods of seismic action. Postpichl et al. (1991), for example, dated different generations of tilted and collapsed speleothems attributed to paleoearthquakes of central Italy, and Lemeille et al. (1999) dated either side of offsets in speleothems to confirm that disruption in Bätterloch and Dieboldslöchli caves, Switzerland, was associated with the 1356 AD Basel seismic event. Kagan et al. (2002) documents uranium-series ages and carbon and oxygen isotope records of phases of speleothem growth precipitated directly on severed stalagmites, collapsed pillars, ceiling blocks, and various stalactites from caves near the Dead Sea Transform Fault System. Eighteen separate seismic events are recognized, which can in some cases be correlated with archaeologically- and geologically- recorded earthquakes. In a similar way, travertines in neotectonic regions can be dated by U-series isochron methods to calculate time-averaged dilation and lateral propagation rates for individual fissures (Hancock et al. 1999).

Archaeology. Some of the most important archaeological and faunal remains have been found in caves and rock shelters and uranium-series ages of cave deposits therein have been instrumental in providing chronological control. An extensive review of the wide range of geochronological approaches that have been applied specifically to cave deposits is provided by Schwarcz and Rink (2001), while Schwarcz and Blackwell (1992) focus on U-series applications. In most cases, ^{230}Th ages have been used to constrain the age of detrital layers that have been washed, blown or carried into caves. Calcite material, such as straw stalactites that have spalled from the cave roof, associated with archaeologically valuable finds in detrital layers can be dated to obtain a maximum, or *terminus post quem* age constraint. Flowstones overlying detrital layers can provide minimum ages. Thin calcite coatings can now be dated using high-precision techniques: Frank et al. (2002), for example, determined mass-spectrometric U-series ages on sub-samples representing < 3 mm of individual calcite layers that grew on walls of artificial water-supply tunnels at Troy/Ilios. Variable quantities of detritus in the samples demanded correction for initial ^{230}Th, and first-order estimates of the actual age of deposition based on an *a priori* estimate for R_0 (Eqn. 6) of 0.75 ± 0.1 were demonstrated to be reasonable after careful evaluation of other sub-samples using isochron methodology. The ^{232}Th-free estimates of ^{230}Th/^{238}U activity ratio and δ^{234}U using the error-weighted regression slope for data in ^{230}Th/^{232}Th vs. ^{238}U/^{232}Th and ^{234}U/^{232}Th vs. ^{238}U/^{232}Th space (Section 2.2), respectively, yielded the same age (4200 ± 750 yr) as the first order estimates (~4350 ± 570 yr) for the oldest overgrowth material. In this way, Frank et (2002) demonstrate that the tunnels must have been built during the Bronze Age (Troy I-II) by Anatolian and south-eastern European cultures.

One of the prime motivators for improved precision of mass-spectrometric U-series ages (and decay constants) is extension of the dateable age range to beyond 500 ka. Numerous important archaeological finds are poorly constrained by only minimum alpha-spectrometric ages of "> 350 ka" and reappraisal of earlier estimates is ongoing for many sites. The Zhoukoudian hominid specimens, from near Beijing, China, for example, have widely been recognized as representative of *Homo erectus*, but attempts to resolve the issue of whether this species was a direct ancestor of later eastern Asian populations or a side branch of human evolution have been confounded by conflicting geochronological results. Prior to the recent study by Shen et al. (2001), ages for the youngest *H. erectus* in the sequence at Zhoukoudian ranged from a time span between 290 and 230 ka, based on ^{230}Th dating of fossils (Yuan et al. 1991), to 414 ± 14 ka based on multiple TIMS ^{230}Th ages of flowstone samples (Shen et al. 1996). Additional ages by Shen et al. (2001) confirm the older age constraint, but cannot be used to limit the age of the youngest skull to a finite range > 400 ka. Fossil remains of *H. erectus* have also been discovered at Tangshan Cave, Nanjing and are morphologically correlated with specimens from Zhoukoudian. High-precision mass-spectrometric U-series ages of flowstone samples overlying the Nanjing Man fossils range from 563 +50/−36 ka to 600 +60/−50 ka (Cheng et al. 1996, Wang et al. 1999, Zhao et al. 2001). It should be borne in mind that these ages are heavily dependent on the precision and accuracy of the decay constants used and careful calibration strategies need to be adopted. Zhao et al. (2001) rely on standardization to a secular equilibrium material (HU-1), which minimizes the fractional errors in age but relies on the fact that the standard is indeed at equilibrium.

4.2. Applications based on proxy evidence for environmental change contained within speleothems

Speleothems and similar deposits contain trace substances and isotopic information that can be used to derive information about the past state of the vadose system overlying the site of deposition. Variations in oxygen and carbon isotopes in both the solid and fluid phase, trace elements such as Mg, Sr, P, Ba, U and Fe, organic acids, pollen and fossil mites, combined with accurate and precise chronology, can be used to construct temporal records of past regional environmental, hydrological or geophysical conditions for the past 500 ka, at resolutions as high as sub-annual in some cases. Secondary calcite deposits are particularly useful because they are often well-preserved, continuous and provide direct radiometric ages. Ocean cores, on the other hand, are subject to bioturbation and can only be directly dated by uranium-series methods in rare circumstances, such as well-preserved aragonitic deposits shed from carbonate platforms (Henderson.and Slowey 2000). Also, ice cores provide multi-proxy records but cannot be directly-dated by radiometric methods.

δ^{18}O in calcite. The distribution of ^{18}O between calcite and water during the precipitation of speleothems and similar deposits is dependent on temperature alone if the system remains in isotopic equilibrium, which is often the case in deeper sections of the cave, where ventilation is minimal and humidity is high. Fractionation between ^{18}O and ^{16}O on precipitation of calcite is about −0.22‰/ºC at 20ºC, increasing to −0.24‰/ºC at 10ºC based on experimental studies of inorganic calcites (O'Neil et al. 1969; Friedman and O'Neil 1977). Hendy and Wilson (1968) optimistically declared that changes in mean annual temperatures as small as 0.2ºC could be achieved based on their preliminary investigations of speleothems from New Zealand. However, since this early work, extensive research has demonstrated that the derivation of paleotemperatures from $\delta^{18}O_{calcite}$ is complex and few reliable quantitative estimates of past temperature have been derived, principally because of the much greater expected temporal amplitude of $\delta^{18}O$ variation in the waters ($\delta^{18}O_{water}$) from which the calcite has precipitated. Variation in $\delta^{18}O_{calcite}$ along the axis of growth, then, is a function of temperature and the isotopic composition of rainfall and percolating vadose waters, the latter attributed to a combination of factors related to the temperature of formation of water in the atmosphere [~0.7‰/ºC for oceanic sites (Dansgaard 1964); generally lower gradient for continental sites (Rozanski et al. (1993)], changes in $\delta^{18}O$ of the sea water, which fluctuates with changing ice volume, and changes in the path of water from source to site of precipitation. The present day geographical distribution of mean annual $\delta^{18}O$ is reasonably well-known, but past spatial patterns must be inferred from models of past atmospheric circulation, ocean $\delta^{18}O$ changes and temperature distributions (Cole et al. 1999; Jouzel et al. 2000; Werner et al. 2000).

In comparing the temporal relationship of $\delta^{18}O$ in speleothem calcite with other proxy records of climate change, both positive and negative relationships with expected mean annual temperature have been observed, dependent on the relative influence of additional factors. For oceanic sites and some continental sites, the temperature dependence of $\delta^{18}O_{water}$ can outweigh the effects of $\delta^{18}O$ of sea water and fractionation at the calcite-water interface, such that calcites deposited during interglacials are less negative (Gascoyne et al. 1981; Goede et al. 1996, Lauritzen 1995, Dorale et al. 1992 1998). In other locations, negative shifts are related to a combination of factors such as glacial-interglacial changes in ocean water $\delta^{18}O$, intensification of rainfall, the "amount effect," seasonal patterns of monsoon rainfall and anomalous shifts in surface water $\delta^{18}O$ in source regions (Bar-Matthews et al. 1997, 1999; Hellstrom et al. 1998, Frumkin et al. 1999 Burns et al. 2001, Wang et al. 2001, Neff et al. 2001, Bard et al. 2002b). It is clear that in some cases, amplitudinal range of $\delta^{18}O_{calcite}$ is too great to be ascribed to temperature variation alone (e.g., −11.65 to −0.82‰ for Crag Cave, south west Ireland; McDermott et al. 2001) and dramatic shifts in $\delta^{18}O$ of water vapour accentuate the apparent relationships. In most recent studies, paleodata are supported by detailed survey of the modern scenario and confirmation that calcite is deposited under isotopic equilibrium conditions. It is recognized that many speleothem samples are likely to be unsuitable for the investigation of the $\delta^{18}O_{calcite}$-$\delta^{18}O_{water}$ relationship because of kinetic effects related to large differences in pCO$_2$ of drip waters and ambient air in the cave, slow drip rates and evaporation. It is now routine to measure $\delta^{18}O$ along distinctive growth layers to determine whether significant variation occurs from the central axis outwards, the so called "Hendy test" (Hendy 1971). While the appearance of kinetic fractionation of the isotopic signal is generally a problem it must be borne in mind that in certain circumstances it may be possible to recognize periodic shifts between equilibrium and non-equilibrium conditions and relate this to regional, not locally-specific, environmental changes (Niggemann et al. in press).

Although the apparent causal mechanisms for $\delta^{18}O_{calcite}$ variation are complicated, consistent regional patterns have been observed with a high degree of correlation with high-resolution $\delta^{18}O$ records from ice and marine cores for compilations of data based on many mass-spectrometric ^{230}Th ages (Winograd et al. 1992; Dorale et al. 1998, Bar-Matthews et al. 1998; McDermott et al. 2001, Burns et al. 2001 Spötl and Mangini 2002; Wang et al. 2002). Where observed patterns are replicated in many samples from the same cave, it is unlikely that non-equilibrium fractionation has occurred because each drip site is likely to be influenced to a different degree by flow path, pCO$_2$, residence times and degassing history (Dorale et al. 1998, 2002).

Perhaps one of the most widely cited $\delta^{18}O_{calcite}$ records is that of the Devils Hole vein calcite (Winograd et al. 1992) which records glacial-interglacial shifts in 1 to 2‰ from

566 to 60 ka. The record is reliably dated by ^{230}Th-^{234}U-^{238}U and ^{234}U-^{238}U methods (Ludwig et al. 1992). The variation in $\delta^{18}O_{calcite}$ exhibited most likely reflects changing $\delta^{18}O_{water}$ in atmospheric precipitation that recharges the groundwaters of the surrounding area. The local T-$\delta^{18}O_{calcite}$ relationship is considered to be positive at all times, such that highest δ^{18}O occurs at times of interglacial periods and is similar to the empirical relationship derived for mid- to high latitude precipitation (e.g., Johnsen et al. 1989) or cave waters (Yonge et al. 1985).

Recently published speleothem $\delta^{18}O_{calcite}$ records (Dorale et al. 1998; Bar-Matthews et al. 1998; Wang et al. 2001; Spotl and Mangini 2002) improve upon the resolution of Devils Hole and extend the investigation of regional variation in $\delta^{18}O_{water}$ and paleorecharge across the globe. These records are of sufficient resolution that leads and lags in the climate system can be investigated by comparison with high resolution polar ice core records. This can only be done, however, if both records are accurate in their timing. Ice core records beyond the last glacial maximum rely on ice flow models because annual layers at such depths no longer exist. Speleothems, on the other hand are directly dated by radiometric methods. Spötl and Mangini (2002) postulate minor differences in the timing of large and abrupt events in the $\delta^{18}O_{water}$ and $\delta^{18}O_{ice}$ from 60 ka to 44 ka. These may possibly be leads and lags, but are more likely to be due to either inaccuracies in the chronologies involved or the correlations between records. A comparison with a similarly dated speleothem record from Hulu Cave, China illustrates the complexities (Fig. 17). Unambiguous markers that are displayed in different paleoenvironmental archives, including speleothems, are required before absolute chronologies can be determined and terrestrial-ocean-cryosphere correlations established with confidence.

Temporal resolution approaching that of the ice deposited during the last glacial period in Greenland can commonly be obtained for stalagmites and stalactites using a drill bit <0.5 mm diameter. To investigate decadal to centennial sensitivity of the ocean-atmosphere-hydrosphere-vegetation system, comparable resolution to ice cores for the Holocene, where annual layers are preserved, is required. McDermott et al. (2001) turned to laser ablation stable isotope measurements using a beam diameter of ~150 μm and recognized features such as the 8200 year cold event that were not apparent in coarser resolution studies (Fig. 1). By matching the resolution of measurements for ice cores, ocean cores and speleothems, researchers in the paleoclimate field are presented with some interesting challenges. Most records at the centennial to millennial scale resolution have a component of global and regional variation. To match these records, one must identify common causal mechanisms that manifest themselves synchronously. If this can be done, leads and lags in the climate system can be investigated. One of the principal difficulties with comparison, however, is that generally only the speleothem records are directly datable.

δ^{13}C in calcite. Dissolved carbon in seepage waters is derived from three sources: atmospheric CO_2, decaying organic matter and root respiration in the soil zone and dissolved limestone along the flow route to the cave void. The net isotopic composition of dissolved HCO_3^- and the precipitated $CaCO_3$ depends, amongst other factors, on the δ^{13}C of reactants in the system, kinetic fractionation factors in the H_2O-$CaCO_3$-CO_2 system, saturation state with respect to $CaCO_3$ (and $CaMg(CO_3)_2$), exchange with gaseous phase and rate of precipitation. The system is complex (see reviews by Wigley et al. 1978; Salomans and Mook 1986; Dulinski and Rozanski 1990) and, while rainfall and temperature variation can cause temporal and spatial variation in δ^{13}C of precipitated calcite by influencing the chemical kinetics of dissolution and precipitation, the most useful information derived from δ^{13}C of speleothems relates to vegetation changes.

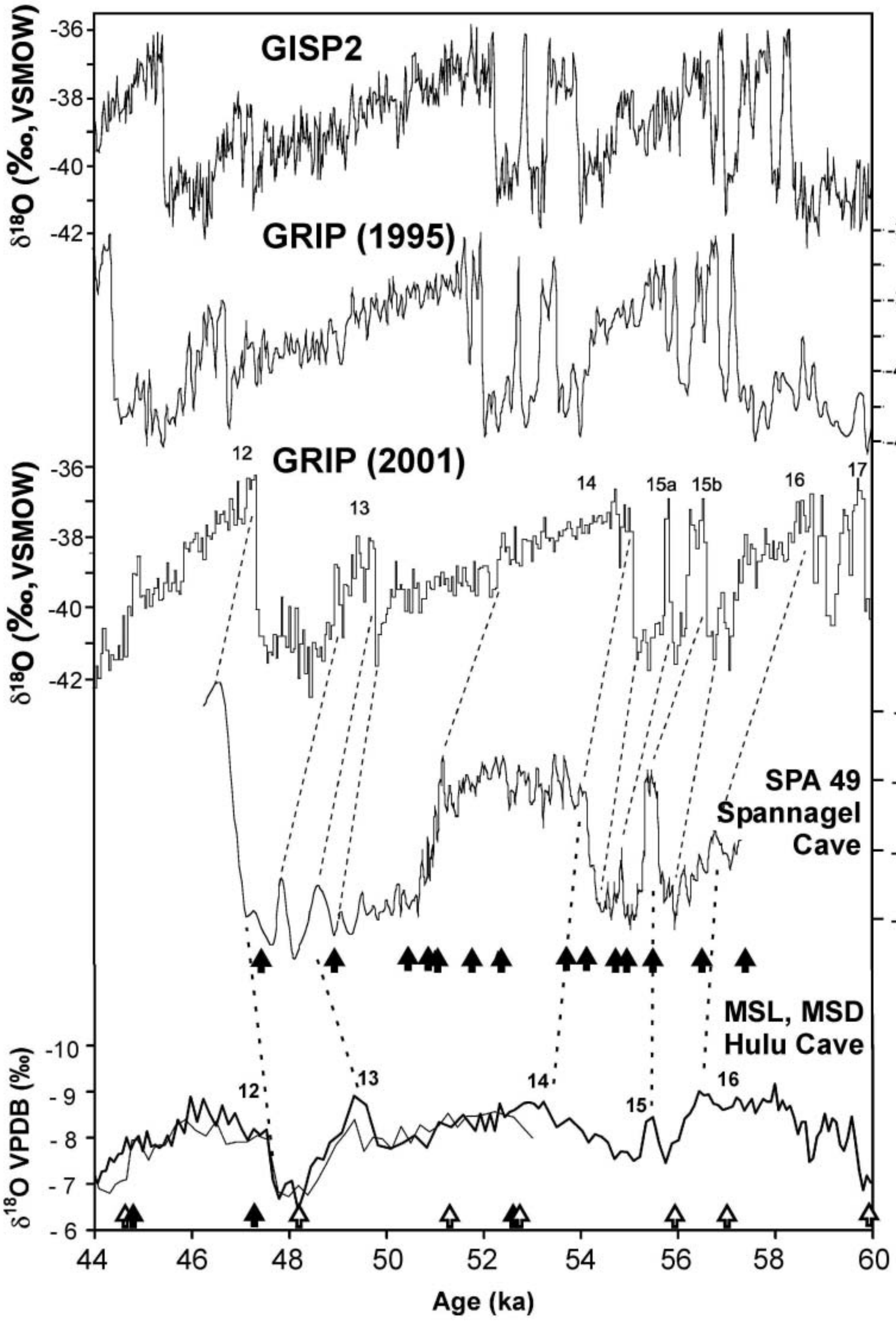

Figure 17. Last glacial period $\delta^{18}O_{calcite}$ for speleothem records from China (Wang et al. 2001) and Austria (Spötl and Mangini 2002), and Greenland $\delta^{18}O_{ice}$ records (Grootes et al. 1993; Johnsen et al. 1995; Johnsen et al. 2001). Ice core records are based on annual band counting and ice flow models. Speleothem records are based on TIMS ^{230}Th ages (shown by arrows). Numbers refer to Dansgaard-Oeschger (D-O) events in ice cores. Climate teleconnections may cause synchronous shifts in atmospheric circulation in different areas of the globe. The abrupt shifts in climate recorded in $\delta^{18}O_{ice}$ in the GRIP and GISP2 ice cores may be synchronous with changes in monsoonal rainfall patterns in China and temperature shifts above the Central Alps recorded in the speleothem records. While broad agreement is demonstrated, apparent discrepancies indicate exceptions to synchronous responses, inaccurate chronologies, or erroneous correlations.

Numerous studies of secondary pedogenic carbonates have successfully interpreted changes in $\delta^{13}C$ as a response to changing vegetation. Geochemical models (Dreybrodt 1980) indicate that the expected range of $\delta^{13}C$ in secondary carbonates precipitated in soils in regions dominated by C_3 (Calvin cycle) plants is −14 to −6‰, whereas those in C_4-dominated regions will have a range of −6 to +2‰ (C_3 plants have $\delta^{13}C$ value of −30 to −24; C_4 plants, −16 to −10‰; Vogel 1993). The differences between these two end-members is sufficiently large than that any temporal variation in their relative abundance should be discernible in secondary carbonates, although vegetation density (Amundson et al. 1988) and soil respiration rates (Quade et al. 1989) are also likely to play a role. Speleothems are likely to display a similar range of $\delta^{13}C$ to pedogenic carbonates under the same conditions.

Studies based on speleothems from the midwestern USA exhibit significant variation in $\delta^{13}C$ that has been related to shifts in the location of prairie and forest ecotones during the last glacial and Holocene periods (Dorale et al. 1992 1998; Denniston et al. 1999a,b, 2000, 2001). If samples can be obtained from locations that experienced the passage of ecotonal boundaries, rapid shifts in $\delta^{13}C$ are observed. A clear example of the relationship between speleothem $\delta^{13}C$ values and the C_3/C_4 biomass ratio was provided by R. G. Baker et al. (1998), who compared well-dated Holocene profiles from Northeast Iowa. Pollen, plant macrofossils, and sedimentary organic matter $\delta^{13}C$ values from alluvial deposits along Roberts Creek were compared to stalagmite $\delta^{13}C$ values from nearby Cold Water Cave. The pollen and plant macrofossil evidence (which in many cases allowed species-level plant identification) showed that a C_4-inclusive prairie replaced a C_3-rich deciduous forest around 6,300 years ago, which in turn was replaced by oak savanna (and a more intermediate C_3-C_4 mixture) approximately 3,500 years ago. The sedimentary organic matter $\delta^{13}C$ values showed a corresponding trend toward heavier isotopic values. The similarity of both the timing and isotopic trend of two speleothem records from Cold Water Cave with the vegetation record from Roberts Creek argues strongly that the speleothems are recording long-terms changes in the isotopic composition of the soil organic matter resulting from regional changes in the vegetation (Fig. 18).

Although changes in $\delta^{13}C$ can be attributed to changing vegetation, there are samples that demonstrate secular variation in regions that have been continuously dominated by either C_3 and C_4 plant types. In these areas, factors other than the distribution of C_3 and C_4 plants must be involved. In New Zealand, no plants are found to use the C_4 photosynthetic pathway except two species (both salt-tolerant lowland species), yet a speleothem from the mountainous region of north-western South Island exhibits substantial variation in $\delta^{13}C$ from 31 ka to present that is reasonably correlated with both $\delta^{18}O$ in the same sample and ice core records of temperature change (Hellstrom et al. 1998). The authors suggest that variability, here, is related to soil moisture conditions with vegetation density. During the last glacial maximum, drier conditions and sparser vegetation produced lower soil atmospheric CO_2 levels and increase in $\delta^{13}C$ (Dulinski and Rozanski 1992).

In a study that ends with a cautionary note, Baker et al. (1997) studied the spatial variation of $\delta^{13}C$ in actively-growing and late Quaternary speleothems from the British Isles, where native C4 plants are non-existent. Despite sampling material predicted to have been deposited under equilibrium conditions (i.e where humidity was high and ventilation minimal), $\delta^{13}C$ values greater than expected for the C_3 pathway (−14 to −6‰) were observed in many cases. They suggest that in some cases, where residence times in the soil are short, waters may not have equilibrated with soil CO_2. Also, kinetic fractionation may occur during degassing of fluids at the location of the sample or *en route* to the cave void. Researchers must study contemporaneous samples from the same cave (or region) to establish whether factors influencing secular variation of $\delta^{13}C$ are regional or local (Dorale et al. 1998, 2002).

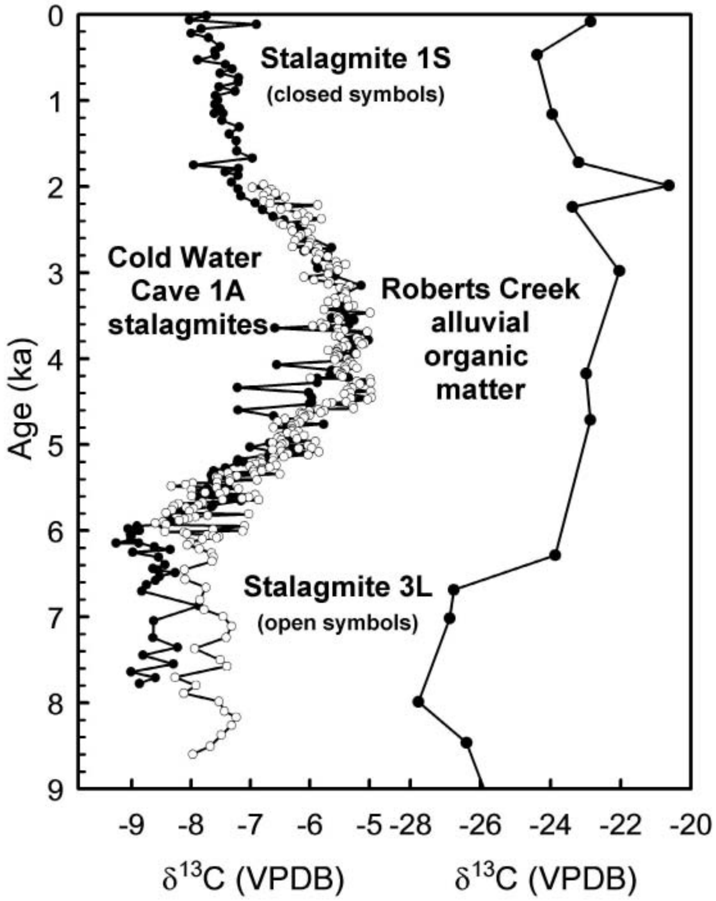

Figure 18. Holocene $\delta^{13}C$ profiles for stalagmites 1S and 3L from Cold Water Cave, Iowa and alluvial sedimentary organic matter from Roberts Creek (~60 km from Cold Water Cave—figure modified from Baker et al. 1998). Note the general similarity in timing and trend of the different $\delta^{13}C$ records. The $\delta^{13}C$ values of the stalagmites reflect the sources of carbon, namely soil CO_2 ultimately derived from the vegetation, for which the Roberts Creek record provides representative data, and the overlying limestone, which typically has $\delta^{13}C$ values close to 0‰ VPDB. In principle, these two sources contribute 50:50 to the dissolved carbonate species, although complex isotopic exchange scenarios are possible that may modify this ratio by the time seepage waters reach the caves. Nonetheless, the carbon which originates as soil CO_2 undergoes isotopic fractionation as it converts from dissolved CO_2 to aqueous CO_2 to HCO_3^- to CO_3^{-2} to solid $CaCO_3$; under equilibrium conditions, this sequence represents an approximate 10‰ enrichment (Hendy 1971). Thus, when soil CO_2 with a $\delta^{13}C$ value of −28‰ (representing a typical C_3 plant value) fractionates approximately 10‰ and mixes 50:50 with bedrock carbonate with a $\delta^{13}C$ value of ~ 0‰, the resultant speleothem carbonate would have a $\delta^{13}C$ value of ~ −9‰, consistent with the observations at Cold Water Cave and Roberts Creek. Because of the 50:50 contributions and the invariant nature of the bedrock component, shifts in the vegetation $\delta^{13}C$ values should cause speleothem shifts that are roughly half the magnitude of the vegetation shifts, again consistent with the observations. Note the factor of two differences in the $\delta^{13}C$ scales.

$\Delta^{14}C$ in calcite. Radiocarbon dating is the most widely-used technique for derivation of timescales for terrestrial and oceanic records of climate change. However, its use in speleothem chronology is considered problematical, principally because of potential variability in the contribution of "dead carbon" from the host limestone (Hendy 1970). While HCO_3^- in the soil zone in many locations may be found to be in equilibrium with soil gas, precipitating waters contain a proportion of carbon inherited from the dissolution of ^{14}C-free limestone in the vadose zone that varies according to the extent of open system conditions and incongruent dissolution (Wigley et al. 1978). Where organic matter turnover rates are relatively short (often <10 years), soil $^{14}CO_2$ can be considered to be effectively in equilibrium with the atmosphere, given the sampling resolution of calcite. Fractionation of carbon isotopes also occurs on precipitation of calcite depending on environmental conditions (see above). Because of these problems, relatively few speleothem chronologies have been based on ^{14}C ages, but where independent estimates of the age were obtained, the dead carbon proportion (dcp) has generally been found to have a range in dcp of 10-20 % (Bastin and Gewelt 1986; Genty et al. 1998, Holmgren et al. 1994), although much greater values are also observed (Vogel and Kronfeld 1997). In a detailed study of ^{230}Th dated speleothems from western Europe, Genty et al. (1999) demonstrate that temporal and spatial changes of dcp can be significant and dependent not only on the extent of open-system conditions, but also the age of the soil organic matter. Uncorrected ^{14}C ages, then, will over estimate the true age of deposition in most cases.

Despite the inherent problems associated with ^{14}C in speleothems, recent work by Beck et al. (2001) has focused attention on this topic because they demonstrated that in certain circumstances the dcp correction may be sufficiently well constrained that calibration of the radiocarbon timescale might be possible. Speleothems have an advantage over marine corals (e.g., Bard et al. 1990, 1998; Edwards et al. 1993), which have been used to extend the calibration curve, because they provide continuous records and are less likely to be affected by post-depositional alteration. Beck et al. (2001) obtained an extensive suite ^{230}Th and ^{231}Pa ages for a submerged speleothem (GB-89-24-1) from the Bahamas that grew continuously from 44 to 11 ka (see Fig. 19). Over 270 AMS ^{14}C ages were obtained for sub-samples along the axis of growth and where the timing of speleothem deposition overlapped with the earliest section (15.6 to 11.1 ka) of the existing radiocarbon calibration curve (Stuiver et al. 1998), a constant dcp of 1450 ± 450 (or 16 ± 5 %) was observed.

AMS ^{14}C ages for the rest of the sample were dcp-corrected and a surprising amount of structure was found in the data that suggests dramatic shifts in atmospheric ^{14}C occurred in the past (Fig. 19). Estimated atmospheric ^{14}C concentrations ($\Delta^{14}C$) were also much greater during the last glacial period, possibly reflecting increased ^{14}C production at times of reduced geomagnetic intensity. Variations in atmospheric ^{14}C concentrations are also related to the distribution of carbon in the Earth's major reservoirs. Detailed study of ^{14}C variation in speleothems could provide valuable information about the timing of changes and nature of carbon exchange between these reservoirs, which is likely to be caused by changes in the pattern of ocean circulation (Stocker and Wright 1996).

***$\delta^{18}O$ and δD in fluid inclusions in calcite*.** Speleothems commonly contain between 0.001 and 0.3 wt. % water trapped within the calcite (Schwarcz et al. 1976). To obtain unambiguous paleoclimate information from the oxygen isotope signal preserved in the speleothem calcite, it would be extremely advantageous to directly measure the isotopic composition of relict drip water that is preserved within fluid inclusions. In this way, the problem of estimating past patterns of $\delta^{18}O_{water}$ in precipitation might be circumvented. Early attempts (Schwarz et al. 1976, Harmon et al. 1979) focused on the hydrogen isotope composition of fluids because it was considered that the $\delta^{18}O_{water}$ in the inclusions could have been altered after exchange with calcite since the time of entrapment. Such an approach is feasible because of the following general relationship observed in meteoric waters (Craig et al. 1961)

$$\delta D_{water} = 8\ \delta^{18}O_{water} + 10 \tag{6}$$

However, few studies have been conducted because of analytical difficulties during extraction and measurement such as re-adsorption or incomplete removal, and the low temporal resolution that can be achieved Also, it is considered likely that the global meteoric water relationship in Equation (6) does not apply consistently across the globe

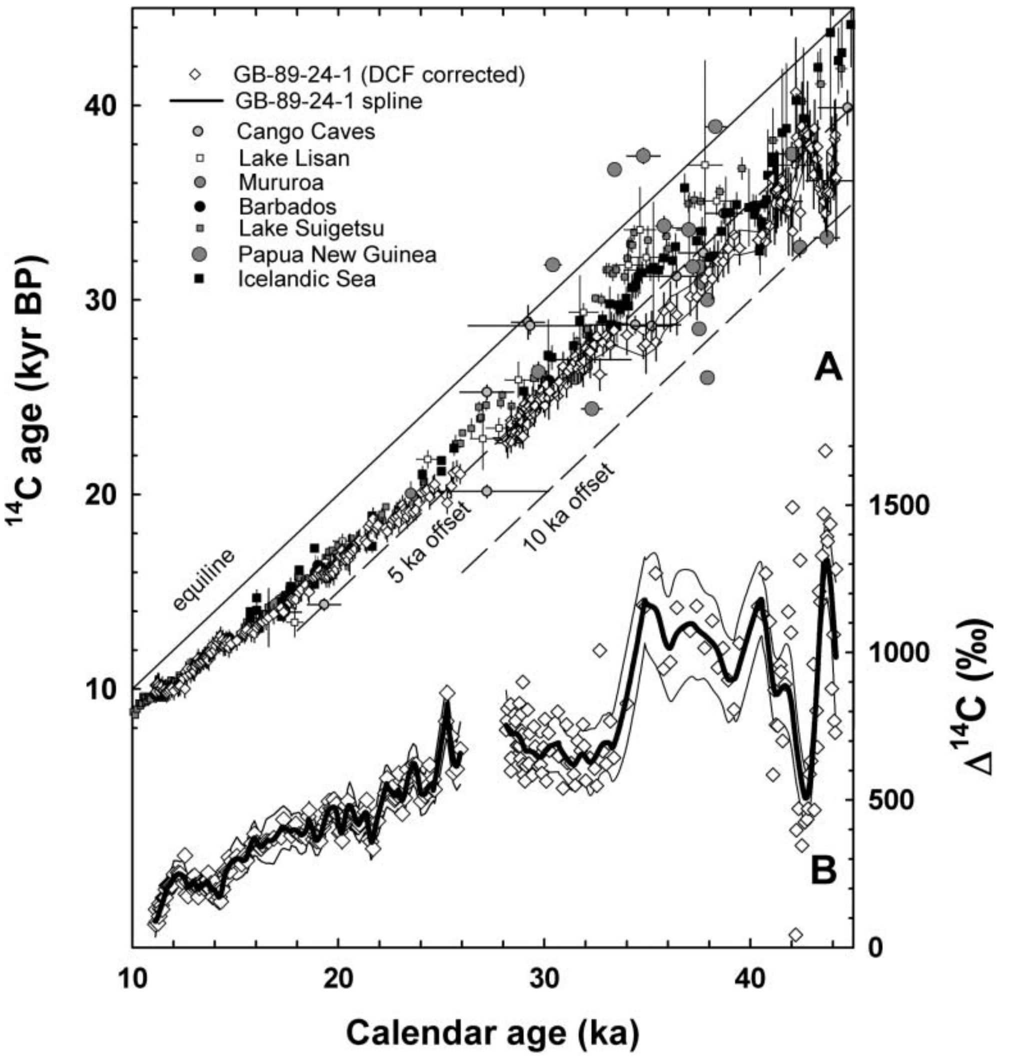

Figure 19. A) Radiocarbon ages vs. calendar ages (45 to 11 ka) for speleothems, coral, lake sediments and a marine core. GB-89-24-1—speleothem from Bahamas (Beck et al. 2001); Cango Caves—speleothem from South Africa (Vogel and Kronfeld 1997); Lake Lisan—lacustrine sediments from paleo-Dead Sea (Schramm 2000) Mururoa, Barbados—corals (Bard et al. 1998); Lake Suigetsu—lacustrine sediments (Kitagawa and van der Plicht 2000), Papua New Guinea (Yokoyama et al. 2000); Icelandic Sea -marine sediments (Voelker et al. 2000). Note increasing scatter in data with increasing and also apparent structure in some of the archives. B) Variations in atmospheric Δ^{14}C based on dcp-corrected ^{14}C age vs. ^{230}Th ages for GB-89-24-1. Both raw data and smoothed spline with 95% confidence bands are plotted. A sharp peak of approximately 1 ka in duration is observed in GB-89-24-1 at circa 44 ka, reaching levels of circa 1300‰—nearly twice as high as the 20th century bomb pulse. This may be related to changes in the atmosphere-ocean exchange of carbon associated with changing mode of ocean circulation during one of the meltwater events that influenced the North Atlantic Ocean during the last glacial period.

or between time periods of with temperature and precipitation regimes (Fritz et al. 1987, Gat and Carmi 1970; Harmon and Schwarz 1981).

Despite the potential problems, two recent studies provide positive results. Matthews et al. (2000) analyzed the δD of fluid inclusions in present-day cave carbonates from Soreq cave (Israel) using the method of thermal vacuum extraction and standard techniques on cave pool water from the same cave to estimate isotopic fractionation during measurement ($\Delta_{ex} = \delta D_{\text{extracted water}} - \delta D_{\text{cave water}}$). After subtracting Δ_{ex} from δD measurements on extracted water from speleothem calcite that is known to be of last glacial age and has previously been analyzed for $\delta^{18}O_{calcite}$ (Bar-Matthews et al. 1997), they demonstrate, by comparing their results with the $\delta^{18}O$ and δD relationship expressed by the Mediterranean Meteoric Water Line (Gat and Carmi 1970), that sea-surface and atmospheric temperatures were indeed cooler during glacial times in this region and closely approximate estimates derived from the global Meteoric Water Line. Dennis et al. (2001) detail robust techniques using a crushing cell, cryogenic vacuum extraction and thermal desorption to analyze artificial and natural samples. Precisions of ± 3‰ for δD and ± 0.4‰ for $\delta^{18}O$ measurements were achieved on samples of $< 1 \mu L$ (which is equivalent to 1 g calcite for samples studied). Gross change of mid-latitude precipitation between glacials and interglacials is only expected to be 5-6 times greater than achievable precisions at present but overall the results are encouraging.

Trace elements. The partitioning of Mg in calcite-water system is known to temperature dependent (Mucci and Morse 1990; Morse and Bender 1990) and early attempts were made by Gascoyne (1983) and Goede and Vogel (1991) to use the secular variation of Mg content in speleothems to derive paleotemperature information. Mg concentrations in speleothems are sufficiently high that high-resolution techniques can be used to investigate its distribution in the calcite. Roberts et al. (1998), for example, used SIMS analysis to investigate the spatial pattern of Mg at 1 μm resolution in SU-80-11, a speleothem from NW Scotland previously dated by TIMS ^{230}Th ages (Baker et al. 1993). This resolution permits observation of annual bands and Roberts et al. suggest that regular fluctuations in Mg/Ca along the axis of growth (mean amplitude 0.00135 ± 0.00045) might be related to a combination of seasonal temperature changes (the sample was collected 50 m from the cave entrance where seasonal variation would have been experienced, which is in contrast to deep sections of a caves where temperatures are constant). Longer term trends of Mg/Ca in SU-80-11 cannot be explained by temperature effects because the amplitude of variation is to large

Information about the environmental conditions in the vadose system above the cave can be derived from the supply of trace elements to the cave void by percolating waters. Concentration of Sr, Mg, Ba, U, P and other constituents is likely to be affected by supply effects and groundwater residence times. Temporal fluctuations of Mg and Sr have been related to evaporative concentration in drip waters (Railsbeck et al. 1994), variation in residence times affecting extent of dolomite dissolution relative to calcite dissolution (Fairchild et al. 1996) and selective leaching of Sr and Mg (Fairchild et al. 2000) and enhanced calcite precipitation along flow route prior to location of drip site in cave void (Fairchild et al. 2000). Each of these factors can be related to paleohydrological condition in the past, and hence well-dated speleothems could provide valuable proxy high-resolution information for past regional climates. The achievable resolution is well-demonstrated by a recent study by Baldini et al. (2002), who combine laser ablation $\delta^{18}O$ and SIMS elemental analysis to obtain a multi-proxy record at sub-annual resolution from a speleothem from Crag Cave, Ireland (Fig. 1).

Organic acid fluorescence. In a similar manner to trace constituents, such as Mg, Sr and P, concentrations of organic acids present in speleothem calcite are sufficient to observe variation at temporal scales of less than annual in some cases (e.g., Baker et al. 1993, Shopov et al. 1994). Organic acids (humic and fulvic) are formed in the soil by humification, and transported to the cave void by percolating waters where they are entrapped in precipitating carbonates. Under certain circumstances, where precipitation patterns are strongly seasonal and the nature of vadose percolation is such that seasonal mixing is incomplete, bands with different luminescent intensities can be differentiated after excitation with UV radiation. In other cases, bands are not observable but secular variation in intensity is found. Such features can be used to derive a variety of paleoenvironmental information (McGarry and Baker 2000).

If annual bands can be distinguished, annual growth rates can be estimated and related to changing environmental conditions to a combination of factors that include drip water rates, soil $p\text{CO}_2$, Ca concentration in percolating waters (see above). Baker et al. (1993) demonstrated that the frequency of banding in a sample from Scotland was annual based on TIMS ^{230}Th ages along the axis of growth. Interpretation of growth rates in terms of palaeoclimatic change is difficult, however, and independent confirmatory records are generally required for sections of the speleothem record. Perhaps more useful are luminescence intensity records, which have been related to past moisture levels in overlying soils and peats: Baker et al. (1999) suggest that 90-100 year oscillations in intensity of luminescence two speleothems from NW Scotland is caused by fluctuations in the extent of humification associated with bog wetness during the past 2500 years. Charman et al. (2001) strengthen this argument for luminescence fluctuation in NW Scotland by analyzing humification, using degree of decay estimated by colorimetry, testate amoebae counts, which indicate water levels, and pollen records in overlying peat cores dated by AMS ^{14}C methods and find a good degree of correlation with the ^{230}Th dated speleothem record.

Secular variation of $\delta^{234}U$ in calcite. Although it has been demonstrated in many studies that there is a wide range in measured δ^{234}U for speleothems from a single cave site, past environmental conditions can be inferred from the variation of δ^{234}U in secondary calcite in certain vadose systems using individual samples or sequences. Elevated δ^{234}U(0), for example, is expected to be related to accumulation of ^{234}U in damaged sites during a period of reduced leaching, either as a result of lower soil pCO2 or reduced soil moisture excess. Richards et al. (1997) relate the saw-tooth pattern of δ^{234}U(0) in speleothem calcite in a submerged sequence on the Bahamas (Fig. 20) to a combination of factors: Uranium in the secondary calcite is primarily inherited from the marine carbonates overlying the cave which were deposited with δ^{234}U(0) similar to present sea water (~145‰). The first-order trend (*A*) towards lower values along the axis of growth can be explained by radioactive decay of U in the overlying carbonates towards secular equilibrium. Superimposed on this is a saw-tooth, or step-like, second order trend. This is likely to be caused by (*B*) deposition of additional marine carbonates with marine δ^{234}U during high sea-stands and accumulation of ^{234}U in damaged sites in the vadose zone under dry conditions, which is then preferential leached, and (*C*) dissolution of increasingly lower and older material during glacials because of stabilization, fissure development and input of organic material.

The pattern of decreasing δ^{234}U(0) at a greater rate than that expected simply from radioactive decay is common in continuous phases of speleothem growth and has been interpreted in terms of paleohydrology in a recent study by Plagnes et al. (2002). Kaufman et al. (1998) recognize a rapid fall in δ^{234}U at 19 ka in speleothems from Soreq cave, Israel, synchronous with shifts in $\delta^{18}\text{O}_{\text{calcite}}$. They interpret this as reflecting the transition from glacial to interglacial conditions in the eastern Mediterranean region, when dramatic increases in precipitation rates elevated the preferential leaching rate of ^{234}U. Also, in a multi-proxy study by Hellstrom and McCulloch (2000), consistent temporal relationships are found between δ^{234}U(0) variation and that of trace elemental concentrations (Sr, Ba, Mg and U), stable isotope data (δ^{13}C and δ^{18}O) and luminescence intensity along the axis of growth of a speleothem from South Island, New Zealand. They relate this to changing effective moisture and vegetation density in this region from the last glacial maximum and the present day.

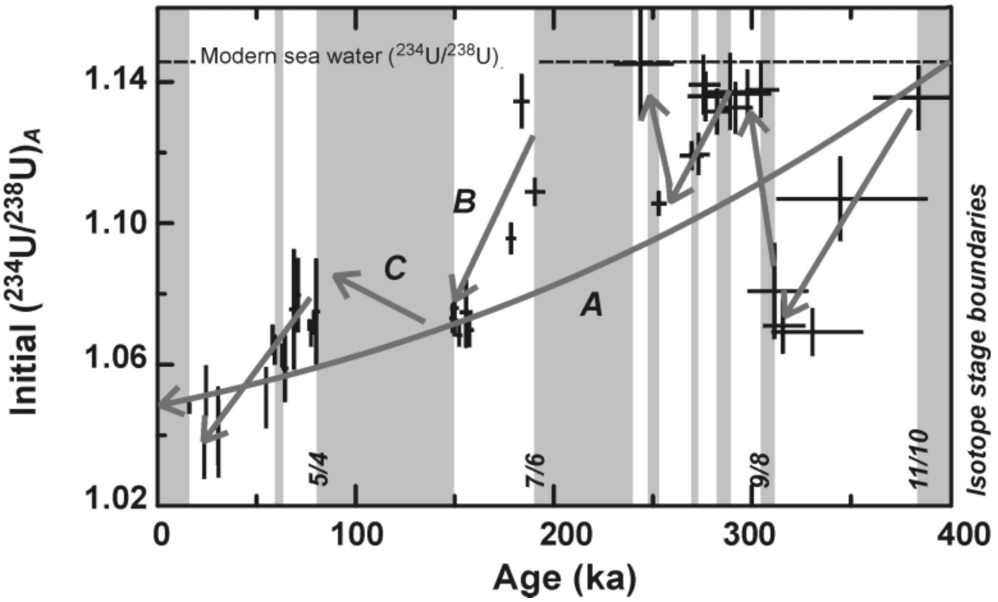

Figure 20. Secular variation in δ^{234}U(0) for Bahamas flowstone sequence. Changes in δ^{234}U(0) are related to uranium-series disequilibrium conditions in host limestone, periodic addition of new material with elevated (marine) δ^{234}U(0), alpha recoil effects and variation in recharge, and hence water-rock interaction times (see text for details).

5. CONCLUDING REMARKS

There is little doubt on the basis of the above review that speleothems are useful in an extremely wide range of applications and the frequency of publications devoted to speleothem-based archives is increasing rapidly. Fundamental to all applications is a robust and high-precision chronology and uranium-series techniques currently set the standard in this regard for speleothems. Reliable ages can be obtained for most samples where material appears to be well-preserved. However, it will become increasingly important to demonstrate reliability as the spatial resolution of analysis improves further.

Most early studies were conducted by researchers from research groups that specialized in karst research. The field is now populated by researchers from a whole host of geochemical and geophysical backgrounds and it can be viewed as truly inter-disciplinary. This is one of the strengths of speleothem research and we envisage even greater collaborative efforts between research teams in the future. Essential to the success of speleothem research, however, is the adherence to a few simple guidelines (see also Smart et al. 1996) that are already routinely observed by many current researchers:

(1) Geochemical evidence from precipitated calcite should be supplemented with study of the present-day processes in the vadose system above the location of the sample.

(2) Analyzes should be conducted on more than one sample, when available, to determine whether inferred environmental factors are indeed regional or global, and not related to specific local effects.

(3) Reliable chronologies should be based on multiple ^{230}Th age determinations at a sampling interval that is appropriate for the spatial resolution of geochemical analysis along the axis of growth and accounts for the possibility of non-linear or discontinuous growth.

(4) Multi-proxy evidence should be obtained along the axis of growth for individual samples. If trace elemental anomalies, related to water-rock interaction, correspond with $\delta^{18}O$ anomalies, related to regional atmospheric circulation or "amount effect," for example, then regional to global scale environmental change is implicated and can be studied at very high resolution.

Speleothems have many advantages over other archives of past geochemical and geophysical information, and we expect their use to become even more widespread. Their value is readily exemplified by recent high-resolution $\delta^{18}O_{calcite}$ records for the last glacial cycle, which have comparable resolution to the polar ice cores. The latter are currently the most widely cited archives for evidence of dramatic and abrupt environmental change for the late Pleistocene and Holocene, yet, in contrast to speleothems, cannot be directly dated for much of their length. Speleothems will play a complimentary role by providing chronological information by way of uranium-series dating and correlation, and more global coverage of regional $\delta^{18}O_{water}$ information. Such information can then be used to verify coupled isotope-atmosphere-ocean models results. We also expect speleothems to be more widely used to provide environmental information prior to the last interglacial-glacial cycle because remarkably well-preserved samples, exhibiting no geochemical or physical alteration, can be obtained. Currently, one of the limiting factors in using speleothems close to limit of uranium-series dating techniques is the precision and accuracy of the half-lives of the shorter-lived nuclides in the uranium-series decay chain. Continued attention must be focused on reducing the precision of these constants if we are to investigate the phasing of environmental change and internal and external forcing during the past 0.5 Ma. Also, more feasibility work should be undertaken in the field of U-Th-Pb dating, because this technique offers the possibility of extending the dateable range to beyond 0.5 Ma. While some researchers will be looking to older deposits, others will be devoting effort to the construction of environmental archives with, perhaps, sub-annual resolution. This is an exciting prospect because such records can be used to test models of the sensitivity of environmental change at much shorter timescales by comparison with historical records and geological evidence from the Holocene. The future then is bright, at least for those stages of research projects that will be undertaken above ground!

ACKNOWLEDGMENTS

Many of the views presented here have been informed by valuable discussions with colleagues at the Universities of Bristol, Leeds, Iowa and Minnesota. The list of names is too long to place here, but special mention should be reserved for the contributions of Peter Smart and Larry Edwards. We have drawn upon numerous examples from our own work in this review and acknowledge the support of the Natural Environment Research Council (UK) and the National Science Foundation (USA). We are grateful for the constructive comments of G. Henderson, A. Mangini and two anonymous reviewers.

REFERENCES

Allègre CJ (1964) De l'extension de la méthode de calcul graphique Concordia aux measures d'âges absolus effctués à l'aide du déséquilibre radioactif. Cas ds minéralisations secondaires d'uanium. C R Acad Sci Paris 259:4086-4089

Alley RB, Mayewski PA, Sowers T, Stuiver M, Taylor KC, Clark PU (1997) Holocene climatic instability: A prominent, widespread event 8200 yr ago. Geology 25:483-486

Amelin Y, Zaitsev AN (2002) Precise geochronology of phoscorites and carbonatites: The critical role of U-series disequilibrium in age interpretations. Geochim Cosmochim Acta 66:2399-2419

Amundson RG, Chadwick OA, Sowers JM, Doner HE (1988) Relationship between climate and vegetation and the stable carbon isotope chemistry of soils in the eastern Mojave Desert, Nevada. Quat Res 29:245-254

Antonioli F, Oliverio M (1996) Holocene sea-level rise recorded by a radiocarbon-dated mussel in a submerged speleothem beneath the Mediterranean Sea. Quat Res 45:241-244

Antonioli F, Silenzi S, Frisia S, (2001) Tyrrhenian Holocene palaeoclimate trends from spelean serpulids Fabrizio. Quat Sci Rev 20:1661-1670

Atkinson TC, Lawson TJ, Smart PL, Harmon, RS, Hess JW (1978) Paleoclimate and geomorphic implications of ^{230}Th/^{234}U dates on speleothem from Britain. Nature 272:24-8

Atkinson TC, Rowe PJ (1992) Applications of dating to denudation chronology and landscape evolution. *In:* Uranium-series disequilibrium: Applications to Earth, Marine and Environmental Sciences, Ivanovich M, Harmon RS (eds) Oxford University Press, Oxford, p 669-703

Auler AS, Smart PL (2001) Late Quaternary paleoclimate in semiarid Northeastern Brazil from U-series dating of travertines and water table speleothems. Quat Res 55:159-167

Ayliffe LK, Marianelli PC, Moriarty KC, Wells RT, McCulloch MT, Mortimer GE, Hellstrom JC (1998) 500 ka precipitation record from southeastern Australia: Evidence for interglacial relative aridity. Geology 26:147-150

Ayliffe LK, Veeh HH (1988) Uranium-series dating of speleothems and bones from Victoria Cave, Naracoorte, South Australia. Chem Geol 72:11-234

Baker A, Barnes WL, Smart PL (1996) Speleothem luminescence intensity and spectral characteristics: Signal calibration and a record of paleovegetation change. Chem Geol 130:65-76

Baker A, Genty D, Dreybrodt W, Barnes WL, Mockler HJ, Grapes J (1998) Testing theoretically predicted stalagmite growth rate with recent annually laminated samples: Implications for past stalagmite deposition. Geochim Cosmochim Acta 62:393-404

Baker A, Genty D, Smart PL (1998) High-resolution records of soil humification and paleoclimatic change from variations in speleothem luminescence excitation and emission wavelengths. Geology 26:903-906

Baker A, Ito E, Smart PL, McEwan R (1997) Elevated ^{13}C in speleothem and implications for palaeo-vegetation studies. Chem Geol 136:263-270

Baker A, Smart PL (1995) Recent flowstone growth rates: Field measurements in comparison to theoretical predictions. Chem Geol 122:121-128

Baker A, Smart PL and Ford DC (1993a) Northwest European palaeoclimate as indicated by growth frequency variations of secondary calcite deposits. Palaeogeog Palaeoclim Palaeoecol 100:291-301

Baker A, Smart PL Edwards RL (1995) Paleoclimate implications of mass spectrometric dating of a British flowstone. Geology 23:309-312

Baker A, Smart PL, Edwards RL (1996) Mass spectrometric dating of flowstones from Stump Cross Caverns and Lancaster Hole, Yorkshire: palaeoclimate implications. J Quat Sci 11:107-115

Baker A, Smart PL, Edwards RL Richards DA (1993b) Annual growth banding in a cave stalagmite. Nature 364:518-520

Baker RG, Gonzalez LA, Raymo M, Bettis EA, Reagan MK, and Dorale JA (1998) Comparison of multiple proxy records of Holocene environments in midwestern USA. Geology 26:1131-1134

Baldini JUL, McDermott F, Fairchild IJ (2002) Structure of the 8200-year Cold Event revealed by a speleothem trace element record. Science 296:2203-2206

Bard E, Antonioli F, Silenzi S (2002a) Sea-level during the penultimate interglacial period based on a submerged stalagmite from Argentarola Cave (Italy). Earth Planet Sci Lett 196:135-146

Bard E, Arnold M, Hamelin B, Tisnerat-Laborde N, Cabioch G (1998) Radiocarbon calibration by means of mass spectrometric Th-230/U-234 and C-14 ages of corals: An updated database including samples from Barbados, Mururoa and Tahiti. Radiocarbon 40:1085-1092

Bard E, Arnold M., Hamelin B, Tisnerat-Laborde N, Cabioch G (1998) Radiocarbon calibration by means of mass spectrometric ^{230}Th/^{234}U and ^{14}C ages of corals. An updated base including samples from Barbados, Mururoa and Tahiti. Radiocarbon 40:1085-1092

Bard E, Delaygue G, Rostek F, Antonioli F, Silenzi S, Schrag DP (2002b) Hydrological conditions over the western Mediterranean basin during the deposition of the cold sapropel 6 event. Earth Planet Sci Lett 202:481-494

Bard E, Hamelin B, Fairbanks RG, Zindler A (1990) Calibration of the ^{14}C timescale over the past 30,000 years using mass spectrometric U-Th ages from Barbados corals. Nature 345:405-410

Bar-Matthews M, Avalon A, Matthews A, Sass E, Halicz L (1996) Carbon and oxygen isotope study of the active water-carbonate system in a karstic Mediterranean cave: Implications for paleoclimate research in semiarid regions. Geochim Cosmochim Acta 60:337-347

Bar-Matthews M, Ayalon A, Kaufman A (1997) Late Quaternary paleoclimate in the eastern Mediterranean region from stable isotope analysis of speleothems at Soreq Cave, Israel. Quat Res 47:155-168

Bar-Matthews M, Matthews A, Avalon A (1991) Environmental controls of speleothem mineralogy in a karstic dolomitic terrain (Soreq Cave, Israel). J Geol 99:189-207

Bassiakos Y (2001) Assessment of the lower ESR dating range in Greek speleothems. J Radioan Nucl Chem 247:629-633

Bastin B, Gewelt M (1986) Analyze pollinique et datation ^{14}C des concretions stalagmitiques Holocenes: Apports complementaires des deaux methods. Geographie Physique et Quaternaire 40:185-196

Beck JW, Richards DA, Edwards RL, Silverman BW, Smart PL, Donahue DL, Hererra-Osterheld S, Burr GS, Calsoyas L, Jull AJT, Biddulph D (2001) Extremely large variations of atmospheric ^{14}C concentration during the last glacial period. Science 29:2453-2458

Bender ML, Fairbanks RG, Taylor FW, Matthews RK, Goddard JG, Broecker WS (1979) Uranium-series dating of the Pleistocene reef tracts of Barbados, West Indies. Geol Soc Am Bull 90:577-594

Betancourt JL, Grissino-Mayer HD, Salzer MW, Swetnam TW (2002) A test of "annual resolution" in stalagmites using tree rings. Quat Res 58:197-199

Bischoff JL, Fitzpatrick JA (1991) U-series dating of impure carbonates: An isochron technique using total-sample dissolution. Geochim Cosmochim Acta 55:543-554

Broecker WS, Olson EA, Orr PC (1960) Radiocarbon measurements and annual rings in cave formations. Nature 185:93-94

Brook GA Sheen S-W, Rafter MA, Railsback LB, Lundberg J (1999) A high-resolution proxy record of rainfall and ENSO since AD 1550 from layering in stalagmites from Anjohibe Cave, Madagascar. Holocene 9:695-705

Buhmann D, Dreybodt W (1985a) The kinetics of calcite dissolution and precipitation in geologically relevant situations of karst areas, 1. Open system. Chem Geol 48:189-211

Buhmann D, Dreybodt W (1985b) The kinetics of calcite dissolution and precipitation in geologically relevant situations of karst areas, 1. Closed system. Chem Geol 53:109-124

Burns SJ, Fleitman D, Matter A, Neff U, Mangini A (2001) Speleothem evidence from Oman for continental pluvial events during interglacial periods. Geology 29:623-626

Burns SJ, Matter A, Frank N, Mangini A (1998) Speleothem-based paleoclimate record from northern Oman. Geology 26:499-502

Charman DJ, Caseldine CJ, Baker A, Gearey B, Hatton J (2001) Palaeohydrological records from peat profiles and speleothems in Sutherland, NW Scotland. Quat Res 55:223-234

Cheng H, Adkins JF, Edwards RL, Boyle EA (2000) ^{230}Th dating of deep-sea corals. Geochim Cosmochim Acta 64:2401-2416

Cheng H, Edwards RL Wang Y (1996) U/Th and U/Pa dating of Nanjing Man. EOS (Trans, Am Geophys Union) 78:F787

Cheng H, Edwards RL, Murrell MT, Benjamin TM (1998) Uranium-thorium-protactinium dating systematics. Geochim Cosmochim Acta 62:3437-3452

Cherdyntsev VV, Kazachevskii IV, Kuz'mina YA (1965) Age of carbonate determined from the isotopes of thorium and uranium. Geochem Int 2:749-756

Chung GS, Swart PK (1990) The concentration of uranium in freshwater vadose and phreatic cements in a Holocene ooid clay: a method of identifying ancient water tables. J Sediment Petrol 60:735-746

Cliff RA, Spötl C (2001) U-Pb dating of speleothems from the Spannagel Cave, Austria. XI EUG Conference, Strasbourg, France. J Conf Abstr 6:601

Cole JE, Rind D, Webb RS, Jouzel J, Healy R (1999) Climatic controls on interannual variability of precipitation δ18O: Simulated influence of temperature, precipitation amount, and vapor source region. J Geophys Res 104:14223-14235

Cole JM, Rasbury ET, Hanson GN, Ashley GM (2001) Evaluating the effect of initial isotopic disequilibrium on U-Pb ages of Quaternary sedimentary carbonates from Olduvai Gorge, Tanzania. 11th Annual V. M. Goldschmidt Conference. Hot Springs, VA. Abstract 3594

Craig H (1961) Isotopic variations in meteoric waters. Science 133:1702-1703

Crowley TJ, Kim K-Y (1994) Milankovitch forcing of the last interglacial sea level. Science 265:1566-1568

Dansgaard W (1964) Stable isotopes in precipitation. Tellus 16:436-468

Dennis PF, Rowe PJ, Atkinson TC (2001) The recovery and isotopic measurement of water from fluid inclusions in speleothems. Geochim Cosmochim Acta 65:871-884

Denniston RF, González LA, Asmerom Y, Baker RG, Reagan MK, Bettis EA (1999a) Evidence for increased cool season moisture during the middle Holocene. Geology 27:815-818

Denniston RF, González LA, Asmerom Y, Polyak V, Reagan MK, Saltzman MR (2001) A high-resolution speleothem record of climatic variability at the Allerod-Younger Dryas transition in Missouri, central United States. Palaeogeog Palaeoclim Palaeoecol 176:147-155

Denniston RF, González LA, Asmerom Y, Reagan MK (2000) Speleothem records of Holocene paleoenvironmental change in the Ozark Highlands, USA. Quat Int 67:21-28

Denniston RF, González LA, Semken HA, Jr, Baker RG, Recelli-Snyder H, Reagan MK, Bettis, EA (1999b) Integrating stalagmite, vertebrate, and pollen sequences to investigate Holocene vegetation and climate change in the southern Midwest. Quat Res 52:381-387

Dervin J, Faucherre J (1973a) Étude des carbonates complexes de thorium et de cérium. II- Constitution des complexes en colution. Bull Soc Chim Fr 11:2926-2929

Dervin J, Faucherre J (1973b) Étude des carbonates complexes de thorium et de cérium. I- Solubilité et nature des ions complexes en solution. Bull Soc Chim Fr 11:2930-2933

Dickson BL, Wheller GE (1992) Uranium-series disequilibrium in exploration geology *In*: Uranium-Series Disequilibrium: Applications to Earth, Marine, and Environmental Sciences, 2nd ed. Ivanovich M, Harmon RS (eds) Clarendon Press, Oxford. p 704-729

Dorale JA, Edwards RL, Alexander CA, Shen CC, Richards DA, Cheng H (2003) Uranium-series dating of speleothems: Current techniques, limits and applications. *In*: Studies of Cave Sediments, Sasowsky ID, Mylroie JE (eds) Kluwer Academic/Plenum Publishers, New York. (in press)

Dorale JA, Edwards RL, Ito E, González LA (1998) Climate and vegetation history of the Midcontinent from 75 to 25 ka: a speleothem record from Crevice Cave, Missouri, USA. Science 282:1871-1874

Dorale JA, Edwards RL, Onac BP (2002) Stable isotopes as environmental indicators in speleothems. *In*: Karst Processes and the Carbon Cycle. Yuan, D-X (ed) Geological Publishing House, Beijing, China. p 107-120

Dorale JA, González LA, Reagan MK, Pickett DA, Murrell MT, Baker RG (1992) A high-resolution record of Holocene climate change in speleothem calcite from Cold Water Cave, northeast Iowa. Science 258:1626-1630

Dreybrodt W (1980) Deposition of calcite from thin films of natural calcareous solutions and the growth of speleothems. Chem Geol 29:89-105

Dreybrodt W (1997) Chemical kinetics, speleothem growth, and climate. *In:* Climate Change: The Karst Record. S-E Lauritzen (ed) Karst Waters Institute Special Publications 2: Charles Town, West Virginia p 23-25

Dulinski M, Rozanski K (1990) Formation of $^{13}C/^{12}C$ isotope ratios in speleothems: A semi-dynamic model. Radiocarbon 32:7-16

Duplessy JC, Labeyrie L, Lalou C, Nguyen HV (1970) Continental climate variations between 130,000 and 90,000 years BP Nature 226:631-632

Edwards RL, Beck JW, Burr GS, Donahue DJ, Chappell JMA, Bloom AL, Druffel ERM, Taylor FW (1993) A large drop in atmospheric C-14/C-12 and reduced melting in the Younger Dryas documented with Th-230 ages of corals. Science 260:962-968

Edwards RL, Cheng H, Murrell MT, Goldstein SJ (1997) Protactinium-231 dating of carbonates by thermal ionization mass spectrometry: Implications for Quaternary climate change. Science 276:782-786

Edwards RL, Gallup CD, Cheng H (2003) Uranium-series dating of marine and lacustrine carbonates. Rev Mineral Geochem 52:363-405

Esat TM, McCulloch MT, Chappell J, Pillans B, Omura A (1999) Rapid fluctuations in sea level recorded at Huon Peninsula during the Penultimate Deglaciation. Science 283:197-201

Fairbanks RG (1989) A 17,000 year glacio-eustatic sea level record: Influence of glacial melting rates on the Younger Dryas event and deep-ocean circulation. Nature 342:637-642

Fairchild IJ, Borsato A, Tooth AF, Frisia S, Hawkesworth CJ, Huang Y, McDermott F, Spiro B (2000) Controls on trace element (Sr-Mg) compositions of carbonate cave waters: implications for speleothem climatic records. Chemical Geology 166:255-269

Fairchild IJ, Tooth AF, Huang Y, Borsato A, Frisia S, McDermott F (1996) Spatial and temporal variations in water and stalactite chemistry in currently active caves: a precursor to interpretations of past climate. *In:* Proc. 4th International Symposium on Geochemistry of the Earth's Surface. Bottrell SH (ed) Ilkley, Yorkshire, University of Leeds, UK p 229-233

Farrant AR, Smart PL, Whitaker FF (1995) Long-term Quaternary uplift rates inferred from limestone caves in Sarawak, Malaysia. Geology 23:357-360

Ford DC (1997) Dating and paleo-environmental studies of speleothems. *In:* Cave Minerals of the World (2nd edn). Hill CA, Forti P (eds) National Speleological Society of America Press, Huntsville, Alabama. p 271-284

Ford DC, Hill CA (1989) Dating results from Carlsbad Cavern and other caves in the Guadalupe Mountains, New Mexico. Isochron/West 54:3-7

Ford DC, Williams PW (1989) Karst geomorphology and hydrology. Unwin Hyman, London

Fornós JJ, Gelabert B, Ginés A, Ginés J, Tuccimei P, Vesica P (2002) Phreatic overgrowths on speleothems: a useful tool in structural geology in littoral karstic landscapes. The example of eastern Mallorca (Balearic Islands). Geodinimica Acta, 15:113-125

Frank N, Mangini A, Korfmann M (2002) $^{230}Th/U$ dating of the Trojan "Water Quarries." Archaeometry 44:305-314

Friedman I, O'Neil JR (1977) Compilation of stable isotope fractionation factors of geochemical interest. U S Geol Surv Prof Paper 440-KK

Frisia S, Borsato A, Fairchild IJ, McDermott F (2000) Calcite fabrics, growth mechanisms, and environments of formation in speleothems from the Italian Alps and southwestern Ireland. J Sediment Res 70:1183-1196

Fritz P, Drimmie RJ, Frape SK, O'Shea K (1987) The isotopic composition of precipitation and groundwater. *In:* Canada International Symposium on the Use of Isotope Techniques in Water Resources Development. IAEA Symposium, Vienna 299:539-550

Frumkin A, Ford DC, Schwarcz HP (1999) Continental oxygen isotopic record of the last 170,000 years in Jerusalem. Quat Res 51:317-327

Gallup CD, Cheng H, Taylor FW, Edwards RL (2002) Direct determination of the timing of sea level change during Termination II. Science 295:310-313

Gallup CD, Edwards RL, Johnson RG (1994) The timing of high sea levels over the past 200,000 years. Science 263:796-800

Gascoyne M (1983) Trace element partition coefficients in the calcite-water system and their paleoclimatic significance. J Hydrol 61:213-222

Gascoyne M (1984) Uranium Series ages of Speleothems from Bahaman Blue Holes and their significance. Trans British Cave Res Assoc 11:45-49

Gascoyne M (1985) Application of the ^{227}Th/^{230}Th method to dating Pleistocene carbonates and comparisons with other dating methods. Geochim Cosmochim Acta 49:1165-1171

Gascoyne M (1992a) Paleoclimate determination from cave deposits. Quat Sci Rev 11:609-632

Gascoyne M (1992b) Geochemistry of the actinides and their daughters. *In*: Uranium-Series Disequilibrium: Applications to Earth, Marine, and Environmental Sciences, 2nd ed. Ivanovich M, Harmon RS (eds) Clarendon Press, Oxford. p 34-61

Gascoyne M, Benjamin GJ, Schwarcz HP, Ford DC (1979) Sea-level lowering during the Illinoian glaciation: evidence from a Bahama "Blue Hole." Science 205:806-808

Gascoyne M, Currant AP, Lord TC (1981) Ipswichian fauna of Victoria Cave and the marine palaeoclimatic record. Nature 294:652-4

Gascoyne M, Ford DC, Schwarcz HP (1981) Late Pleistocene chronology and paleoclimate of Vancouver Island determined from cave deposits. Ca J Earth Sci 18:1643-1652

Gascoyne M, Harmon RS (1992) Palaeoclimatology and palaeoselevels. *In:* Uranium-series disequilibrium: Applications to Earth, Marine and Environmental Sciences. Ivanovich M, Harmon RS (eds) Oxford University Press, Oxford. p 553-582

Gascoyne M, Schwarcz HP (1982) Carbonate and sulphate precipitates. *In:* Uranium series disequilibrium: Applications to environmental problems (1st edn). Ivanovich M, Harmon RS (eds) Calrendon Press, Oxford. p 268-301

Gascoyne M, Schwarcz HP, Ford DC (1978) Uranium-series dating and stable-isotope studies of speleothems. Part 1. Theory and techniques. Trans Brit Cave Res Assoc 5:91-112

Gascoyne M, Schwarcz HP, Ford DC (1983) Uranium-series ages of speleothem from northwest England: correlation with Quaternary climate. Phil Trans Royal Soc London B301:143-164

Gat JR, Carmi I (1970) evolution of the isotopic composition of stamospheric waters in the Mediterranan Sea area. J Geophys Res 75:3039-3048

Genty D, Baker A, Massault M, Proctor C, Gilmour M, Pons-Branchu E, Hamelin B (2001) Dead carbon in stalagmites: Carbonate bedrock paleodissolution vs. ageing of soil organic matter. Implications for ^{13}C variations in speleothems. Geochim Cosmochim Acta 65:3443-3457

Genty D, Massault M (1999) Carbon transfer dynamics from bomb-^{14}C and δ^{13}C time series of a laminated stalagmite from SW France - Modeling and comparison with other stalagmite records. Geochim Cosmochim Acta 63:1537-1548

Genty D, Quinif Y (1996) Annually laminated sequences in the internal structure of some Belgian stalagmites - importance for paleoclimatology. J Sediment Res 66:275-288

Genty D, Vokal B, Obelic B, Massault M (1998) Bomb ^{14}C time history recorded in two modern stalagmites - importance for soil organic matter dynamics and bomb ^{14}C distribution over continents. Earth Planet Sci Lett 160:795-809

Getty SR, Asmerom Y, Quinn TM (2001) Accelerated Pleistocene coral extinctions in the Caribbean Basin from uranium-lead (U-Pb) dating. Geology 29:639-642

Getty SR, DePaolo DJ (1995) Quaternary geochronology using the U-Th-Pb method. Geochim Cosmochim Acta 59:3267-3272

Geyh M (1970) Isotopenphysikalische Untersuchungen an Kalksinter, ihre Bedeutung fur die 14C-Alterbestimmung von Gründwasser und die erforshung des paläoklimas. Geol Jahrb 88:149-159

Goede A, Green DC, Harmon RS (1986) Late Pleistocene palaeotemperature record from a Tasmanian speleothem. Aust J Earth Sci 33:333-342

Goede A, Vogel JC (1991) Trace element variations and dating of a late Pleistocene Tasmanian speleothem. Palaeogeog Palaeoclim Palaeoecol 88:121-131

Goldstein SJ, Stirling CH (2003) Techniques for measuring uranium-series nuclides: 1992-2002. Rev Mineral Geochem 52:23-57

González LA, Carpenter SJ, Lohmann KC (1992) Inorganic calcite morphology: roles of fluid chemistry and fluid flow. J Sediment Petrol 62:382-399

Gordon D, Smart PL (1984) Comments on "Speleothems Travertines and Paleoclimates" by G.J. Hennig, R. Grün and K. Brunnacker. Quat Res 22:144-147

Gordon D, Smart PL, Ford DC, Andrews JN, Atkinson TC, Rowe PJ, Christopher NSJ (1989) Dating of late Pleistocene interglacial and interstadial periods in the United Kingdom from speleothem growth frequency. Quat Res 31:14-26

Grenthe I, Fuger J, Konings RJM, Lemire RJ, Muller AB, Nguyen-Rung C, Wanner H (1992) Chemical Thermodynamics of Uranium. Nuclear Energy Agency. North-Holland, Amsterdam

Grootes PM, Stuiver M, White JWC, Johnsen S, Jouzel JJ (1993) Comparison of oxygen isotope records from the GISP2 and GRIP Greenland ice cores. Nature 366:552–554

Grün R (1989) Electron spin resonance (ESR) dating. Quat Int 1:65-109

Hancock PL, Chalmers RML, Altunel E, Cakir Z (1999) Travitonics: using travertines in active fault studies. J Struct Geol 21:903-916

Harmon RS, Ford DC, Schwarcz HP (1977) Interglacial chronology of Rocky and Mackenzie Mountains based upon ^{230}Th-^{234}U dating of speleothems. Can J Earth Sci 14:2543-2552

Harmon RS, Land LS, Mitterer RM, Garrett P, Schwarcz HP, Larson GJ (1981) Bermuda sea levels during the last interglacial. Nature 289:481-3

Harmon RS, Mitterer RM, Kriausakul N, Land LS, Schwarcz HP, Garrett P, Larson GJ, Vacher HL, Rowe M (1983) U-Series and amino-acid racemization geochronology of Bermuda: Implications for eustatic sea-level fluctuation over the past 250,000 years. Palaeogeog Palaeoclim Palaeoecol 44:41-70

Harmon RS, Schwarcz HP (1981) Changes of ^{2}H and ^{18}O enrichment of meteoric water and Pleistocene glaciation. Nature 290:125-128

Harmon RS, Schwarcz HP, O'Neil JR (1979) D/H ratios in speleothem fluid inclusions: A guide to variations in the isotopic compositions of meteoric precipitation? Earth Planet Sci Lett 42:254-266

Harmon RS, Thompson P, Schwarcz HP, Ford DC (1975a) Late Pleistocene paleoclimates of North America as inferred from stable isotope studies of speleothems. Quat Res 9:54-70

Harmon RS, Thompson P, Schwarcz HP, Ford DC (1975b) Uranium-series dating of speleothems. Nat Speleological Soc Bull 37:21-33

Hearty PJ, Kindler P, Cheng H, Edwards RL (1999). Evidence for a +20 m middle Pleistocene sea-level highstand (Bermuda and Bahamas) and partial collapse of Antarctic ice. Geology 27:375-378

Hellstrom J, McCulloch M, Stone J (1998) A detailed 31,000-year record of climate and vegetation change from the isotope geochemistry of two New Zealnd speleothems. Quat Res 50:167-178

Hellstrom JC, McCulloch MT (2000) Multi-proxy constraints on the climatic significance of trace element records from a New Zealand speleothem. Earth Planet Sci Lett 179:287-297

Henderson GM, Slowey NC (2000). Evidence against northern-hemisphere forcing of the penultimate deglaciation from U-Th dating. Nature 402:61-66

Henderson GM, Slowey NC, Fleisher MQ (2001) U-Th dating of carbonate platform and slope sediments. Geochim Cosmochim Acta 65:2757-2770

Hendy CH (1970) The use of ^{14}C in the study of cave processes. *In*: Twelfth Nobel Symposium, Radiocarbon Variations and Absolute Chronology. Olsson IU (ed) Almqvist and Wiksell, Stockholm, and Wiley and Sons, New York, p 419-443

Hendy CH (1971) The isotopic geochemistry of speleothems. I. The calculation of the effects of different modes of formation on the composition of speleothems and their applicability as paleoclimatic indicators. Geochim Cosmochim Acta 35:801-824

Hendy CH, Wilson AT (1968) Paleoclimatic data from speleothems. Nature 219:48-51

Hennig GJ, Grün H, Brunnacker K (1983) Speleothems, travertines, and paleoclimates. Quat Res 20:1-29

Hercman H (2000) Reconstruction of palaeoclimatic changes in Central Europe between 10 and 200 thousand years BP, based on analysis of growth frequency of speleothems. Studia Quat 17:35-70

Hill CA, Forti P (1997) Cave Minerals of the World (2nd edn). National Speleological Society, Huntsville

Holmgren K, Lauritzen S-E, Possnert G (1994) ^{230}Th/^{234}U and ^{14}C dating of a Late Pleistocene stalagmite in Lobatse II Cave, Botswana. Quat Sci Rev 13:111-119

Huang Y, Fairchild IJ (2001) Partitioning of Sr^{2+} and Mg^{2+} into calcite under karst-analog experimental conditions. Geochim Cosmochim Acta 65:47-62

Huang Y, Fairchild IJ, Borsato A, Frisia S, Cassidy NJ, McDermott F, Hawkesworth CJ (2001) Seasonal variations in Sr, Mg and P in modern speleothems (Grotta di Ernesto, Italy). Chem Geol 175:429-448

Ikeya M (1975) Dating a stalactite by electron paramagnetic resonance. Nature 255:48-50

Israelson C, Halliday AN Buchardt B (1996) U-Pb dating of calcite concretions from Cambrian black shales and the Phanerozoic time scale. Earth Planet Sci Lett 141:153-159

Jahn B-m, Cuvellier H (1994) Pb-Pb and U-Pb geochronology of carbonate rocks: An assessment. Chem Geol 115:125-151

Joao A, Bigot S, Fromage F (1987) Study of the carbonate complexes of IVB elements: I. Determination of the stability constant of Th(IV) pentacarbonate. Bull Soc Chim Fr, Issue 1, p. 42-44

Johnsen SJ, Dahl-Jensen D, Dansgaard W, Gundestrup N (1995) Greenland palaeotemperatures derived from GRIP bore hole temperature and ice core isotope profile. Tellus 47B:624-629

Johnsen SJ, Dahl-Jensen D, Gundestrup N, Steffensen JP, Clausen HB, Miller H, Masson-Delmotte V, Sveinbjörnsdottir AE, White J (2001) Oxygen isotope and palaeotemperature records from six Greenland ice-core stations: Camp Century, Dye-3, GRIP, GISP2, Renland and NorthGRIP J Quat Sci 16**:**299-307

Johnsen SJ, Dansgaard W, White JWC (1989) The origin of arctic precipitation under present and glacial conditions. Tellus 41B:452-468

Jones B (1995) Processes associated with microbial biofilms in the twilight zone of caves: examples from the Cayman Islands. J Sediment Res A65:552-560

Jones CE, Halliday AN, Lohmann KC (1995) The impact of diagenesis on high-precision U-Pb dating of ancient carbonates: An example from the Late Permian of New Mexico. Earth Planet Sci Lett 134:409-423

Jouzel J, G. Hoffmann G, Koster RD, Masson V (2000) Water isotopes in precipitation: data/model comparison for present-day and past climates. Quat Sci Rev 19:363-379

Kagan E, Agnon A, Bar-Matthews M, Ayalon A (2002) Cave deposits as recorders of paleoseismicity: A record from two caves located 60 km west of the Dead Sea Transform (Jerusalem, Israel). *In:* Environmental Catastrophes and Recoveries in the Holocene (online abstract http://atlas-conferences.com/cgi-bin/abstract/caiq-38)

Kashiwaya K, Atkinson TC, Smart PL. (1991). Periodic variations in late Pleistocene speleothem abundance in Britain. Quat Res 35:190-196

Kaufman A (1993) An evaluation of several methods for determining ^{230}Th/U ages in impure carbonates. Geochim Cosmochim Acta 57:2303- 2317

Kaufman A, Broecker WS (1965) Comparison of ^{230}Th and ^{14}C ages for carbonate materials from Lakes Lahontan and Bonneville. J Geophys Res 70:4039-4054

Kaufman A, Ku T-L, Luo S (1995) Uranium-series dating of carnotites: Concordance between Th-230 and Pa-231 ages. Chem Geol 120:175-181

Kaufman A, Wasserburg GJ, Porcelli D, Bar-Matthews M, Ayalon A, Halicz L (1998) U-Th isotope systematics and U-series ages of speleothems from Soreq Cave, Israel and climatic correlations. Earth Planet Sci Lett 156:141-155

Kendall AC, Broughton PL (1978) Origin of fabrics in speleothems composed of columnar calcite crystals. J Sediment Petrol 48:519-538

Kitagawa H; van der Plicht J (2000) Atmospheric radiocarbon calibration beyond 11,900 cal BP from Lake Suigetsu laminated sediments. Radiocarbon 42:369-380

Ku T-L (2000) Uranium-Series Methods. *In:* Quaternary Geochronology: Methods and Applications. Stratton Noller J, Sowers JM, Lettis WR (eds) American Geophysical Union, Washington DC, p 101-114

Ku T-L, Kimmel MA, Easton WH, O'Neil TJ (1974) Eustatic sea level 120,000 years ago on Oahu Hawaii. Science 183:959-962

Ku T-L, Liang ZC (1984) The dating of impure carbonates with decay series isotopes. Nucl Instr Meth 223:563-571

Langmuir D (1997) Aqueous Environmental Geochemistry. Prentice Hall, New Jersey

Langmuir D, Herman JS (1980) The mobility of thorium in natural waters at low temperatures. Geochim Cosmochim Acta 44:1753-1766

Latham AG, Ford DC (1993) The paleomagnetism and rock magnetism of cave and karst deposits. *In:* Applications of Paleomagnetism to Sedimentary Geology. Aissaoui DM, McNeill DF, Hurley NF (eds). SEPM Special Publications. 49:149-155

Latham AG, Schwarz HP (1992) Carbonate and sulphate precipitates. *In:* Uranium-series disequilibrium: Applications to Earth, Marine and Environmental Sciences, Ivanovich M, Harmon RS (eds) Oxford University Press, Oxford, p 423-459

Lauritzen S-E (1991) Karst resources and their conservation in Norway. Norsk Geografisk Tidskrift 45:119-142

Lauritzen S-E (1993) Natural environmental change in karst: The quaternary record. Catena Supp 25:21-40

Lauritzen S-E (1995) High-resolution paleotemperature proxy record for the last interglaciation based on Norwegian speleothems. Quat Res 43:133-146

Lauritzen S-E (2003) Reconstructing Holocene climate records from speleoethems. *In*: Global Change in the Holocene. Mackay AW, Battarbee RW, Birks HJB (eds) Oldfield F. Arnold, London (in press)

Lauritzen S-E, Mylroie JE Results of a Speleothem U/Th Dating Reconnaissance from the Helderberg Plateau, New York. J Cave Karst Studies 62(1):20-26

Lauritzen S-E, Onac BP (1995) Uranium-series dating of speleothems from Romanian caves. Theor Appl Karst 8:25-36

Lemeille F, Cushing M, Carbon D, Grellet B, Bitterli T, Flehoc C (1999) Co-seismic ruptures and deformations recorded by speleothems in the epicentral zone of the Basel earthquake. Geodinam Acta 12:179-191

Li W-X, Lundberg J, Dickin AP, Ford DC, Schwarcz HP, McNutt R, Williams D (1989) High-precision mass-spectrometric uranium-series dating of cave deposits and implications for paleoclimate studies. Nature 339:534-536

Lin JC, Broecker WS, Anderson RF, Hemming S, Rubenstone JL, Bonani G (1996) New Th-^{230}/U and C-14 ages from Lake Lahontan carbonates, Nevada, USA, and a discussion of the origin of initial thorium. Geochim Cosmochim Acta 60:2817-2832

Lively RS (1983) Late Quaternary U-series speleothem growth record from southeastern Minnesota. Geology 11:259-262

Lomitschka M, Mangini A (1999) An ascorbic acid/Na_2EDTA cleaning procedure for precise Th/U-dating of small samples of deep sea corals. Earth Planet Sci Lett 170:391-401

Ludwig KR (1977) Effect of initial radioactive-daughter disequilibrium on U-Pb isotope apparent ages of young minerals. J Res United States Geol Surv 5:663-667

Ludwig KR (1999) Using Isoplot/Ex, Version 2.01: A geochronological toolkit for Microsoft Excel. Berkeley Geochronology Center Special Publication 1a:47

Ludwig KR (2003) Mathematical–statistical treatment of data and errors for ^{230}Th/U geochronology. Rev Mineral Geochem 52:631-636

Ludwig KR, Paces JB (2002) Uranium-series dating of pedogenic silica and carbonate, Crater Flat, Nevada. Geochim Cosmochim Acta 66:487–506

Ludwig KR, Simmons KR, Szabo BJ, Winograd IJ, Landwehr JM, Riggs AC, Hoffman RJ (1992) Mass-spectrometric ^{230}Th-^{234}U-^{238}U dating of the Devils Hole calcite vein. Science 258:284-287

Ludwig KR, Simmons KR, Winograd IJ, Szabo BJ, Riggs AC (1993) Dating of the Devils Hole calcite vein. Science 259:1626-1627

Ludwig KR, Szabo BJ, Moore JG, Simmons KR (1991) Crustal subsidence rate off Hawaii determined from ^{234}U/^{238}U ages of drowned coral reefs. Geology 19:171-174

Ludwig KR, Titterington DM (1994) Calculation of ^{230}Th/U isochrons, ages, and errors. Geochim Cosmochim Acta 58:5031-5042

Lundberg J (1997) Paleoclimatic reconstruction and timing of sea level rise at the end of the Penultimate Glaciation, from detailed stable isotopic study and TIMS dating of submerged Bahamian speleothem. Proceedings of the 12th Int. Confr. Speleology, Switzerland 1:101

Lundberg J, Ford DC (1994) Late Pleistocene sea level change in the Bahamas from U-series dating of speleothem by mass spectrometry. Quat Sci Rev 13:1-14

Lundberg J, Ford DC, Hill CA (2000) A preliminary U-Pb date on cave spar, Big Canyon, Guadalupe Mountains, New Mexico, USA. J Cave Karst Studies 62:144-148

Luo S, Ku T-L (1991) U-series isochron dating: A generalized method employing total sample dissolution. Geochim Cosmochim Acta 55:555-564

Lyons RG, Crossley PC, Ditchburn RG, McCabe WJ, Whitehead N (1989) Radon escape from New Zealand speleothems. Appl Radiat Isot 40:1153-1158

Martinson DG, Pisias NG, Hays JD, Imbrie J, Moore TC, Shackleton NJ (1987) Age dating and the orbital theory of the Ice Ages: Development of a high-resolution 0 to 300,000 yr chronostratigraphy. Quat Res 27:1-29

Matthews A, Ayalon A, Bar-Matthews M (2000) D/H ratios of fluid inclusions of Soreq cave (Israel) speleothems as a guide to the Eastern Mediterranean Meteoric Line relationships in the last 120 ky. Chem Geol 166:183-191

McDermott F, Mattey DP, Hawkesworth CJ (2001) Centennial-scale Holocene climate variability revealed by a high-resolution speleotherm ð^{18}O record from SW Ireland. Science 294:1328-1331

McGarry SF, Baker A (2000) Organic acid fluorescence: applications to speleothem paleoenvironmental reconstruction. Quat Sci Rev 19:1087-1101

Moorbath S, Taylor PN, Orpen JL, Treloar P, Wilson JF (1987) First direct radiometric dating of Archaen stromatolitic limestone. Nature 326:865-867

Morse JW, Bender ML (1990) Partition coefficients in calcite: Examination of factors influencing the validity of experimental results and their application to natural systems. Chem Geol 82:265–277

Mucci A, Morse JW (1990) The chemistry of low temperature abiotic calcites: Experimental studies on coprecipitation, stability and fractionation. Rev Aquatic Sci 3:217-254

Musgrove ML, Banner JL, Mack LE, Combs DM, James EW, Cheng H, Edwards RL (2001) Geochronology of late Pleistocene to Holocene speleothems from central Texas: Implications for regional paleoclimate. Geol Soc Am Bull 113:1532-1543

Neff U, Burns SJ, Mangini A, Mudelsee M, Fleitmann D, Matter A (2001) Strong coherence between solar variability and the Monsoon in Oman between 9 and 6 kyrs ago. Nature 411:290-293

Neymark LA, Amelin YV, Paces JB (2000) ^{206}Pb-^{230}Th-^{234}U-^{238}U and ^{207}Pb-^{235}U geochronology of Quaternary opal, Yucca Mountain, Nevada. Geochim Cosmochim Acta 64:2913-2928

Neymark LA, Paces JB (2000) Consequences of slow growth for 230Th/U dating of Quaternary opals, Yucca Mountain, Nevada, USA. Chem Geol 164:143-160

Niggemann S, Mangini A, Richter DK, Wurth G (in press) A paleoclimate record of the last 17,600 years in stalagmites from the B7-cave, Sauerland, Germany. Quat Sci Rev

Oberli F, Meier M, Berger A , Rosenberg C, Gieré R (1996) ^{230}Th/^{238}U disequilibrium systematics in U-Th-Pb dating: Nuisance or powerful tool in geochronology. 6th V.M. Goldchmidt Conference, Heidelberg, Germany. J Conf Abstr 1:439

Olley JM, Roberts RG, Murray AS (1997) A novel method for determining residence times of river and lake sediments based on disequilibrium in the thorium decay series. Water Resour Res 33:1319-1326

Onac BP, Lauritzen S-E (1996) The climate of the last 150,000 years recorded in speleothems: preliminary results from north-western Romania. Theor Appl Karstology 9:9-21

O'Neil JR., Clayton RN, Mayeda TK (1969) Oxygen isotope fractionation in divalent metal carbonates. J Chem Phys 51:5547-5558

Osmond JK, Cowart JB (1982) Groundwater *In:* Uranium series disequilibrium: Applications to environmental problems (1st edn). Ivanovich M, Harmon RS (eds) Calrendon Press, Oxford, p 202-245

Osmond JM, May JP, Tanner WF (1970) Age of the Cape Kennedy barrier-and-lagoon complex. J Geophys Res 75:469-479

Pickett DA, Murrell MT, Williams RW (1994) Determination of femtogram quantities of protactinium in geologic samples by thermal ionization mass spectrometry. Anal Chem 66:1044-1049

Plagnes V, Causse C, Genty D, Paterne M, Blamart D (2002) A discontinuous climatic record from 187 to 74 ka from a speleothem of the Clamouse Cave (south of France). Earth Planet Sci Lett 201:87-103

Polyak VJ, Asmerom Y (2001) Late Holocene climate and cultural changes in the southwestern United States. Science 294:148-151

Polyak VJ, McIntosh WC, Provencio P, Güven N (1998) Age and Origin of Carlsbad Caverns and related caves from ^{40}Ar/ ^{39}Ar of alunite. Science 279:1919-1922

Porcelli D, Swarzenski PW (2003)The behavior of U- and Th- series nuclides in groundwater. Rev Mineral Geochem 52:317-361

Postpichl D, Agostini S, Forti P, Quinif Y (1991) Paleoseismicity from karst sediments: "Grotta del Cervo" cave, Central Italy. Tectonophysics 193:33-44

Quade J, Cerling TE, Bowman JR (1989) Systematic variations in the carbon and oxygen isotopic composition of pedogenic carbonate along elevation transects in the southern Great Basin. United States Geol Soc Am Bull 101:464-475

Railsback LB (2000) An Atlas of Speleothem Microfabrics: *http://www.gly.uga.edu/speleoatlas/SAIndex1.html*

Railsback LB, Brook GA, Webster JW (1999) Petrology and paleoenvironmental significance of detrital sand and silt in a stalagmite from Drotsky's Cave, Botswana. Phys Geography 20:331-347

Railsback LB, Brook, GA, Chen J, Kalin R, Fleisher CJ (1994) Environmental controls on the petrology of a Late Holocene speleothem from Botswana with annual layers of aragonite and calcite: J Sediment Res A64:147-155

Rasbury ET, Hanson GN, Meyers WJ, Saller AH (1997) Dating of the time of sedimentation using U-Pb ages for paleosol calcite. Geochim Cosmochim Acta 61:1525-1529

Richards DA (1995) Pleistocene sea levels and paleoclimate of the Bahamas based on ^{230}Th ages of speleothems. PhD dissertation. University of Bristol, Bristol

Richards DA, Bottrell SH, Cliff RA, Ströhle K, Rowe PJ (1998) U-Pb dating of a Quaternary-age speleothem. Geochim Cosmochim Acta 62:3683-3688

Richards DA, Smart PL Edwards RL (1994) Maximum sea levels for the last glacial period from U-series ages of submerged speleothems. Nature 367:357-360

Richards DA, Smart PL, Borton CJ, Edwards RL, Roberts MS (1997) Uranium-series disequilibria in speleothems form the Bahamas: Sea levels, carbonate deposition and diagenesis. Seventh Annual V. M. Goldschmidt Conference, LPI Contribution 921, Lunar and Planetary Institute, Houston. p 173

Richards DA, Smart PL, Edwards RL (1992) Late Pleistocene sea-level change based on high-precision mass-spectrometric ^{230}Th ages of submerged speleothems from the Bahamas. EOS Trans, Am Geophys Union 73:172

Rink WJ (1997) Electron spin resonance (ESR) dating and ESR applications in Quaternary science and archaeometry. Rad Meas 5-6:975-1025

Roberts MS, Smart PL, Baker A (1998) Annual trace element variations in a Holocene speleothem. Earth Planet Sci Lett 154:237-246

Roberts MS, Smart PL, Hawkesworth CJ, Perkins WT, Pearce NJP (1999). Trace element variations in coeval Holocene speleothems from GB Cave, southwest England. The Holocene 9:138-139

Robinson LF, Henderson GM, Slowey NC (2002) U-Th dating of marine isotope stage 7 in Bahamas slope sediments. Earth Planet Sci Lett 196:175-187

Rogers JJW, Adams JAS (1969) Uranium. *In:* Handbook of Geochemistry. Wedepohl, KH (ed) Spinger-Verlag, Berlin

Rosholt JN, Antal PS (1962) Evaluation fo the Pa^{231}/U-Th^{230}/U method for dating Pleistocene carbonate rocks. US Geol Surv Pro Paper 450-E:108-111

Rowe PJ, Austin T, Atkinson TC (1988) The Quaternary evolution of cave deposits at Cresswell Crags gorge, England. Cave Science. Trans Brit Cave Res Assoc 16:3-17

Rozanski KL, Araguas-Araguas L, Gonfiantini R (1993) Isotopic patterns in modern global precipitation. *In:* Climatic Change in Continental Isotope Records. Swart PK, Lohmann KC, MacKenzie J, Savin S (eds) American Geophysical Union, Washington D.C., p 1-36

Salomans W, Mook WG (1986) Isotope geochemistry of carbonates in the weathering zone *In:* Handbook of Environmental Isotope Geochemistry: Vol 2 The Terrestrial Environment. Fritz P, Fontes JC (eds), Elsevier, Amsterdam, p 239-269

Schramm A, Stein M, Goldstein SL (2000) Calibration of the ^{14}C time scale to 50 kyr by ^{234}U-^{230}Th dating of sediments from Lake Lisan (the paleo-Dead Sea). Earth Planet Sci Lett 175:27-40

Schwarcz HP (1986) Geochronology and isotope geochemistry of speleothems. *In:* Handbook of Environmental Isotope Geochemistry: Vol 2 The Terrestrial Environment. Fritz P, Fontes JC (eds) Elsevier, Amsterdam, p 271-303

Schwarcz HP, Blackwell BA (1992) Archaeological applications. *In:* Uranium-series disequilibrium: Applications to Earth, Marine and Environmental Sciences. Ivanovich M, Harmon RS (eds) Oxford University Press, Oxford, p 513-552

Schwarcz HP, Harmon RS, Thompson P, Ford DC (1976) Stable isotope studies of fluid inclusions in speleothems and their paleoclimatic significance. Geochim Cosmochim Acta 40:657-665

Schwarcz HP, Rink WJ (2001) Dating methods for sediments of caves and rock shelters. Geoarchaeology 16:355-372

Shen GJ (1996) ^{227}Th/^{230}Th dating method: Methodology and application to Chinese speleothem sample. Quat Sci Rev 15:699-707

Shen GJ, Ku T-l, Cheng H, Edwards RL, Yuan ZX, Wang Q (2001) High-precision U-series dating of Locality 1 at Zhoukoudian, China. J Human Evol 41:679-688

Shen GJ, Ku T-L, Gahleb B, Yuan ZX (1996) Preliminary results on U-series dating of Peking Man site with high precision TIMS. Acta Anthropol Sinica 15:210-217 (in Chinese)

Shopov YY, Ford DC, Schwarcz HP (1994) Luminescent micro-banding in speleothems: high-resolution chronology and paleoclimate. Geology 22:407-410

Short SA, Lowson RT, Ellis J (1988) ^{234}U/^{238}U and ^{230}Th/^{234}U activity ratios in the colloidal phases of aquifers in lateritic weathered zones. Geochim Cosmochim Acta 52:2555-2563

Smart PL, Richards DA, Edwards RL (1998) Uranium-series ages of speleothems from South Andros, Bahamas; implications for Quaternary sea-level history and palaeoclimate. Cave Karst Sci 25:67-74

Smart PL, Roberts MS, Baker A, Richards DA (1996) Palaeoclimate determination from speleothems. A critical appraisal of the state of the art. *In:* Climate Change: The Karst Record. Lauritzen S-E (ed) Karst Waters Institute Special Publications 2. Charles Town, West Virginia, p 157-159

Smith PE, Brand U, Farquhar RM (1994) U-Pb systematics and alteration trends of Pennsylvanian-aged aragonite and calcite. Geochim Cosmochim Acta 58:313-322

Smith PE, Farquhar RM (1989) Direct dating of Phanerozoic sediments by the ^{238}U/^{206}Pb method. Nature 341:7-20

Smith PE, Farquhar RM Hancock RG (1991) Direct radiometric age determination of carbonate diagenesis using U-Pb in secondary calcite. Earth Planet Sci Lett 105:474-491

Spalding RF, Mathews TD (1972) Submerged stalagmites from caves in the Bahamas: Indicators of low sea level stand. Quat Res 2:470-472

Spötl C, Mangini A, Frank N, Eichstädter R, Burns SJ (2002) Start of the last interglacial period at 135 ka: Evidence from a high alpine speleothem. Geology 30:815-818

Spötl C, Mangini A. (2002) Stalagmite from the Austrian Alps reveals Dansgaard-Oeschger events during isotope stage 3: Implications for the absolute chronology of Greenland ice cores. Earth Planet Sci Lett 203:507-518

Stirling CH, Lee DC, Christensen JM, Halliday AN (2000) High-precision *in situ* U-238-U-234-Th-230 isotopic analysis using laser ablation multiple-collector ICPMS. Geochim Cosmochim Acta 64:3737-3750

Stocker TF, Wright DG (1996) Rapid changes in ocean circulation and atmospheric radiocarbon. Paleoceanogaphy 11:773-796

Stuiver M, Reimer PJ, Bard E, Beck JW, Burr GS, Hughen KA, Kromer B, McCormac G, van der Plicht J, Spurk M (1998) INTCAL98 radiocarbon age calibration, 24,000-0 cal BP Radiocarbon 40:1041-1083

Sutcliffe AJ, Lord TC, Harmon RS, Ivanovich M, Rae A, Hess JW (1985) Wolverine in northern England about 83,000 years BP: Faunal evidence for climatic change during Isotope stage 5. Quat Res 24:73-86

Swarzenski PW, Porcelli D, Andersson PS, Smoak JM (2003) The behavior of U- and Th- series nuclides in the estuarine environment. Rev Mineral Geochem 52:577-606

Szabo BJ (1979) ^{230}Th, ^{231}Pa and open system dating of fossil corals and shells. J Geophys Res 84:4927-4930

Szabo BJ, Kolesar PT, Riggs AC, Winograd IJ, Ludwig KR (1994) Paleoclimatic inferences from a 120,000-year calcite record of water-table fluctuations in Browns Room of Devils Hole, Nevada. Quat Res 41:59-69

Taylor SR, McLennan SM (1995) The geochemical evolution of the continental crust. Rev Geophys 33:241-265

Tera F, Wasserburg GJ (1972) U-Th-Pb systematics in three Apollo 14 basalts and the problem of initial Pb in lunar rocks. Earth Planet Sci Lett 14:281-304

Thompson P, Schwarcz HP, Ford DC (1976) Stabke isotope geochemistry, geothermometry, and geochronology of speleothems from West Virginia. Geol Soc Am Bull 87:1730-1738

Vaks A, Ayalon A. Gilmour M, Frumkin A, Kaufman A, Matthews A, Bar-Matthews M. (2001) Pleistocene paleoclimate evidences from speleothem record of a karstic cave located at the desert boundary - Maale-Efraim, Eastern Shomron, Israel. PAGES - PEPIII: Past Climate Variability Through Europe and Africa Conference Abstr (*http://atlas-conferences.com/c/a/g/c/54.htm*)

Venables WN, Ripley BD (1999) Modern Applied Statistics with S-PLUS. Springer-Verlag, New York

Vesica PL, Tuccimei P, Turi B, Fornós JJ, Ginés A, Ginés J (2000) Late Pleistocene paleoclimates and sea-level change in the Mediterranean as inferred from stable isotope and U-series studies of overgrowths on speleothems, Mallorca, Spain. Quat Sci Rev 19:865-879

Voelker AHL, Grootes PM, Nadeau M-J, Sarnthein M (2000) Radiocarbon levels in the Iceland Sea from 25-53 kyr and their link to the Earth's magnetic field intensity. Radiocarbon 42:437-452

Vogel JC (1993) Variability of carbon isotope fractionation during photosynthesis. *In:* Stable isotopes and plant carbon-water relations. Ehleringer JR, Hall AE, Farquhar GD (eds) Academic Press, San Diego, p 29-38

Vogel JC, Kronfeld J (1997) Calibration of radiocarbon dates for the late Pleistocene using U/Th dates on stalagmites. Radiocarbon 39:27-32

Wang YG, Cheng H, Edwards RL, An ZS, Wu JY, Shen C-C, Dorale JA (2001) A high-resolution absolute-dated late Pleistocene monsoon record from Hulu Cave, China. Science 294:2345-2348

Wang YJ, Hai, C, Luo CL, Xia, YF, Wu JY, Chen J (1999) TIMS U-series ages of speleoethem from Tangshan caves, Nanjing. Chinese Sci. Bull. 44:1987-1991

Wedepohl KH (1995) The composition of the continental crust. Geochim Cosmochim Acta 59:1217-1239

Wendt I (1984) A three-dimensional U-Pb discordia plane to evaluate samples with common lead of unknown isotopic composition. Chem Geol 2:1-12

Wendt I, Carl C (1985) U/Pb dating of discordant 0.1 Ma old secondary U minerals. Earth Planet Sci Lett 73:278-284

Werner M, Mikolajewicz U, Hoffmann G, Heimann M (2000) Possible changes of δ^{18}O in precipitation caused by a meltwater event in the North Atlantic. J Geophys Res 10:10161-10167

Whitehead NE, Ditchburn RG, Williams PW, McCabe WJ (1999) ^{231}Pa and ^{230}Th contamination at zero age: a possible limitation on U/Th series dating of speleothem material. Chem Geol 156:359-366

Wigley TML, Plummer LN, Pearson FJ (1978) Mass transfer and carbon isotope evolution in natural water systems. Geochim Cosmochim Acta 42:1117-1140

Winograd IJ, Coplen, TB, Landwehr JM, Riggs AC, Ludwig KR, Szabo BJ, Kolesar PT, Revesz KM (1992) Continuous 500,000-year climate record from vein calcite in Devils Hole, Nevada. Science 258:255-260

Winograd IJ, Landwehr JM, Ludwig KR, Coplen TB, Riggs AC (1997) Duration and structure of the past four interglaciations. Quat Res 48:141-154

Winograd IJ, Szabo BJ, Coplen TB, Riggs AC (1988) A 250,000-year climatic record from Great Basin vein calcite: implications for Milankovitch theory. Science 242:1275-1280

Yokoyama Y, Esat TM, Lambeck K, Fifield LK (2000) Last ice age millennial scale climate changes recorded in Huon Peninsula corals. Radiocarbon 42:383-401

Yonge CJ, Ford DC, Gray JP, Schwarcz HP (1985) Stable isotope studies of cave seepage water. Chem Geol 58:97-105

Yuan SX, Chen TM, Gao SJ, Hu YQ (1991) Study on uranium series dating of fossil bones from Zhoukoudian sites Acta Anthropol. Sinica 10:189-193 (in Chinese)

Zhao J-X, Hu K, Collerson KD, Xu H-K (2001) Thermal ionization mass spectrometry U-series dating of a hominid site near Nanjing, China. Geology 29:27-30